Tropospheric Ozone Assessment Report: A critical review of changes in the tropospheric ozone burden and budget from 1850 to 2100

Article · January 2021

CITATIONS
63

READS
710

39 authors, including:

Hideharu Akiyoshi
National Institute for Environmental Studies
155 PUBLICATIONS **7,350** CITATIONS
SEE PROFILE

Richard Anthony Cox
University of Cambridge
302 PUBLICATIONS **30,268** CITATIONS
SEE PROFILE

Mhairi Coyle
UK Centre for Ecology & Hydrology/The James Hutton Institute
79 PUBLICATIONS **7,535** CITATIONS
SEE PROFILE

Makoto Deushi
Meteorological Research Institute, Japan Meteorological Agency
179 PUBLICATIONS **7,242** CITATIONS
SEE PROFILE

ELEMENTA
Science of the Anthropocene

Archibald, A. T., et al. 2020. Tropospheric Ozone Assessment Report: A critical review of changes in the tropospheric ozone burden and budget from 1850 to 2100. *Elem Sci Anth*, 8: 1. DOI: https://doi.org/10.1525/elementa.2020.034

RESEARCH ARTICLE

Tropospheric Ozone Assessment Report: A critical review of changes in the tropospheric ozone burden and budget from 1850 to 2100

A. T. Archibald[1,2,*], J. L. Neu[3], Y. F. Elshorbany[4], O. R. Cooper[5,6], P. J. Young[7,8,9], H. Akiyoshi[10], R. A. Cox[1], M. Coyle[11,12], R. G. Derwent[13], M. Deushi[14], A. Finco[15], G. J. Frost[6], I. E. Galbally[16,17], G. Gerosa[15], C. Granier[5,6,18], P. T. Griffiths[1,2], R. Hossaini[7,8], L. Hu[19], P. Jöckel[20], B. Josse[21], M. Y. Lin[22], M. Mertens[20], O. Morgenstern[23], M. Naja[24], V. Naik[25], S. Oltmans[26], D. A. Plummer[27], L. E. Revell[28], A. Saiz-Lopez[29], P. Saxena[30], Y. M. Shin[1], I. Shahid[31], D. Shallcross[32], S. Tilmes[33], T. Trickl[34], T. J. Wallington[35], T. Wang[36], H. M. Worden[33], and G. Zeng[23]

Our understanding of the processes that control the burden and budget of tropospheric ozone has changed dramatically over the last 60 years. Models are the key tools used to understand these changes, and these underscore that there are many processes important in controlling the tropospheric ozone budget. In this critical review, we assess our evolving understanding of these processes, both physical and chemical.

[1] Yusuf Hamied Department of Chemistry, University of Cambridge, United Kingdom
[2] National Centre for Atmospheric Science, United Kingdom
[3] Jet Propulsion Laboratory, California Institute of Technology, Pasadena, CA, USA
[4] School of Geosciences, College of Arts and Sciences, University of South Florida, St. Petersburg, FL, USA
[5] Cooperative Institute for Research in Environmental Sciences, University of Colorado, Boulder, CO, USA
[6] NOAA Chemical Sciences Laboratory, Boulder, CO, USA
[7] Lancaster Environment Centre, Lancaster University, United Kingdom
[8] Centre of Excellence in Environmental Data Science, Lancaster University,United Kingdom
[9] Institute for Social Futures, Lancaster University, United Kingdom
[10] Climate Modeling and Analysis Section, Center for Global Environmental Research, National Institute for Environmental Studies, Tsukuba, Japan
[11] UK Centre for Ecology & Hydrology Edinburgh, Bush Estate, Penicuik, Midlothian, United Kingdom
[12] The James Hutton Institute, Craigiebuckler, Aberdeen, United Kingdom
[13] rdscientific, Newbury, United Kingdom
[14] Meteorological Research Institute, Japan Meteorological Agency, Tsukuba, Ibaraki, Japan
[15] Dipartimento di Matematica e Fisica, Università Cattolica del S.C., Brescia, Italy
[16] Climate Science Centre, CSIRO Oceans and Atmosphere, Aspendale, Victoria, Australia
[17] Centre for Atmospheric Chemistry, University of Wollongong, Wollongong, New South Wales, Australia
[18] Laboratoire d'Aérologie, Université de Toulouse, CNRS, UPS, France
[19] Department of Chemistry and Biochemistry, University of Montana, Missoula, MT, USA
[20] Deutsches Zentrum für Luft- und Raumfahrt, Institut für Physik der Atmosphäre, Oberpfaffenhofen, Germany
[21] Centre National de Recherches Météorologiques, Université de Toulouse, Météo-France, CNRS, Toulouse, France
[22] Atmospheric & Oceanic Sciences, Princeton University and NOAA Geophysical Fluid Dynamics Laboratory, Princeton, NJ, USA
[23] National Institute of Water and Atmospheric Research, Wellington, New Zealand
[24] Aryabhatta Research Institute of Observational Sciences, Nainital, Uttarakhand, India
[25] NOAA Geophysical Fluid Dynamics Laboratory, Princeton, NJ, USA
[26] NOAA Global Monitoring Laboratory, Boulder, CO, USA
[27] Climate Research Division, Environment and Climate Change Canada, Montreal, Canada
[28] School of Physical and Chemical Sciences, University of Canterbury, Christchurch, New Zealand
[29] Department of Atmospheric Chemistry and Climate, Institute of Physical Chemistry Rocasolano, Spanish National Research Council (CSIC), Madrid, Spain
[30] School of Environmental Sciences, Jawaharlal Nehru University, New Delhi, India
[31] Institute of Space Technology, Islamabad, Pakistan
[32] School of Chemistry, Cantock's Close, University of Bristol, United Kingdom
[33] Atmospheric Chemistry Observations & Modeling Laboratory National Center for Atmospheric Research, Boulder, CO, USA
[34] Karlsruher Institut für Technologie, IMK-IFU, Garmisch-Partenkirchen, Germany
[35] Research & Advanced Engineering, Ford Motor Company, Dearborn, MI, USA
[36] Department of Civil and Environmental Engineering, The Hong Kong Polytechnic University, Hong Kong, China

* Corresponding author:
Email: ata27@cam.ac.uk

We review model simulations from the International Global Atmospheric Chemistry Atmospheric Chemistry and Climate Model Intercomparison Project and Chemistry Climate Modelling Initiative to assess the changes in the tropospheric ozone burden and its budget from 1850 to 2010. Analysis of these data indicates that there has been significant growth in the ozone burden from 1850 to 2000 (approximately 43 $\pm$ 9%) but smaller growth between 1960 and 2000 (approximately 16 $\pm$ 10%) and that the models simulate burdens of ozone well within recent satellite estimates. The Chemistry Climate Modelling Initiative model ozone budgets indicate that the net chemical production of ozone in the troposphere plateaued in the 1990s and has not changed since then inspite of increases in the burden. There has been a shift in net ozone production in the troposphere being greatest in the northern mid and high latitudes to the northern tropics, driven by the regional evolution of precursor emissions. An analysis of the evolution of tropospheric ozone through the 21st century, as simulated by Climate Model Intercomparison Project Phase 5 models, reveals a large source of uncertainty associated with models themselves (i.e., in the way that they simulate the chemical and physical processes that control tropospheric ozone). This structural uncertainty is greatest in the near term (two to three decades), but emissions scenarios dominate uncertainty in the longer term (2050–2100) evolution of tropospheric ozone. This intrinsic model uncertainty prevents robust predictions of near-term changes in the tropospheric ozone burden, and we review how progress can be made to reduce this limitation.

Keywords: Ozone, Tropospheric chemistry, Ozone budget, Chemistry transport models, Tropospheric ozone

1. Introduction

Tropospheric ozone is a greenhouse gas and, at elevated levels, a pollutant detrimental to human health and crop and ecosystem productivity (REVIHAAP, 2013; U.S. Environmental Protection Agency, 2013; Long-Range Transport of Air Pollution [LRTAP] Convention, 2015; Monks et al., 2015). Since 1990, a large portion of the anthropogenic emissions of gases that react in the atmosphere to produce ozone have shifted from North America and Europe—due to pollution controls—to Asia, driven by economic growth and more limited pollution controls (Granier et al., 2011; Cooper et al., 2014; Zhang et al., 2016b; Hoesly et al., 2018). This rapid shift, coupled with limited ozone monitoring in developing nations, has left scientists with a number of basic questions still to answer: Which regions of the world have the greatest human and plant exposure to ozone pollution? Is ozone continuing to decline in nations with strong emission controls? To what extent is ozone increasing in the developing world? How can we best quantify ozone's impact on climate, human health, and crop/ecosystem productivity?

To answer these questions, the International Global Atmospheric Chemistry (IGAC) project developed the Tropospheric Ozone Assessment Report (TOAR): Global metrics for climate change, human health and crop/ecosystem research (www.igacproject.org/activities/TOAR). Initiated in 2014, TOAR's mission is to provide the research community with an up-to-date scientific assessment of tropospheric ozone's global distribution and trends from the surface to the tropopause. TOAR's primary goals are to produce the first tropospheric ozone assessment report underpinned by all available surface, ozonesonde, aircraft, and satellite observations to document an understanding of ozone distributions and trends from the peer-reviewed literature and new analyses and to generate easily accessible, well-documented ozone exposure metrics relevant to human health and ecosystems at thousands of measurement sites around the world. Through the TOAR Surface Ozone Database (Schultz et al., 2017), these ozone metrics are freely accessible for research on the global-scale impact of ozone on climate, human health, and crop/ecosystem productivity. The assessment report is organized as a series of papers in a Special Feature of *Elementa: Science of the Anthropocene*.

In addition to measurements, numerical modeling plays a critical role in understanding the burden and budget of tropospheric ozone (see *TOAR-Model Performance*: Young et al., 2018). Atmospheric chemistry models typically incorporate (1) tropospheric (and stratospheric) chemical reaction schemes, (2) anthropogenic precursor emission inventories, (3) schemes for natural emissions, (4) removal of ozone at physical surfaces and interfaces, and (5) schemes for representing atmospheric fluid dynamics, thermodynamics, and radiation. Alleviating uncertainties in model representation of these processes is necessary for improved understanding of the drivers of past and future changes in tropospheric ozone and how these changes may affect climate, human health, and ecosystems.

This article, abbreviated as *TOAR-Ozone Budget*, focuses on the physical and chemical processes that affect the budget of ozone in the troposphere. *TOAR-Ozone Budget* begins with a brief historical overview of the evolution of the scientific understanding of tropospheric ozone and the fundamental processes known to control it (Sections 1–3). The main focus of this article is a detailed analysis of our current understanding of the sources and sinks of ozone in the troposphere (Section 4), while we discuss new insights into the chemical and physical processes that control ozone and challenges associated with the accurate simulation and prediction of ozone abundances (Sections 5 and 6). Section 7 provides a summary and future outlook.

1.1. A brief history of tropospheric ozone research

The history of tropospheric ozone research has been reviewed in detail recently (Staehelin et al., 2017; Wallington et al., 2019), and here, we provide a brief overview. The

greatest challenges in tropospheric ozone research over the last few decades have included quantifying and understanding (1) the role and interactions of physical processes, including transport of ozone-rich air from the stratosphere to the troposphere and the removal of ozone at plant, soil, water, snow, and ice surfaces and (2) chemical processes including the emission and transformation of ozone precursors and the production and destruction of ozone in the troposphere by gas and aerosol phase chemistry. Recently, it has been recognized that the rates and spatial distributions of these different processes have changed over the past decades and will most likely continue to change in the future as the locations of precursor emissions change (Zhang et al., 2016b).

1.2. Evolution in understanding of the physical and chemical processes controlling the distribution of ozone

The starting point of this historical review is the identification of the transport of ozone-rich air from the stratosphere into the troposphere (Regener, 1938). Here, we follow the terminology of Stohl et al. (2003a) and use stratosphere to troposphere transport (STT) in reference to air and ozone transport from the stratosphere across the tropopause and into the troposphere, and stratosphere–troposphere exchange (STE) in reference to air and ozone exchange across the tropopause in both directions. The large-scale processes driving transport of stratospheric air to the troposphere were first identified with the discovery of the Brewer–Dobson circulation, in which tropospheric air passes into the stratosphere in the upper arm of the ascending Hadley circulation at low latitudes and stratospheric air returns to the troposphere in midlatitudes (Brewer, 1949). Further analysis showed that most of the actual transport occurs during tropopause folding in the vicinity of a jet stream (Danielsen, 1968; Shapiro, 1976, 1978, 1980; Danielsen and Mohnen, 1977; Keyser and Shapiro, 1986), with other mechanisms of STT being subsidence in cutoff lows (Price and Vaughan, 1993) and gravity-wave breaking (Lamarque et al., 1996). Subsequently, there have been attempts to quantify STT and its temporal evolution through observational constraints (Murphy and Fahey 1994; Beekmann et al., 1997; Scheel, 2003; Stohl et al., 2003a; Olsen et al., 2004; Trickl et al., 2020).

Ozone destruction on surfaces has been recognized since the earliest laboratory experiments (Schönbein, 1840). Early research showed that ozone is present in much lower concentrations in the lower atmosphere than in the upper atmosphere implying one or more ozone loss mechanisms in the troposphere (Hartley, 1881; Fabry and Buisson, 1913; Colange and Lepape, 1929; Chapman, 1942). These ideas on the loss of ozone by destruction at the Earth's surface were first formalized by Auer (1939), with the classical view of tropospheric ozone being regulated by STT of ozone and surface destruction being put forth by Junge (1962; **Figure 1A**). **Figure 1** shows, schematically, how this understanding has evolved over time. By the 1980s (**Figure 1B**), there were sufficient measurements of ozone deposition rates at the Earth's surface (e.g., Regener, 1957; Galbally, 1971), sufficient observations of ozone in surface air, and sufficient understanding of the interaction of meteorology and ozone deposition that a global budget of ozone deposition of $1{,}000 \pm 500$ Tg (O_3) yr^{-1} was estimated by Galbally and Roy (1980). These early studies have been proven accurate, with estimates of STT and dry deposition remaining within a factor of two over the last 30 years, each having uncertainties of around $\pm 30\%$ at present (see Section 7).

Up until 1970, there was no knowledge of the kinetic basis of photochemistry of ozone in the lower atmosphere. This changed dramatically when decomposition products of ozone photolysis in the near ultraviolet (UV) were determined, revealing that the long wavelength limit for a significant yield of $O(^1D)$ was 310 nm (Jones and Wayne, 1970). Levy (1971) noted that although the majority of $O(^1D)$ atoms are deactivated to ground state $O(^3P)$ atoms through collision with a third molecule (N_2 or O_2), a small fraction reacts with water vapor to produce hydroxyl radicals (OH). Levy showed that UV radiation in the troposphere and at the Earth's surface was sufficient to initiate the formation of hydroxyl radicals. There was a rapid development of the understanding of the photochemistry of the troposphere in the 1970s (Levy, 1971, 1972, 1973; Crutzen, 1973; Chameides and Walker, 1973). It was shown that hydroxyl radicals, in the presence of nitrogen oxides and carbon monoxide or volatile organic compounds (VOCs), initiate chemical cycles that, utilizing the oxidation products of carbon monoxide and VOCs, lead to net ozone production (**Figure 1B**); this chemistry is applicable in both the remote troposphere and the urban atmosphere (e.g., Monks et al., 2015). The basic mechanism of photochemical production of ozone in the troposphere was confirmed in part by the identification of positive correlations of carbon monoxide and ozone in many regions of the background troposphere (Fishman and Seiler, 1983).

An early combined experimental and modeling study of ozone chemistry in the background troposphere was the Mauna Loa Observatory Photochemistry Experiment in 1988 (MLOPEX; Liu et al., 1992; Ridley et al., 1992), which was followed by MLOPEX 2 at the same site in 1991 and 1992 (Atlas and Ridley, 1996; Brasseur et al., 1996; Hauglustaine et al., 1996). Since then, it has been shown that net photochemical production of ozone can occur in a wide range of environments, including in biomass burning plumes (Jaffe and Wigder, 2012), the polar boundary layer in summer (Oltmans et al., 2008), and in polluted air in snow-covered rural environments in winter (Schnell et al., 2009), as well as in the background troposphere and polluted urban atmosphere. New processes that have been added to the original understanding of tropospheric ozone production and loss processes over the past two decades are discussed in Section 5.

1.3. Regional differences in ozone photochemistry

There are some marked differences in ozone chemistry in remote regions, including the free troposphere, compared to the urban boundary layer (**Figure 1C**). Methane plays an important role for the global ozone background level.

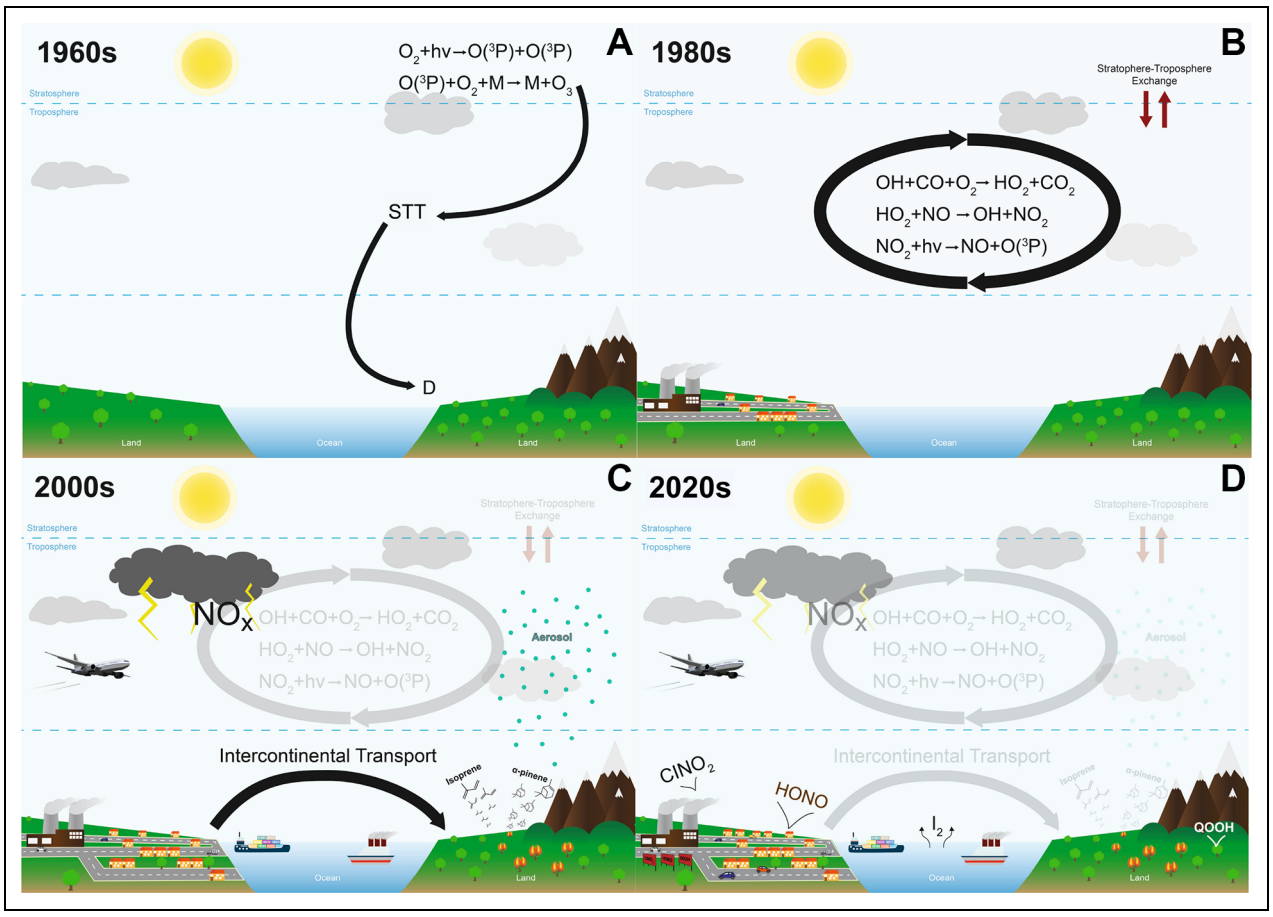

Figure 1. Schematic illustration of how our understanding of the chemical and physical processes controlling tropospheric ozone has evolved. The panels highlight the key processes identified in the different time periods. The labeling of dates in the subpanels (A–D) is indicative. DOI: https://doi.org/10.1525/elementa.2020.034.f1

The increase in methane over the last decade has been a major driver for increases in background ozone. However, its reactivity makes it a relatively smaller contributor to ozone in the urban atmosphere, where directly emitted reactive organic compounds and CO dominate ozone production. In remote regions, as well as methane, the VOCs that contribute to ozone chemistry are first- and many-generation oxidation products, carbon monoxide (which comes from direct emissions and secondary production from VOCs), and a range of oxygenated organic compounds. Another major difference is the availability of NO_x, whose sources are abundant in the urban atmosphere. The primary sources of NO_x in the remote atmosphere are lightning, particularly in the tropical-free troposphere (Ridley et al., 1994; Zhang et al., 2003; DeCaria et al., 2005; Schumann and Huntrieser, 2007) and peroxyacetyl nitrate (PAN). In the remote continental boundary layer, there are additional sources of NO_x from soils (Galbally and Roy, 1978; Davidson and Kingerlee, 1997) and biomass burning. PAN is a temporary reservoir species for NO_x that is thermally unstable. It is formed primarily in the urban atmosphere from where it can be transported long distances in the free troposphere, facilitating ozone production in the remote atmosphere. In NO_x-poor environments such as the marine boundary layer (MBL) and much of the free troposphere, ozone is mainly destroyed by photolysis (Ayers et al., 1992). International field experiments (Carpenter et al., 1997; Penkett et al., 1997; Monks et al., 1998) have identified the NO compensation point between ozone production and destruction (Galbally et al., 2000), a key parameter for defining those regions of the troposphere that are net sinks and those that are net sources for tropospheric ozone (Fishman et al., 1979).

A key component of the tropospheric ozone budget is the destruction of ozone at the Earth's surface via deposition, a process absent in the free troposphere. The lack of deposition, coupled with colder temperatures and lower water vapor concentrations, extends the lifetime of ozone in the free troposphere from about a week or so in lower altitudes to a few months in the upper troposphere, based on a globally averaged tropospheric lifetime of 22–23 days (Stevenson et al., 2006). These long atmospheric lifetimes explain the efficiency of the observed transport of ozone from the stratosphere to the middle and lower troposphere and the importance of intercontinental ozone transport in contributing to ozone trends in the background regional atmosphere (**Figure 1C**). The importance of such long-range transport mechanisms for ozone was recognized in the 1970s (Cox and Eggleton, 1975) and formed the cornerstone of the United Nations Economic Commission for Europe Convention on the LRTAP and

continues to be a topic of important research. In the late 1990s, the intercontinental transport of ozone and its precursors from Asia to North America and from North America to Europe was observed, demonstrating the link between the emissions from one continent and the trace gas mixing ratios above a downwind continent (Hemispheric Transport of Air Pollution [HTAP], 2010).

1.4. Development of emissions inventories

On a global scale, the emissions of ozone precursors have increased dramatically over the last 60 years (Lamarque et al., 2010; van Marle et al., 2017; Hoesly et al., 2018). Initially, inventories of ozone precursors were globally integrated estimates (Junge, 1972; Söderlund and Svensson, 1976). Regional emissions inventories were then developed, with the first urban emissions inventory focusing on carbon monoxide, VOCs, and NO_x for Los Angeles in the early 1970s to address air quality issues (Roth et al., 1974). A modern approach is the progressive merging of urban, regional, and global emission inventories under the IGAC Global Emissions Initiative project (http://www.geiacenter.org/) and the Emissions of atmospheric Compounds and Compilation of Ancillary Data project. The history of these inventories and attempts at their harmonization are discussed by Granier et al. (2011) and references therein and in Granier et al. (n.d.). The state of biomass burning and anthropogenic emissions inventories in 2011 was such that the regional estimates for carbon monoxide and NO_x from different inventories differed by up to a factor of two for the period 1980–2005 (Granier et al., 2011). Similar levels of uncertainty apply to VOC emission estimates too (e.g., McDonald et al., 2018). This highlights the importance for uncertainty estimates associated with emission inventories. Although earlier inventories usually completely neglected uncertainty, the latest generation of historic emissions for chemistry-climate model (CCM) studies is making efforts to move toward enabling quantitative uncertainty estimates (Hoesly et al., 2018).

Another complexity of emission inventories is natural emissions, whose emission rates and their temporal and spatial distribution are dependent on many physical, chemical, and biological processes and states in the environment. Four key processes that contribute to ozone precursor emissions are the production of VOCs from vegetation, NO_x from lightning and soils, and both VOCs and NO_x from naturally occurring biomass burning. These processes have been recognized as important contributors to total budgets of NO_x and VOCs for many decades, but the problems of quantifying emissions have been formidable. Interactive process-based models now simulate VOC emissions from vegetation and are embedded within most CCMs, for example, the Biogenic Emission Inventory System (Guenther et al., 1995) and the Model of Emissions of Gases and Aerosols from Nature (Guenther et al., 2006). However, there is still considerable work to be undertaken in verifying these models (e.g., Marais et al., 2012; Hu et al., 2015; Emmerson et al., 2016). Similarly, interactive models exist for simulating NO_x emissions from lightning (e.g., those based on Price et al., 1997), but major uncertainties still need to be addressed to refine these models (Schumann and Huntrieser, 2007; Clark et al., 2017; Luo et al., 2017).

2. Physical processes regulating tropospheric ozone

2.1. Loss of ozone to the surface

Historically, the ozone deposition process was discussed first by Regener (1957) who proposed a surface destruction coefficient(s), based on the concept of a kinetic coefficient as used to describe a chemical reaction taking place at the surface. Galbally (1971, 1974) combined this concept with the ideas based on studies of gas transfer to surfaces introduced by Chamberlain (1966) to develop a generalized framework. The ozone deposition process is now widely described using a resistance analogy, first employed by Galbally and Roy (1980), where the various stages of transfer from the bulk atmosphere to a surface are modeled as serial resistance terms. The destruction at the surface can also be expressed as an equivalent resistance. The advantage of the resistance approach is that the terms are additive, and the reciprocal of the sum of the resistances is the deposition velocity, v_d (Galbally, 1974; Galbally and Roy, 1980; Wesely, 1989), such that

$$v_d = (R_a + R_b + R_c)^{-1},$$

where R_a is the aerodynamic resistance, representing the role of atmospheric turbulence in transporting ozone down from a reference height in the boundary layer; R_b is the resistance arising from molecular diffusion in the sublaminar boundary layer just above the surface; and R_c is the total surface resistance, arising from when ozone passes through the boundary layer or canopy and makes contact with the surface, where it rapidly reacts and is destroyed. R_c has stomatal and nonstomatal pathways (**Figure 2**) and is the dominant factor controlling daytime ozone deposition to vegetated surfaces. The rate of this nonstomatal surface destruction is represented by either a combination of cuticular resistance (R_{ct}, which also includes all external plant surfaces) and soil resistance (R_g) or a total surface resistance for nonvegetated areas, as appropriate.

In the case of plant canopies (which make up a large component of the total ozone deposition flux), there may also be an additional aerodynamic transport term (R_{a_inc}) that represents transport of ozone down to the soil or vegetated understory. Gas phase loss of ozone by reaction with NO emitted from the soil and highly reactive VOCs emitted from plants (Kurpius and Goldstein, 2003; Fares et al., 2010) takes place both above and within the canopy, and these losses can affect ozone deposition rates over forests and other plant systems with canopies. All these processes and their connections are illustrated in **Figure 2.**

Over vegetation, ozone can enter the plants' stomata if they are open. The stomatal uptake of ozone is largely regulated by the physiological activity and associated gas exchanges of the vegetation, with light, temperature, and water availability in the plant–soil system as the dominant

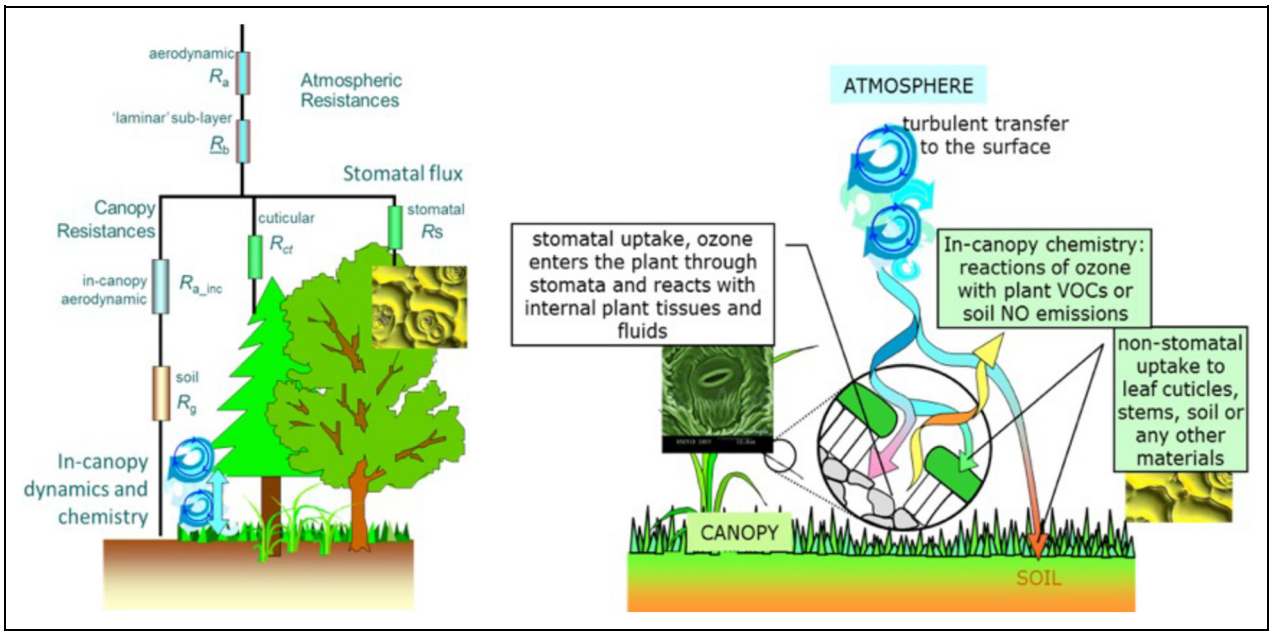

Figure 2. Pathways of ozone deposition on vegetated surfaces (with or without the resistance analogue used to quantify and model the processes). DOI: https://doi.org/10.1525/elementa.2020.034.f2

controlling factors (Fowler et al., 2009; Gerosa et al., 2009; Lin et al., 2019). To estimate the stomatal resistance, it is normally assumed that the concentration of ozone in the intercellular airspace is very small compared to the external concentration so that it can be neglected. However, studies of plant physiology show that this is not always the case (de la Torre, 2008), and so a modified resistance term may be needed. Furthermore, the widely used Wesely scheme does not account for the effects of soil moisture or vapor pressure deficits on the stomatal uptake. Recent observational analyses and coupled plant physiology-CCMs indicate a key role for water availability in modulating ozone deposition rates on seasonal to interannual time scales via changes in stomatal conductance, with the effects on monthly mean daytime v_{d,O_3} variability as large as a factor of two (Lin et al., 2019). Substantial reductions in ozone removal by drought-dressed vegetation in the warming climate have been shown to exacerbate ozone air pollution extremes and offset much of the ozone air quality improvements gained from regional emission controls over Europe in recent decades (Lin et al., 2020).

Previously, this stomatal uptake, which can be calculated using plant physiology models, was thought to be the dominant removal process over all vegetated surfaces. The nonstomatal terms were assumed to be constant, only differing depending on whether the surface is dry, wet, or frozen (Wesely, 1989). However, more recent studies have shown that nonstomatal deposition to surfaces can be highly variable and is influenced by temperature, solar radiation, surface moisture, and composition, as well as by emissions from the surface. In certain periods and conditions, nonstomatal deposition may dominate surface losses, but there are still large uncertainties in the processes involved (e.g., Fowler et al., 2001; Rannik et al., 2012; Clifton et al., 2017). These concepts are incorporated to some degree in interactive ozone deposition modules within air quality and CCMs (e.g., Tuovinen et al., 2004; Franz et al., 2017; Lin et al., 2019).

A review of ozone deposition estimates from multiple global-scale CCMs was undertaken by Hardacre et al. (2015). They looked at 15 models that contributed to the model intercomparison coordinated by the Task Force on HTAP (Fiore et al., 2009). Thirteen of these models incorporated a resistance scheme based on the work of Wesely (1989), while the other two used prescribed deposition rates (fixed v_d for each land cover class). The calculated annual global deposition fluxes ranged between 818 and 1,256 Tg yr^{-1} across the models, with an ensemble mean of 978 $\pm$ 127 Tg yr^{-1}, which is similar to predictions from other studies (e.g., Stevenson et al., 2006; Wild, 2007; Young et al., 2013a, 2013b, 2018). Comparing the model results with some of the limited measurement data available showed considerable variation in model performance with season, land cover type, and location. The study concluded that the uncertainties in deposition to oceans, grasslands, and tropical forests were the main cause of differences between the models and that improving them would have the greatest benefit. Although the Wesely (1989) scheme has success in some applications (e.g., Silva and Heald, 2018), the lack of sensitivity to soil water availability is problematic, as reviewed by Lin et al. (2019).

Recent work has also highlighted the effects of structural uncertainty in the dry deposition mechanism on trends and interannual variability in the ozone deposition flux (Wong et al., 2019). Wong et al. (2019) also show that different deposition schemes result in biases in surface ozone of around 2–5 nmol/mol in the Northern Hemisphere (NH) and up to 8 nmol/mol in tropical rainforests. Silva et al. (2019, 2020) have shown that a combination of reduced complexity as well as increased complexity

models and more novel efforts using advanced statistical or machine learning techniques are possible now. However, the ability of any of these schemes to capture observations is currently critically hampered by a dearth in observed ozone deposition fluxes, particularly long-term measurements over a range of land cover types in the tropics.

Early studies of ozone dry deposition rates and processes for deposition to oceans and snow (Galbally and Roy, 1980; Garland et al., 1980) derived deposition rates around an order of magnitude lower than those for soil and plants. More recent studies have established even lower ozone deposition rates over the open ocean (Helmig et al., 2007; Fowler et al., 2009; Ganzeveld et al., 2009; Helmig et al., 2012). These observations can be largely reproduced if the reaction between ozone and iodide ($I^-_{(aq)}$) in the ocean surface layer is included along with turbulent and molecular diffusion processes (Carpenter et al., 2013; Luhar et al., 2017, p. 18). Incorporating such a deposition scheme into the UK Chemistry and Aerosol CCM (UKCA; Luhar et al., 2018) decreases ozone deposition over the ocean by almost half, which corresponds to a 10 % decrease in the model calculated total global ozone deposition. Similar results are obtained in a study with an updated surface ocean iodide distribution and the Luhar et al. (2018) scheme with the GEOS-Chem chemical transport model (CTM; Pound et al., 2020). An overall downward revision of global ozone deposition rates can be expected as these rates are more widely adopted. The net impact of the ozone-iodide reaction on the ozone budget is not well known, however, given that the ocean surface emits iodine in response to ozone deposition and the released iodine may catalytically destroy ozone in the near surface air, with feedback on other factors such as radiative forcing (Prados-Roman et al., 2015; Sherwen et al., 2017b). Further model studies are needed to assess the importance of these ozone-iodine feedbacks and reduce the uncertainties in iodine's global impact on ozone as well as more observations of surface ocean iodide concentrations, which currently limits the evaluation of the deposition schemes in models.

There are several areas that require further investigation to improve models, allow feedbacks and interactions such as climate change and associated changes in plant activity to be properly assessed, and reduce uncertainty in ozone loss on surfaces. These are (1) ozone chemistry within plant tissue, on plant and soil surfaces, and within the ocean surface layer; (2) interactions between ozone deposition and near surface ozone loss via gas phase chemistry, including the coupled ozone deposition and iodine emission cycle at the ocean surface and VOC-ozone reactions in plant canopies; and (3) reduced ozone removal by drought-stressed vegetation and associated feedbacks on surface ozone levels during heatwaves and drought (e.g., Lin et al., 2020). Detailed interactive ozone deposition schemes that include these processes are needed for use in CCMs to assess how changes in deposition due to changes in land use and climate change affect the global tropospheric ozone budget.

2.2. Transport of ozone from the stratosphere to the troposphere

The stratosphere has long been recognized as an important source of tropospheric ozone. With regard to the impact of stratospheric ozone on the tropospheric ozone budget, the key questions are as follows: (1) What is the net annual flux of ozone from the stratosphere to the troposphere, and what is its interannual variability? (2) What are the relative contributions of the various STT transport mechanisms (see below) to the annual STT ozone flux? (3) How well do global atmospheric chemistry models simulate STT transport mechanisms and their contributions to the tropospheric ozone burden? and (4) How will this source of tropospheric ozone change under climate change, in particular under a geoengineered climate (Xia et al., 2017)?

The dynamical processes that transport ozone from the lowermost stratosphere into the troposphere are generally well understood. These were summarized by Stohl et al. (2003), who reviewed the first 40 years of research on STT, beginning with the pioneering airborne explorations of E. F. Danielsen in 1963 (Danielsen, 1968). At the global scale, STT is driven by the Brewer–Dobson circulation. The 380K isentropic surface of the extra tropics is a key boundary for quantifying the global annual downward flux of ozone into the troposphere because any ozone that descends from the stratospheric "overworld" (above 380K) into the lowermost stratosphere (below 380K) will eventually enter the troposphere regardless of the exact transport mechanism or the location or timing thereof (Appenzeller et al., 1996; Olsen et al., 2004). Based on MERRA-2 reanalyses, the NH extratropical STT flux has a broad peak from February to May and a minimum in September–October (Jaeglé et al., 2017).

Recent estimates of the flux across the 380K isentropic surface based on the latest global reanalysis data (with assimilated total column ozone from satellites) are 489 Tg yr^{-1} (NH: 275 Tg yr^{-1}; Southern Hemisphere [SH]: 214 Tg yr^{-1}; Olsen et al., 2013), 448 $\pm$ 35 Tg yr^{-1} (NH: 256 $\pm$ 20; SH: 191 $\pm$ 19; Yang et al., 2016), and 492 Tg yr^{-1} (NH: 281 Tg yr^{-1}; SH: 211 Tg yr^{-1}; Jaeglé et al., 2017), with the hemispheric disparity arising from the hemispheric asymmetry in the strength of the Brewer–Dobson circulation (stronger in the NH). Estimates of the net stratospheric ozone flux into the troposphere (i.e., the downward flux minus the much smaller flux of tropospheric ozone into the stratosphere) have been inferred from a range of contemporary global atmospheric chemistry models as a residual term of the tropospheric ozone budget, after accounting for the large terms associated with ozone production, loss, and surface deposition. TOAR-Model Performance provides a summary of estimates produced from stand-alone simulations and coordinated activities (Atmospheric Composition Change: the European Network of excellence [ACCENT] and Atmospheric Chemistry and Climate Model Intercomparison Project [ACCMIP]; ensembles of opportunity), over the last two decades, which yield a net flux of stratospheric ozone into the troposphere of 520 $\pm$ 100 Tg (O_3) yr^{-1} through closure of the ozone budget (Young et al., 2018). Few of the ACCENT and

ACCMIP models included full stratospheric chemistry, but following the early work of Jöckel et al. (2006), more and more models are beginning to include this more realistic method of simulating the stratospheric ozone burden. Some of the most recent estimates for the present day from a model with full stratospheric chemistry are 325–360 Tg, at the low end of the ACCENT and ACCMIP ranges (Banerjee et al., 2016; Hu et al., 2017).

The flux estimates above are representative of average conditions, but the values vary interannually due to changes in the stratospheric circulation driven, for example, by El Niño-Southern Oscillation (ENSO) and the stratospheric quasi-biennial oscillation (QBO). Interannual variations in the strength of the stratospheric circulation of around 40% affect the STT flux leading to changes in tropospheric ozone at northern midlatitudes of around 2%, which is approximately half of the interannual variability (Neu et al., 2014). Olsen et al. (2013) found the extratropical STT ozone flux varied by $\pm 15\%$ in the NH and $\pm 6\%$ in the SH from year to year, concluding that 35–39 years would be required to detect a 2%–3% decade^{-1} trend in the STT ozone flux. The STT ozone flux has been affected by the decrease of stratospheric ozone due to ozone depleting substances, but the impact on tropospheric ozone has been relatively small. Hsu and Prather (2009) estimated STT reductions of approximately 25% in the SH and approximately 10% in the NH from ozone depletion that occurred from 1979 to 2004, corresponding to a mean decrease in tropospheric ozone of 2.1 nmol/mol and 1 nmol/mol, respectively.

The transport mechanisms by which STT occurs are (1) intrusions of stratospheric air into the troposphere via the tropopause folds associated with the dry airstream of extratropical cyclones, (2) intrusions of stratospheric air within decaying cutoff lows (a subset of extratropical cyclones), (3) gravity wave breaking, and (4) deep convection penetrating the tropopause (Stohl et al., 2003b). A recent analysis of all NH extratropical cyclones for the period 2005–2012 estimates that stratospheric intrusions associated with these cyclones account for $42 \pm 20\%$ of the NH extratropical STT ozone flux (Jaeglé et al., 2017). Notable findings regarding the location and seasonality of these intrusions are that shallow intrusions occur most frequently along the subtropical jet stream, a region known for Rossby wave breaking processes conducive to STT, and are particularly prevalent during winter (Scott and Cammas, 2002; Waugh and Funatsu, 2003; Trickl et al., 2010, 2011; Homeyer and Bowman, 2013; Nath et al., 2017). Deep intrusions that reach the lower troposphere are frequent at midlatitudes in winter and spring, with the Southwestern United States being a region of high activity, especially in spring. These intrusions also impact the chemistry of the troposphere as they mix with other air masses (Esler et al., 2001); the degree of mixing can be partially gauged via observations of the intrusion's water vapor mixing ratio (Trickl et al., 2016). Intrusions often occur in close proximity to polluted airstreams of extratropical cyclones, and over time, these air masses can intermingle and eventually mix (Stohl and Trickl, 1999; Parrish et al., 2000; Cooper et al., 2004a; Stohl et al., 2007). Intrusions have also been observed to mix with biomass burning plumes above North America and Europe (Brioude et al., 2007; Trickl et al., 2015).

Although winter and springtime intrusions are cited as most important to the tropospheric burden, summertime stratospheric contributions to tropospheric column ozone amounts (not surface ozone) measured by sondes were estimated at 20%–25% over Northeastern North America in the 2004 INTEX-A and ICARTT studies (Thompson et al., 2007). The latter budget was based on the identification of ozone and potential temperature laminae throughout the soundings. A similar conclusion was reached for the same data set by Cooper et al. (2006) using the FLEXible PARTicle dispersion model (FLEXPART), a particle-trajectory approach. A 20%–25% contribution for summer STT impacts on tropospheric column ozone was estimated by Colette and Ancellet (2005) using a 30-year European sonde climatology. Furthermore, Stauffer et al. (2018) used a clustering technique and meteorological reanalysis and estimated that, depending on the location, between 25% and 40% of ozonesonde profiles at midlatitude stations exhibited STT characteristics with anomalously low tropopause heights. The ozonesonde profiles in STT-influenced clusters were not confined to just winter and spring seasons.

Model-based intrusion climatologies and observation-based case studies have demonstrated that high altitude regions such as the Western United States (Cooper et al., 2004b, 2011; Brioude et al., 2007; Langford et al., 2009, 2015a, 2015b, 2017; Pan et al., 2010; Lefohn et al., 2011, 2012, 2014; Lin et al., 2012a, 2015; Yates et al., 2013; Škerlak et al., 2014, 2019; Dolwick et al., 2015; Lin et al., 2016), the Tibetan Plateau (Ding et al., 2006; Cristofanelli et al., 2010; Chen et al., 2011, 2013; Yin et al., 2017; Škerlak et al., 2019), and the Andes (Anet et al., 2017) are important regions for STT, not only because of frequent deep intrusions but also because their high elevation and very deep daytime boundary layers facilitate the mixing of the diluted intrusions down to the surface. Research aircraft have also documented the occurrence of stratospheric intrusions above Siberia (Berchet et al., 2013), the remote regions of the tropical and midlatitude South Indian Ocean (Clain et al., 2010; Baray et al., 2012), and at the surface of the high-altitude Antarctic ice sheet (Cristofanelli et al., 2018). The Western United States has been intensely studied, with the depth and frequency of the intrusions above the region providing an important test of Eulerian models and global reanalysis data, which have traditionally been limited in their ability to simulate the filamentary features of individual intrusions due to their coarse resolution. However, recent improvements in vertical and horizontal resolution now enable simulation of individual stratospheric intrusions above the Western United States and their contribution to surface ozone observations (Lin et al., 2012a; Knowland et al., 2017). The interannual variability of intrusions above the region and their impact at the surface have been shown to be strongly influenced by ENSO-driven transport patterns (Lin et al., 2015).

Observational analyses have been crucial for our understanding of STT (see Tarasick et al., 2019a, for a summary). Recent STT research is providing increasing evidence for important interactions between intrusions and deep convection. The potential vorticity anomalies in the mid- and upper troposphere associated with intrusions can trigger deep convection (Waugh and Funatsu, 2003). This can result in mixing between stratospheric and tropospheric air, as observed during a research flight that encountered deep convective clouds penetrating the bottom of an intrusion above Hawaii, with subsequent mixing of tropical tropospheric and midlatitude stratospheric air masses (Cooper et al., 2005). This phenomenon has also been observed above the Western United States during springtime (Homeyer et al., 2011). Deep convective clouds can also entrain ozone-rich lower stratospheric air into the upper troposphere, as observed by three research aircraft on multiple surveys of thunderstorm anvils during the summer 2012 Deep Convective Clouds and Chemistry experiment (DC3) above the central United States (Pan et al., 2014; Schroeder et al., 2014). Tang et al. (2011) used a CTM with parameterized deep convection and found that deep convection contributes to half of the STT ozone flux above northern midlatitudes during June.

3. Chemical processes regulating tropospheric ozone

Our understanding of the chemical sources and sinks and hence the budget of ozone in the troposphere has increased significantly over the last four decades (**Figure 1**). Much of the chemistry is now "textbook," but the analysis of new laboratory and field observations (enabled by developments in new instruments and improved numerical models) has produced important new discoveries, which we discuss here.

3.1. The photochemical formation mechanism of tropospheric ozone

It is well established that tropospheric ozone is mainly a secondary photochemical product that results from the photolysis of NO_2.

(R1a) $RO_2/HO_2 + NO \rightarrow NO_2 + RO/OH$
(R1b) $RO_2 + NO + M \rightarrow RONO_2 + M$ (minor)
(R2) $NO_2 + h\nu \rightarrow NO + O(^3P)$ ($\lambda \leq 400$ nm)
(R3) $O_2 + O(^3P) + M \rightarrow O_3 + M$

RO_2/HO_2 are organic peroxy radicals (R refers to an alkyl, aryl, or alkenyl group) and the hydroperoxy radical, respectively. These compounds are key intermediates in the production of ozone in the troposphere (see Section 5.5 for more details) as they convert NO into NO_2 without destroying ozone. They are formed from the oxidation of VOCs and CO with OH. $RONO_2$ represent organic nitrates that can act as a local sink of oxidants and a reservoir for ozone precursors. The OH radical is the primary oxidant in the troposphere, for which ozone itself is the primary source via reactions R4 and R5.

(R4) $O_3 + h\nu \rightarrow O(^1D) + O_2$ ($\lambda \leq 315$ nm)
(R5) $O(^1D) + H_2O \rightarrow 2\ OH$

Several studies have reviewed OH chemical formation in great detail (e.g., Elshorbany et al., 2010; Stone et al., 2012), and we only briefly mention it here.

Other sources of radicals include alkene ozonolysis (e.g., Paulson and Orlando, 1996; Rickard et al., 1999; Johnson and Marston, 2008), the photolysis of carbonyl compounds, and the photolysis of HONO (Platt and Perner, 1980; reaction R6).

(R6) $HONO + h\nu$ ($\lambda < 400$ nm) $\rightarrow OH + NO$

This reaction has received attention over the last decade as an important source of OH in the urban atmosphere (Kleffmann et al., 2005, Ren et al., 2006; Dusanter et al., 2009; Elshorbany et al., 2009, 2012a, 2012b) with associated impacts on the production of ozone (see Section 5.2 for more details).

Recent calculations employing a detailed chemistry scheme (including over 1,630 reactions) highlight that secondary production of OH and OH recycling reactions of oxidized VOCs could outweigh the source of OH in the troposphere from R4 and R5 (Lelieveld et al., 2016). But more work is needed to identify the consistency of this result across a range of models.

The ozone forming reactions, R1a, R2, and R3, can be considered as a sequence of chain propagating reactions. Under high NO_x conditions, the chain termination is dominated by R7 (where M is a third body), which leads to the formation of nitric acid ($HONO_2$).

(R7) $OH + NO_2 + M \rightarrow HONO_2 + M$

Under low NO_x conditions, R10 and R11 are the more important forms of chain termination.

(R8) $HO_2 + O_3 \rightarrow OH + 2\ O_2$
(R9) $OH + O_3 \rightarrow HO_2 + O_2$
(R10) $HO_2 + HO_2 \rightarrow H_2O_2 + O_2$
(R11) $HO_2 + RO_2 \rightarrow ROOH + O_2$

In addition to these chemical sinks of ozone, there are a number of physical sinks of ozone—deposition to surfaces (see Section 2.1) and uptake (including of oxidant reservoirs) onto particles (see Section 5.6)—that remove ozone from the troposphere.

Owing to the fast photolysis of NO_2 during the day, reactions that convert NO into NO_2 without the consumption of ozone are considered as ozone producing reactions (i.e., R12a), and reactions that convert NO_2 into other members of the NO_z family (the molecules of oxidized nitrogen [NO_y] excluding NO and NO_2) are considered as ozone destroying (e.g., R7 and R12b). Experimental evidence for a minor, but potentially important, channel of the reaction between HO_2 and NO producing nitric acid ($HONO_2$; channel 12b) has been reported (Butkovskaya et al., 2005, 2007, 2009). The main sink of $HONO_2$ is surface deposition.

(R12a) $HO_2 + NO \rightarrow HO + NO_2$
(R12b) $HO_2 + NO + M \rightarrow HONO_2 + M$

Several modeling studies (e.g., Søvde et al., 2011; Gottschaldt et al., 2013; Archibald et al., 2020) have investigated the impact of including channel R12b and shown that it could lower tropospheric ozone production rates considerably (20%). Urgent laboratory studies are required to corroborate the $HONO_2$ forming channel R12b.

Traditionally, the modeled chemical budget for "ozone" has actually been the budget of odd oxygen ($O_x = O_3 + O(^1D) + O(^3P) + NO_2 \ldots$) to remove the dominance of null cycles between O_3, and $O(^1D)$ and $O(^3P)$. This diagnosed two terms: the production, predominantly from the conversion of NO to NO_2 via peroxy radicals (R1a), and the loss, from the reaction of $O(^1D)$ with H_2O (R5), the direct reaction of HO_x radicals with O_3 (R8 and R9) and other terms. Although this diagnostic framework offered some utility, it has not over the years provided significant insight into why the O_3 budgets of different models differed so substantially. Recently, Edwards and Evans (2017) and Bates and Jacob (2019b) proposed alternative frameworks. Edwards and Evans (2017) showed that tracking the electron spin angular momentum (a spin budget) within the GEOS-Chem model resulted in similar results to the traditional model of ozone production in the troposphere described above but has the advantage of framing the budget in terms of emissions of ozone precursors (VOCs) and specific chemical processes that reduce the efficiency of O_3 production by VOCs. The benefit of this is that more insight can be gained about the role of specific emission changes on the ozone budget (as there is less emphasis on R12a, which ultimately almost every emitted VOC experiences) and specific chemical mechanism details. The spin budget is similar to the ideas implemented in the Common Representative Intermediates (CRI) mechanism (Jenkin et al., 2008, 2019) where individual VOCs are indexed according to their potential to generate RO_2, which propagate NO to NO_2 (F_{NO} in Edwards and Evans, 2017). However, as described, this approach comes at a computational cost as a large amount of output from the model is required. Bates and Jacob (2019b) took an alternative approach and extended the idea of chemical families to a wider O_y family ($O_y = O_x + O_z$). In this framework, O_z represents the ozone forming species such as RO_2 and HO_2 (as well as many other species), without which ozone cannot be produced. Within this "ozone" budget, R1a is an amplifier in the cycling of odd oxygen between O_z and O_x rather than the main source. These reactions add to the O_y burden, with addition of a primary stratospheric source and photolysis of carbonyl compounds. Although the total magnitude of production and loss of ozone is unchanged using their budget framework, the lifetime of O_y in the troposphere is dramatically increased (from 24 to 73 days), and the role of the stratosphere is significantly enhanced (acting as a source of 26% of the O_y budget as opposed to 9% of the O_x budget).

These new approaches offer a new capability in our ability to understand the ozone budget within models. However, their relative newness and the need to diagnose a large number of chemical fluxes have not resulted in these approaches being adopted by the current generation of model intercomparison exercises. Future efforts may thus allow a better understanding of the model budgets of ozone and why they may disagree with each other.

4. The tropospheric ozone budget

Atmospheric chemistry models are the principal tools available to understand the interplay between the complex sources and sinks of tropospheric ozone described above and hence to understand the response of ozone to changes in these sources and sinks. These models vary greatly in complexity (see Young et al., 2018). Increasingly, models used to study the chemistry of tropospheric ozone include not only the reactions discussed above but also reactions that are important for stratospheric ozone chemistry (Morgenstern et al., 2017). They can be used to diagnose the spatial and temporal dependence of ozone production in the troposphere, how it has evolved over the past, and, in the case of CCMs, how it will continue to evolve into the future (Young et al., 2018).

Models not only simulate the distribution of ozone, they can also be used to diagnose the ozone budget that controls this distribution. The traditional budget discussed above has four terms: (1) photochemical production (*P*), whose major terms are described by the constituent reactions of R1a (the number depending on the model's complexity); (2) photochemical loss (*L*), whose major terms are given by R5, R8, and R9, sometimes including additional minor reactions (e.g., R7, R12b, and several others); (3) deposition of ozone to the Earth's surface (*D*), usually including both dry and wet deposition (which can include loss via clouds); and (4) net transport from the stratosphere (*S*), which is usually calculated as the residual of the ozone budget, assuming it to be in balance ($S = P - L - D$). *S* can also be explicitly calculated, but this method is much less frequently used because it is more computationally expensive, and traditional definitions of the tropopause surface do not allow for an unambiguous measure of transport in complex dynamical situations (see Prather et al., 2011).

The first three ozone budget terms (*P*, *L*, and *D*) are usually calculated in each model grid box and can be globally integrated to give the tropospheric ozone budget. The net photochemical tendency (often found in the literature as net chemical production: $d[O_3]/dt|chem = P - L = NCP$) provides a useful measure of regions that are chemical sources and sinks of ozone. An example of the spatial structure in net chemical production is shown in **Figure 3** for the UKCA CCM under year 2000 conditions (Banerjee et al., 2014).

Figure 3 shows that the most intense net chemical production occurs near the surface over land, with the exception of regions with very high NO_x emissions (e.g., over parts of Western Europe, East Asia, and North America). Ozone destruction is widespread over the tropical oceans, especially over the tropical Pacific. Zonally, the net ozone tendency shows a double peak structure in altitude (Panel B). Within the boundary layer, ozone production dominates, especially in northern midlatitudes. The net ozone tendency decreases with altitude above the boundary layer; in the tropics, photochemical ozone destruction dominates the lower tropospheric signal. The net ozone

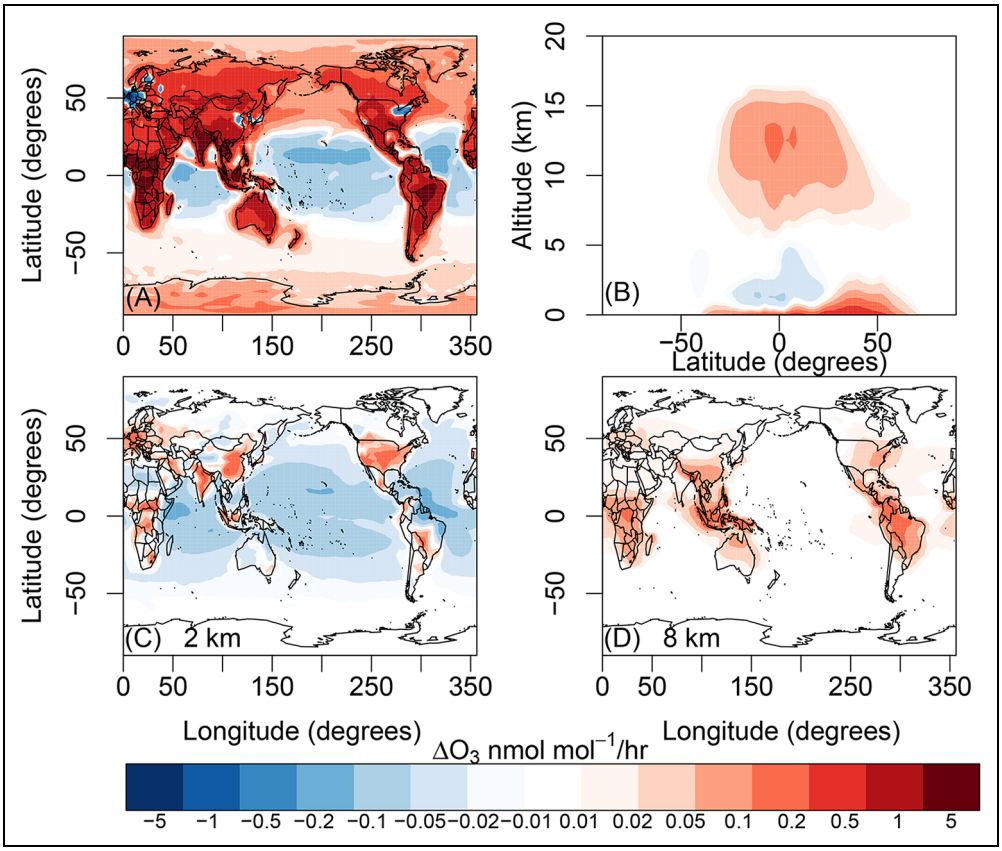

Figure 3. Surface annual mean (Panel A) and zonal mean net chemical production (Panel B) of ozone from the UKCA model for the year 2000 following the Atmospheric Chemistry and Climate Model Intercomparison Project historical scenario (Lamarque et al., 2010). Panels C and D show annual mean net chemical production at 2 and 8 km, respectively. DOI: https://doi.org/10.1525/elementa.2020.034.f3

tendency then has a secondary peak in the tropical upper troposphere, where lightning NO_x emissions have an important role in ozone production (Banerjee et al., 2014). The influence of lightning and deep convection on the net ozone tendency is seen in Panel D, where the regions of high annual mean net chemical production at 8-km altitude correlate with regions of high convective activity and outflow.

The majority of the published literature on the tropospheric ozone budget focuses on single model studies. A meta-analysis of the literature is thus problematic because these studies invariably use specific and unique emissions and meteorological conditions or simulate different periods in time. It could be, in principle, considerably easier to quantify and understand the drivers for change in the tropospheric ozone budget from multimodel studies. *TOAR-Model Performance* summarized the present-day ozone budget from a range of different model assessments published between 2005 and 2012 (ACCENT, ACCMIP, and Fifth Assessment Report [AR5]; see Table 8.1 of Young et al., 2018). These gave an inferred STT (S) of 520 $\pm$ 100 Tg (O_3) yr^{-1} and a surface destruction term (D) of 1,000 $\pm$ 200 Tg (O_3) yr^{-1}. Analysis of multimodel ensembles can prove problematic, however, owing to differences in the level of chemical complexity each model is capable of representing (especially with respect to nonmethane VOCs (NMVOCs); see Young et al., 2013a, 2013b), as well as other pragmatic decisions made by modeling groups that make different model setups incongruent (e.g., whether natural emissions evolve with the climate or not). A further specific challenge for the tropospheric ozone budget is in the development of consistent terms of reference for diagnosing the main budget terms, which appears trivial but still to this day causes consternation due largely to disagreements regarding the suite of reactions to be included in the chemical production (P) and loss (L) terms (Young et al., 2013a, 2013b, 2018). For example, there were several models in ACCMIP that incorrectly include terms like R2 in their diagnosed P, rendering a comprehensive assessment of the models impossible (i.e., only 5 of the 15 models analyzed in Young et al., 2013a, had comparable P and L terms).

4.1. How has our understanding of the tropospheric ozone budget changed over time?

As our understanding of the processes that impact tropospheric ozone has changed with time (e.g., **Figure 1**), so too has the representation of those processes in models. Note that we discuss the change in the ozone budget due to improved knowledge captured through model simulations themselves, not the actual atmospheric trend. Here, we have provided a meta-analysis of the published literature to identify some general features of the changes in model ozone budget terms from the mid-1990s to the

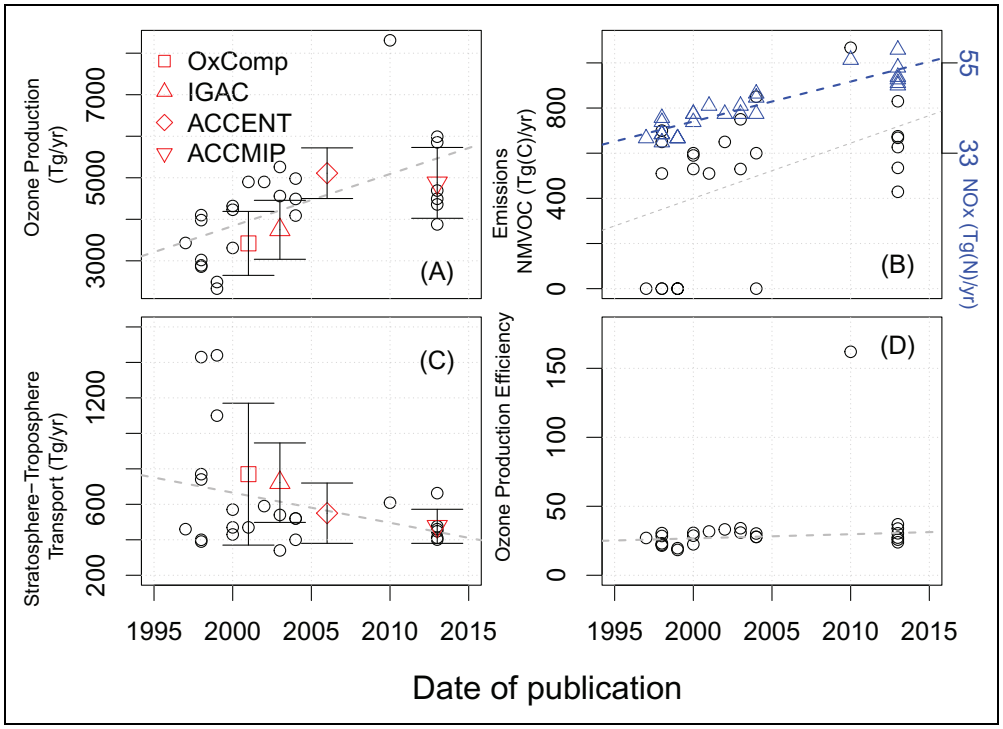

Figure 4. Model simulated (A) production of ozone, (B) emissions of nonmethane volatile organic compounds and NO_x (blue triangles), (C) stratosphere–troposphere transport, and (D) ozone production efficiency (Tg ozone produced/Tg NO_x emitted), all as a function of publication date. Where data exist, multimodel estimates and their uncertainties are indicated. Indicative linear fits through the data are added as dashed lines in each panel, and assessment report means and standard deviations are added to Panels A and C. DOI: https://doi.org/10.1525/elementa.2020.034.f4

present, during which time models have become more sophisticated in their representation of both chemical and physical processes. Hu et al. (2017) recently performed a similar analysis of simulations using the GEOS-Chem CTM. Here, we examine a range of single model studies and multimodel studies. **Figure 4** compares calculations from the ACCMIP and ACCENT projects and earlier studies cited by Stevenson et al. (2006) of (a) gross ozone production (*P*), (b) emissions of NMVOCs and NO_x, (c) STT, and (d) ozone production efficiency (OPE; calculated as *P*/emissions of NO_x). In all cases, these models analyzed the budget terms for the late 1990s to early 2000s facilitating qualitative comparison.

Several trends are evident from the data in **Figure 4.** First, there has been an increase in the model-diagnosed photochemical production of ozone as models have evolved over the last two decades (**Figure 4A**, about 100 Tg per publication year). This in general agrees with the work of Hu et al. (2017) for GEOS-Chem, where the rate of ozone production increased by approximately 80 Tg per publication year. The increase in ozone production (**Figure 4A**) at first glance coincides with an apparent increase in NMVOC emissions with publication year (**Figure 4B**), but in reality, there are two populations of models: those that include NMVOC emissions (which exhibit a large spread, with average values of 600 $\pm$ 200 Tg(C)/yr) and those with zero NMVOC emissions. The models without NMVOC emissions are those focused on stratospheric chemistry, with very simple tropospheric ozone chemistry schemes (i.e., with zero or little NMVOCs). Owing to the high level of scatter, it is not possible to confirm whether the increase in ozone production is linked to increases in NMVOC in the models. More likely, a major contribution to the increase in *P* is the increase in NO_x emissions (**Figure 4B**, blue triangles), which have steadily risen for model studies of the "present day" as emissions inventories have been revised (see Section 6.2 for more on trends and uncertainty in emissions of ozone precursors).

Although the ozone production term in models appears to have increased over time, **Figure 4C** suggests that the STT term has decreased. One explanation for this decrease in modeled STT over the publication period (1998–2013) is the tendency for more recent model studies to include combined stratosphere–troposphere chemistry schemes. These models are more susceptible to errors in large-scale transport of ozone from the stratosphere than earlier CTM-based studies that applied fixed stratospheric ozone boundary conditions (e.g., OxComp and ACCENT). Hu et al. (2017) hypothesized the change in STT may be related to early model simulations being run at coarse resolution and a trend for higher resolution model simulations as time has progressed. This resolution change could affect the parameterized vertical transport, in particular deep convection, resulting in lower ozone in the tropical upper troposphere and hence a lower tropical upwelling flux to compensate for the midlatitudes downwelling flux. Further targeted studies would be required to clarify the exact mechanisms behind this trend.

Figure 4D shows that the OPE, defined as the ratio of the amount of ozone produced to the NO_x emitted, has increased by 1.2 units per publication year, based on a linear fit to these data. This slight increase in OPE with time could, in principle, account for at least part of the increase in *P* over this publication record (**Figure 4A**). One possible cause for the increase in OPE is a redistribution of NO_x emissions; a shift of NO_x emissions to lower latitudes can lead to more efficient ozone production (Zhang et al., 2016b). However, it is not possible to definitively identify the cause of the increase in OPE from these multimodel data. The average OPE over the publication period is 27.8 $\pm$ 4.85. There is one significant outlier: the CRI-STOCHEM model (Utembe et al., 2010), which has an OPE of 161. This OPE is consistent with the fact that the *P* term in CRI-STOCHEM is the highest documented in the literature (*P* = 8,310 Tg/yr). CRI-STOCHEM makes use of the CRI mechanism (Jenkin et al., 2008), which is traceable to the Master Chemical Mechanism (Jenkin et al., 1997) and includes a much more complete description of NMVOC than is used in other models. The high *P* value may reflect greater ozone photochemical production associated with a more complete description of NMVOC chemistry. Interestingly, the ozone burden in CRI-STOCHEM is in broad agreement with other models, as the increased photochemical activity in the model also increases *L*, which counteracts the effects of such a high *P*. It is clear that observational constraints on tropospheric OPE rather than just the ozone burden would be very useful for constraining models. Recent advances in instrumentation may make this possible (Sklaveniti et al., 2018).

Although the ACCMIP and ACCENT intercomparisons have generated a large amount of useful data for the community, a lack of consistent model design makes it difficult to understand how model simulations of the ozone budget have evolved over time. For example, the different sets of precursor emissions used in ACCENT and ACCMIP (and the upcoming Aerosol and Chemistry Model Intercomparison Project [AerChemMIP]) make it difficult to understand what is driving the change in tropospheric ozone from one intercomparison to the next. An outstanding question is how the impacts of changes in chemical mechanisms and rate constants have affected model simulations of the ozone budget. Newsome and Evans (2017) showed that uncertainty in the inorganic rate constants leads to a notable uncertainty in the calculated composition of the atmosphere. Within the GEOS-Chem model, they showed approximately 10% uncertainties in the present-day ozone burden and 16% uncertainties in the present-day global mean OH due to uncertainties in the inorganic rate constants alone, with even larger changes in tropospheric ozone radiative forcing (16% uncertainties). These uncertainties are comparable to the intermodel variability for these parameters. Hu et al. (2017) have been able to quantify some of this using the GEOS-Chem model and have shown, for example, that changing the representation of isoprene chemistry, in particular a decreased role of isoprene nitrates as sink for NO_x, had a significant effect on tropospheric ozone production rates (increasing *P* and *L* by approximately 12%). Moreover, although model analysis of the ozone budget provides a means of understanding what drives changes in tropospheric ozone, there are no available observations with which to constrain these model calculations, with the exception of the global ozone burden and to some extent STT. It is currently impossible to say that a model that simulates a *P* of 3,000 Tg/yr is wrong and one that simulates 7,000 Tg/yr is correct. However, with recent aircraft campaigns that are designed to survey the global composition of reactive gases, such as the NASA Atmospheric Tomography mission (ATom; Prather et al., 2017) and NERC North Atlantic Climate System: Integrated Study (Sutton et al., 2018) campaigns, there may be additional constraints on the budget in the future.

4.2. Modeled trends in the ozone burden: 1850–2016

The preindustrial (defined here as the period ca. 1850 CE) burden and distribution of ozone remains highly uncertain despite recent advances in measuring potential ozone proxies in ice cores (Yeung et al., 2019). Ozone concentrations in the 19th century are virtually unknown as reliable rural observations can only be traced back as far as 1896, as assessed by *TOAR-Observations* (Tarasick et al., 2019b). Tarasick et al. (2019b) could only conclude that surface ozone in the northern extra-tropics increased by 30%–70% from the mid-20th century to the present day (1990–2014), but with large uncertainty and drawing largely on historical data from Europe. With respect to free tropospheric ozone, there are even fewer independent historical observations from balloons and aircraft, but these indicate similar changes to those near the surface (Tarasick et al., 2019b), albeit again limited to the northern midlatitudes. However, estimates of the preindustrial ozone burden can range widely among models due to uncertainties associated with fossil fuel emissions, biomass burning emissions (Rowlinson et al., 2020), and global halogen chemistry due to different feedbacks between ambient ozone concentrations and oceanic halogen emissions during preindustrial times (Sherwen et al., 2017a; see also the discussion of this topic in Section 5.3).

At present, model simulations remain our best tools for quantifying changes in the ozone burden since the preindustrial (Stevenson et al., 2013; Young et al., 2013a; Griffiths et al., 2020). Modeled trends are for the entire global tropospheric ozone burden, while the historical observations are heavily weighted toward the surface and northern midlatitudes.

Figure 5 shows the trends in the burden of tropospheric ozone as simulated by a subset of models that took part in the ACCMIP project (Young et al., 2013a) in support of the AR5 of the United Nations Intergovernmental Panel on Climate Change (IPCC, 2013; Myhre et al., 2013), as well as from a subset of models that participated in the Chemistry Climate Model Initiative (CCMI; Morgenstern et al., 2017). In addition, **Figure 5** shows satellite estimates of the tropospheric ozone burden from *TOAR-Climate* (Gaudel et al., 2018). For the models, we define the tropopause using the 125 nmol/mol ozone isopleth determined from monthly mean output; the satellite data are tropospheric columns, with the tropopause

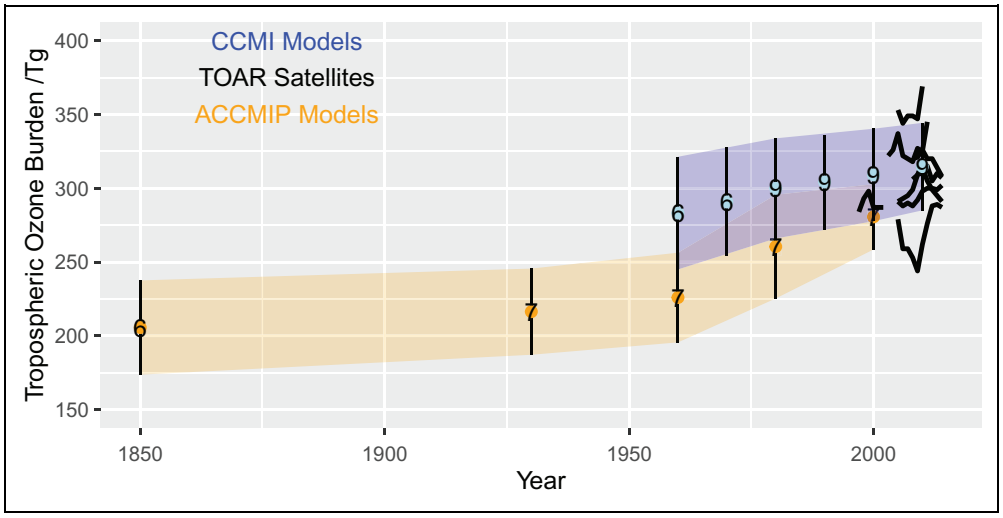

Figure 5. Comparison of modeled (orange and blue envelopes) and satellite-observed (gray envelope) trends in the tropospheric ozone burden between 60°N and 60°S. Means of the model data are shown as circles with the vertical lines reflecting ± 1 standard deviation of the mean. The number of models used in calculating the means are displayed in the circles. TOAR Satellites refers to the range of satellite tropospheric ozone burden estimates presented in *TOAR-Climate*. DOI: https://doi.org/10.1525/elementa.2020.034.f5

levels described by Gaudel et al. (2018). Previous analyses have often used a 150 nmol/mol ozonopause (Stevenson et al., 2006; Young et al., 2013a); however, as discussed in detail in Prather et al. (2011), the global tropospheric ozone burden is sensitive to this definition, and we have opted for a lower definition (125 vs. 150 nmol/mol) that results in a smaller burden and less stratospheric influence. We direct the reader to Prather et al. (2011) for a more complete discussion on the impacts of tropopause definition on the ozone budget, but note here that these can be significant. We also note that the TOAR satellite products shown in **Figure 5** use a range of different estimates of the tropopause, with the majority of them using lapse-rate–based tropopauses based on meterological reanalyses. As the ACCMIP models only provided output as decadal average values, the annually varying CCMI data have been averaged over each decade. We limit the analysis to the latitude range 60°S–60°N, where the satellite measurements are densest. This geographically limited focus results in a difference between the calculations of the ozone burden presented here from those discussed by Young et al. (2013a, 2013b) for the ACCMIP models but enables a more robust comparison of the model and satellite data.

Stevenson et al. (2013) show that the ACCMIP models generally perform reasonably well against a very limited set of preindustrial near surface ozone observations. Young et al. (2013a, 2018) and Revell et al. (2018) show that the ACCMIP and CCMI models also perform well against recent satellite estimates of the tropospheric ozone column (within $\pm$ 30%).

The model simulations summarized in **Figure 5** highlight several key points. First, the tropospheric ozone burden has increased considerably over the historic period. The models indicate that there has been an approximately 30% growth in the burden of ozone over the period 1850–2010, consistent with isotopic constraints using heavy oxygen (^{18}O) from ice cores (Yeung et al., 2019). Simulated increases in the tropospheric ozone burden since the mid-20th century are consistent with that observed at the surface, as assessed by *TOAR-Observations* (Tarasick et al., 2019b). Second, although there is an agreement in the growth of the ozone burden, there is a significant spread in model simulations. However, this spread decreases over the simulation period. For example, the spread in the ACCMIP models, measured as the multimodel standard deviation divided by the multimodel mean, decreases from 15% in 1850 to 7% in 2000. Similarly, for the CCMI models, the model spread decreases from 13% in 1960 to 9% in 2010. The cause of these features is currently unresolved. Finally, in spite of the large spread in the multimodel simulations, both model ensembles lie within the range of satellite estimates of the tropospheric ozone burden, as reviewed by Gaudel et al. (2018).

The overlap between the two model intercomparisons (ACCMIP and CCMI) with each other, and with the TOAR satellite-observations, is promising and highlights a good degree of understanding and capability in simulating the burden of tropospheric ozone. **Figure 5** shows that the variability in the CCMI models is larger than the variability in the ACCMIP models. This could be a function of more models being included in the averages (see the numbers in the circles in **Figure 5**), but importantly, the model spread lies within the spread of the satellite observations, although we note that this is also quite large (21–107 Tg). We can also note that over the period 1960–2000, the ACCMIP models show a stronger increase in the tropospheric ozone burden than the CCMI models (**Figure 5**).

Understanding the causes for the differences in the growth of the ozone burden over this period is an outstanding challenge and would require systematic studies to isolate the key drivers. As Young et al. (2018) highlight,

there is need for urgent progress in this area. One consideration, as discussed in general terms in Section 4.1, is the impact of changes in the models themselves; it is possible that models underwent significant process improvements between ACCMIP and CCMI, particularly with respect to the number of models that simulate both stratospheric and tropospheric ozone (Morgenstern et al., 2017). What is certain is that the emissions and boundary conditions used in the ACCMIP and CCMI studies are different (Young et al., 2013a; Morgenstern et al., 2017).

Young et al. (2018) discuss the history of model intercomparison projects (MIPs) and highlight that CCMI coordinated the largest scale chemistry-climate modeling ozone intercomparison to study the transient evolution of ozone from 1960 through to 2100 (Morgenstern et al., 2017). The CCMI simulations allow us to investigate how well the models agree on the timing of trends in the ozone burden. **Figure 6** displays time-series plots of the relative change in the tropospheric ozone burden for a subset of the CCMI models. Each panel in **Figure 6** shows an individual simulation with its details (model name, experiment, etc.) included in the caption. There were three core types of experiments in the CCMI experimental design: refC1, refC2, and refC1SD. **Figure 6** focuses on the refC1 and refC2 simulations, which differ with respect to the time period of the simulations (refC2 covers 1960–2100, whereas refC1 covers 1960–2010) and the forcings used (refC1 uses observed historic sea-surface temperature fields, whereas refC2 uses modeled sea-surface fields either in a fully coupled sense or from a separate climate model run). The ozone burdens displayed in **Figure 6** have been normalized to the maximum value for each simulation in the time series; this normalization is necessary as there are large absolute differences between models (approximately 80 Tg), whereas the trends over the period are much smaller (approximately 50 Tg). For the EMAC family of models, there are not only differences in the simulations analyzed (refC1 and refC2) but also the physical model used. For example, the vertical resolution was different between versions (47 vs. 90 vertical levels) and the EMAC-L47MA_revC2_r2i1p1 was simulated including an interactive deep ocean model. See Jöckel et al. (2016) for more details.

Figure 6 highlights that the CCMI models analyzed generally all show increasing burdens of ozone over the period 1960–2010 but that there is a significant amount of spread across the simulations. Broadly speaking, most models tend to agree that the tropospheric ozone burden reached a plateau around 1990–2000 and did not change significantly over the following decade. **Figure 6** also highlights that although there is spread between simulations from a specific model (i.e., the rows), this is much smaller than the spread between simulations from different models (i.e., the columns; see Section 4.3 for more on this).

Table 1 shows how the decadal average net chemical tendency (P–L or $d[O_3]/dt_{|chem}$) has changed in a subset of the CCMI models for which these data are available. This quantity diagnoses the net change in the ozone burden as a result of chemical processes only. $d[O_3]/dt_{|chem}$ is analogous to P–L, but differences can arise in the upper troposphere, where traditional diagnosis of P omits the photolysis of O_2 (see Section 3), which can become important in this region (Prather, 2009). As $d[O_3]/dt_{|chem}$ is not tied to accounting for specific reactions, this tends to give a cleaner and "pure" account of the tendency of ozone due to chemical processes. In many respects, the CCMI simulations mirror the results from the ACCMIP models (Young et al., 2013a). First, **Table 1** in this study and **Table 2** of Young et al. (2013) both emphasize that, in general, fewer models provide data associated with diagnosing drivers for change in the tropospheric ozone budget than provide data on the ozone burden itself. **Table 1** highlights that as with the individual budget terms themselves, there is large spread in the absolute magnitude of the net chemical tendency of tropospheric ozone as simulated in the models. EMAC-L90MA and CMAM have very large and very weak photochemical production of ozone, respectively (not surprising given the extremely simple tropospheric chemistry in CMAM), while CESM1-CAM4Chem and GEOSCCM fall between the two extremes. However, when comparing the relative trend in the net chemical tendency in tropospheric ozone, it becomes apparent that there is a very high level of agreement between the models. The relative trends in net chemical production over time are plotted for the CCMI models in **Table 1 Figure 7. Figure 7** shows that the relative trend in net chemical production peaked in the 1990s and has leveled off since then, that is, on average, the troposphere has provided less of a chemical source of ozone since the 1990s. This result is generally consistent with the trend in the major precursor emissions. **Figure 8B** shows that emissions of NO_x rose only slightly over the period 1990–2010 at the global scale. There is consistency therefore between **Figures 5** and **7**, which emphasizes that the growth in the burden of ozone in the CCMI models was very small over the period 1960–2010, particularly over the period 1990–2010, where **Figure 6** shows that for most models, the tropospheric ozone burden has plateaued and that this muted trend in the ozone burden in a large part may be attributed to a decrease in the rate of net production of ozone in the troposphere (**Figure 7**).

To further understand the changes in the modeled net chemical production, **Figure 9** shows a latitudinal breakdown of the data in **Table 1. Figure 9** highlights that the picture at the global scale of a gradual decline in net production of tropospheric ozone since the 1990s (**Figure 7**) is masked by opposing trends at the hemispheric scale. In fact, there are some complex changes occurring in the tropospheric net chemical production that appear to be associated with the redistribution of global emissions (**Figure 8**). Normalized to the 1960s, the SH (**Figure 9A** and **B**) shows much smaller trends in $d[O_3]/dt_{|chem}$ than the NH, where the trends are roughly doubled (note different y-axes for the two hemispheres). The general feature of **Figure 9** is that there was global growth in $d[O_3]/dt_{|chem}$ from 1960 to 1990, but since 1990, two opposing trends are apparent: (1) At high latitudes, there has been a decrease in NCP of ozone, and (2)

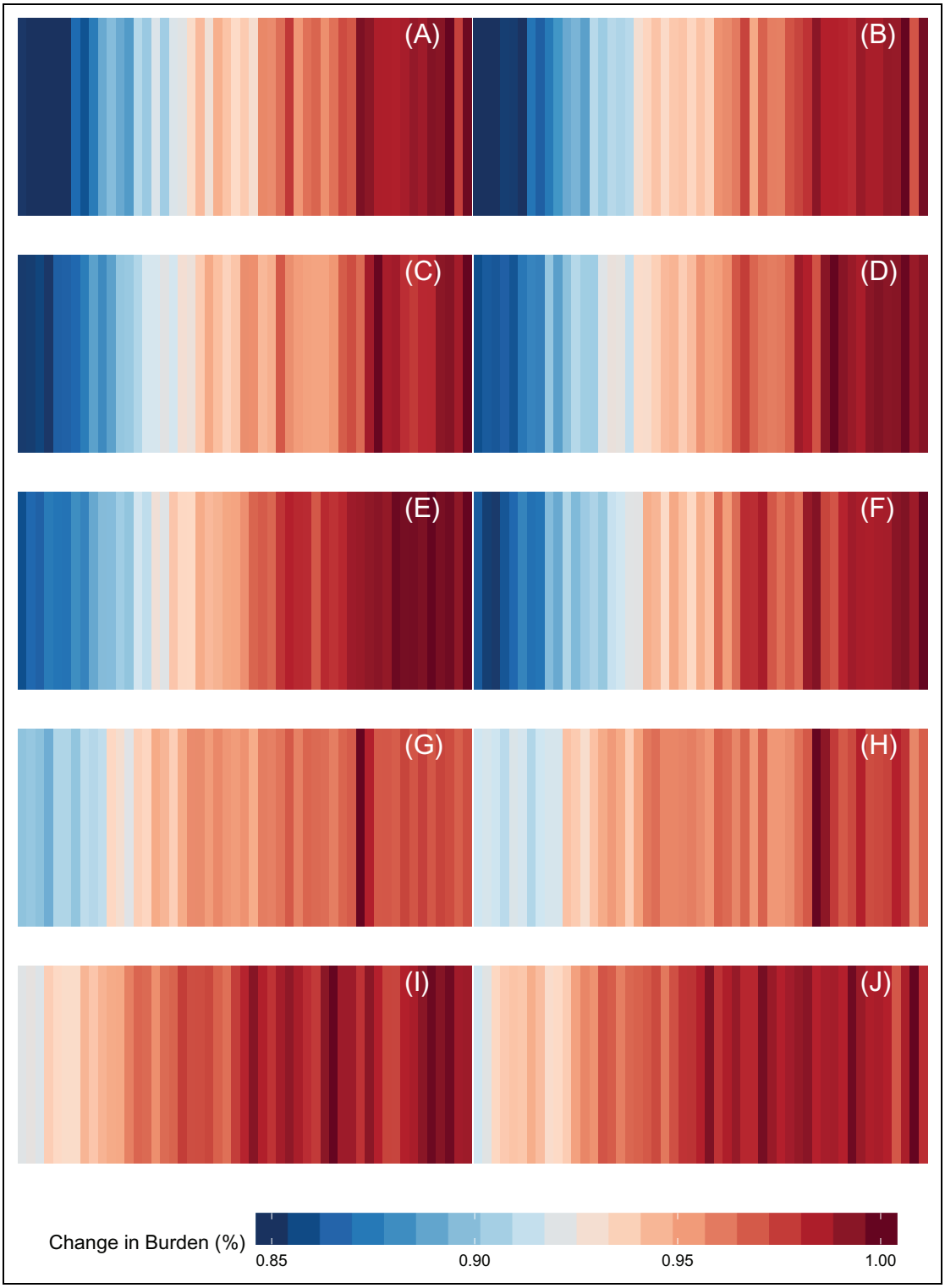

Figure 6. Changes in the tropospheric ozone burden from 1960 to 2010 relative to the maximum simulated burden over the five decades in a subset of the Chemistry Climate Model Initiative models. Each year is plotted as a horizontal colored bar, which represents the fraction of the maximum burden of tropospheric ozone over the time series. Increases in color from blue to red denote increases in the burden. Individual model simulations are displayed in each panel. Panels A–F highlight models with significant changes in the burden over the time period of focus. (A) CESM1-CAM4Chem_refC1_r1i1p1. (B) CESM1-CAM4Chem_refC1_r2i1p1. (C) CMAM_refC1_r1i1p1. (D) CMAM_refC1_r2i1p1. (E) EMAC-L47MA_refC2_r2i1p1. (F) EMAC-L90MA_refC1_r1i1p1. (G) NIWA-UKCA_refC1_r1i1p1. (H) NIWA-UKCA_refC1_r2i1p1. (I) NIWA-UKCA_refC2_r1i1p1. (J) NIWA-UKCA_refC2_r2i1p1. Styled on the Climate Warming stripes (https://showyourstripes.info/). See the Supplement for more details. DOI: https://doi.org/10.1525/elementa.2020.034.f6

Table 1. Comparison of net chemical production of ozone ($\Delta[O_3]/\Delta t$] computed by a subset of the Chemistry Climate Model Initiative models analyzed in **Figures 5** and **6**. DOI: https://doi.org/10.1525/elementa.2020.034.t1

Model	1960	1970	1980	1990	2000	2010
CESM1-CAM4Chem	273 (±39)	337 (±44)	405 (±33)	442 (±36)	411 (±32)	396
CMAM	52 (±15)	102 (±28)	142 (±26)	188 (±24)	185 (±15)	174
EMAC-L90MA	495 (±36)	568 (±38)	642 (±25)	683 (±26)	658 (±18)	663 (±18)
GEOSCCM	257 (±24)	309 (±21)	373 (±16)	399 (±23)	370	NA

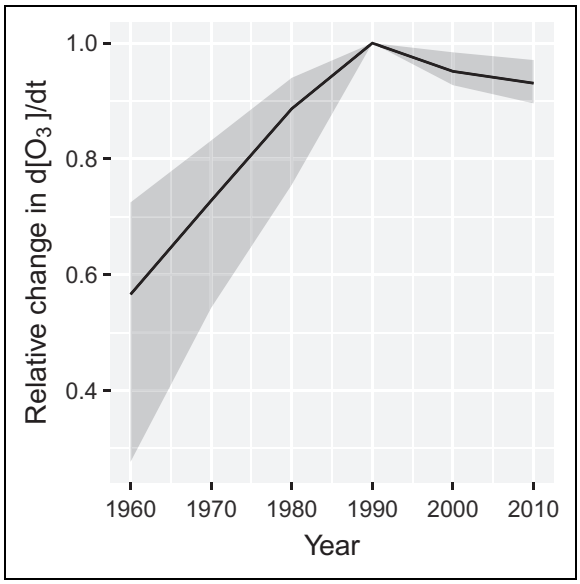

Figure 7. Multimodel estimates (based on **Table 1**) of the relative changes (fractional) in the net chemical production of ozone in the troposphere as a function of time. The black solid lines show the multimodel mean and the gray envelope the range of the model calculations. DOI: https://doi.org/10.1525/elementa.2020.034.f7

in the tropics, there has been a strong increase in NCP of ozone, especially in the northern tropics (**Figure 9C**). However, with such a small number of models, and without good observational constraints on $d[O_3]/dt_{|chem}$, it is hard to be definitive with respect to these trends, but nonetheless, these data suggest the need for some further targeted studies to identify and quantify the drivers of these trends and to understand how they will affect the future tropospheric ozone burden. To a first order, the main drivers seem partly linked to the variability in emissions of NO_x, as was highlighted in several previous studies (i.e., Parrish et al., 2014), but as **Figure 8** reflects, there is uncertainty in our understanding of these changes.

4.3. Can we project trends in the tropospheric ozone burden with confidence?

There is robust information suggesting that models have some skill in simulating the burden of ozone in the troposphere (Young et al., 2013a, 2018; Griffiths et al., 2020), and the results presented above further add to this. But do we have confidence in predicting trends in the evolution of tropospheric ozone into the future? Although we have the ability to diagnose some of the drivers for changes in tropospheric ozone, particularly the role of chemical production, we cannot presently constrain all of these drivers. Furthermore, the expected changes in the global tropospheric ozone burden over the next few decades are small and will be difficult to detect given the current observing system (Young et al., 2013a, 2018; Griffiths et al., 2020). Even the ACCMIP Representative Concentration Pathway 8.5 scenario (RCP8.5; van Vuuren et al., 2011), which had the largest projected increases in ozone precursor emissions of any of the representative concentration pathways, led to a predicted increase in global ozone of only 8% from 2000 to 2030 (Young et al., 2013a). Given the results from *TOAR-Climate* showing large spatial heterogeneity in measured surface and airborne ozone trends over the past 15 years, the tendency for trends in a given location to be strongly influenced by meteorological variability (e.g., Bloomer et al., 2009; Lin et al., 2014; Strode et al., 2015), and the large differences in satellite measurements of ozone (Gaudel et al., 2018), it is likely that observational records longer than 30 years are required to robustly test modeled ozone trends (e.g., Barnes et al., 2016; Brown-Steiner et al., 2018).

To examine the systematic uncertainties that affect our ability to make confident predictions of the future evolution of tropospheric ozone, we have analyzed tropospheric column ozone from a subset of six transient CMIP5 model simulations (Myhre et al., 2013) for three scenarios (RCP2.6, RC4.5, and RCP8.5), relying on the models that included interactive chemistry (the "CHEM" models described by Eyring et al., 2013). **Figure 10** shows the future evolution of the tropospheric ozone column (in Dobson Units; left-hand panels) and the fractional variance in the response of the tropospheric column due to internal variability (i.e., short timescale fluctuations driven by natural climatic variability), scenario variability (i.e., driven by the different assumptions about emissions), and intrinsic model differences (right-hand panels), following Hawkins and Sutton (2009).

Mirroring the CCMI global burden results (**Figure 5**), **Figure 10A** highlights a very modest degree of uncertainty arising from interannual variability at the global scale. A much larger uncertainty comes from the models themselves and, given that there are only three independent models, is likely underestimated compared to using a larger ensemble (e.g., if transient data were available from ACCMIP or ACCENT). The model variability is shown to be the leading source of uncertainty in near-term

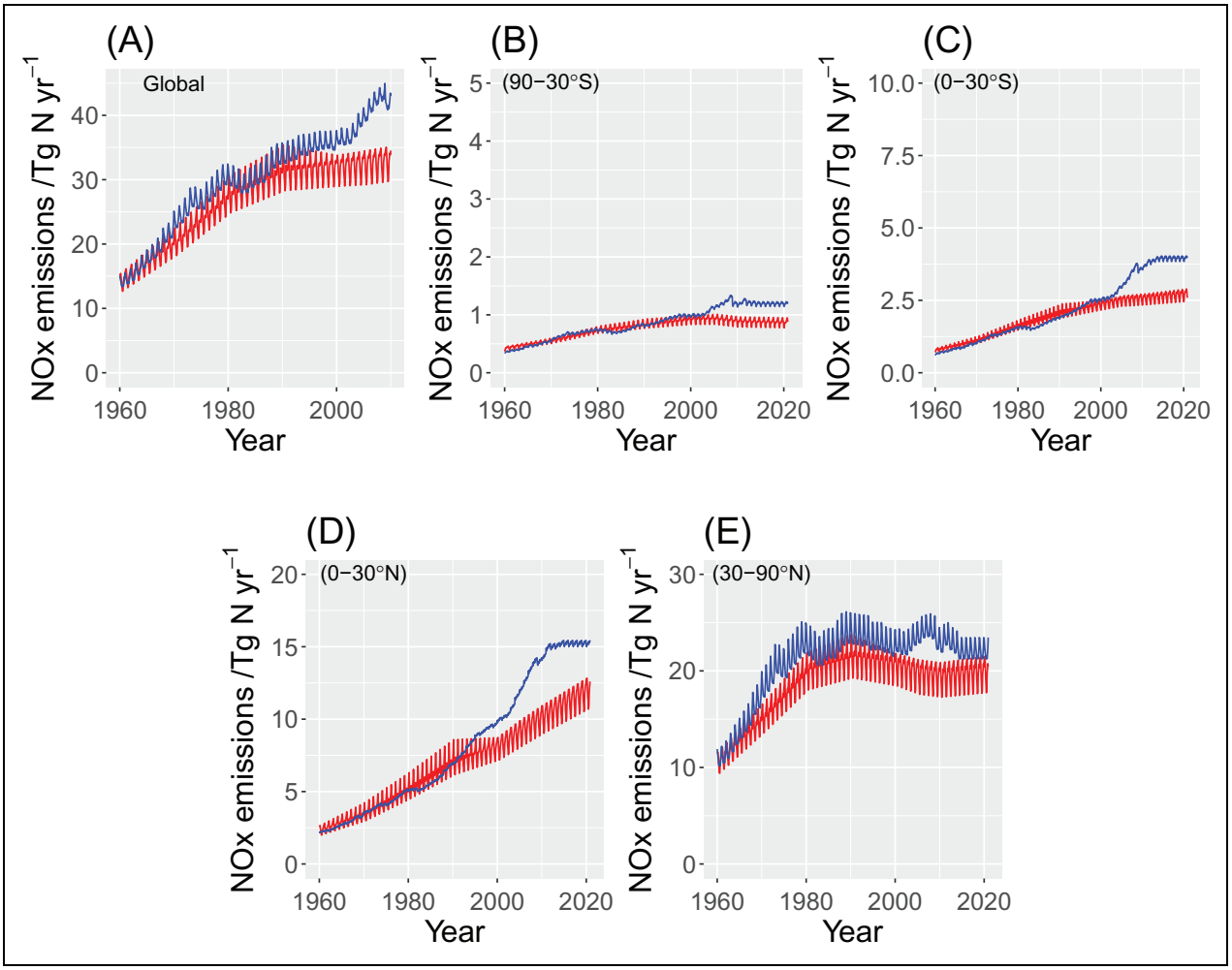

Figure 8. Anthropogenic (land based) NO_x emissions (blue) from the bottom-up Community Emissions Database System inventory (Hoesly et al., 2018) for the period 1960–2010 and (red) from the MACCity implementation of the CMIP5 emissions inventory of Lamarque et al. (2010) through 2000 and the RCP8.5 scenario thereafter (as used in the Chemistry Climate Model Initiative simulations; Granier et al., 2011). Panels B–D show the same latitude regions as analyzed in **Figure 9.** DOI: https://doi.org/10.1525/elementa.2020.034.f8

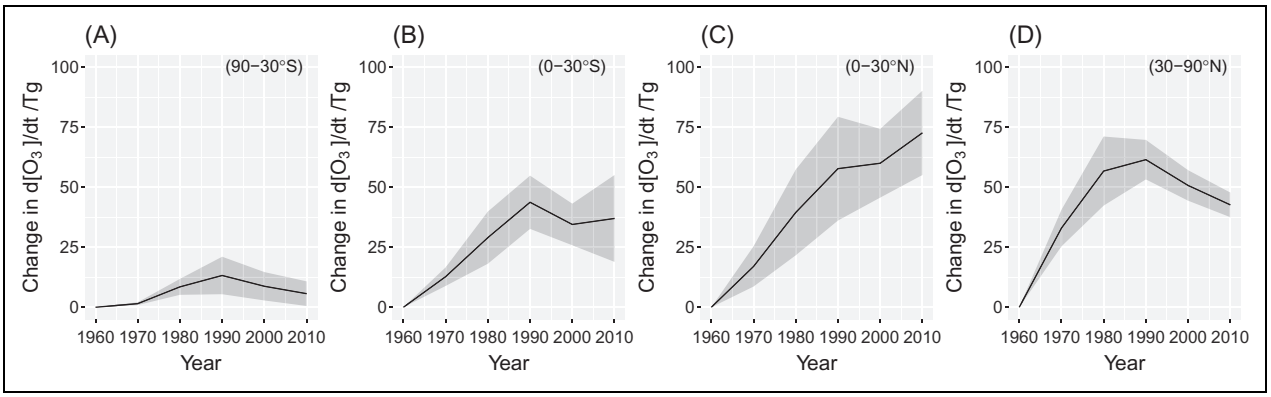

Figure 9. Changes in the decadal average ozone chemical tendency in the troposphere from 1960 to 2010 relative to the 1960 levels, as simulated by a subset of the Chemistry Climate Model Initiative models (see **Table 1** for details). In all panels, the dark line shows the multimodel mean change in ozone tendency and the colored envelope the standard deviation around the multimodel mean. Panel A shows the relative change in the Southern Hemisphere (SH) extratropics (–90° to –30°), Panel B the SH tropics (–30° to 0°), Panel C the Northern Hemisphere (NH) tropics (0° to 30°), and Panel D the NH extratropics (30° to 90°). Note the NH and SH data are on different *y*-axis scales. DOI: https://doi.org/10.1525/elementa.2020.034.f9

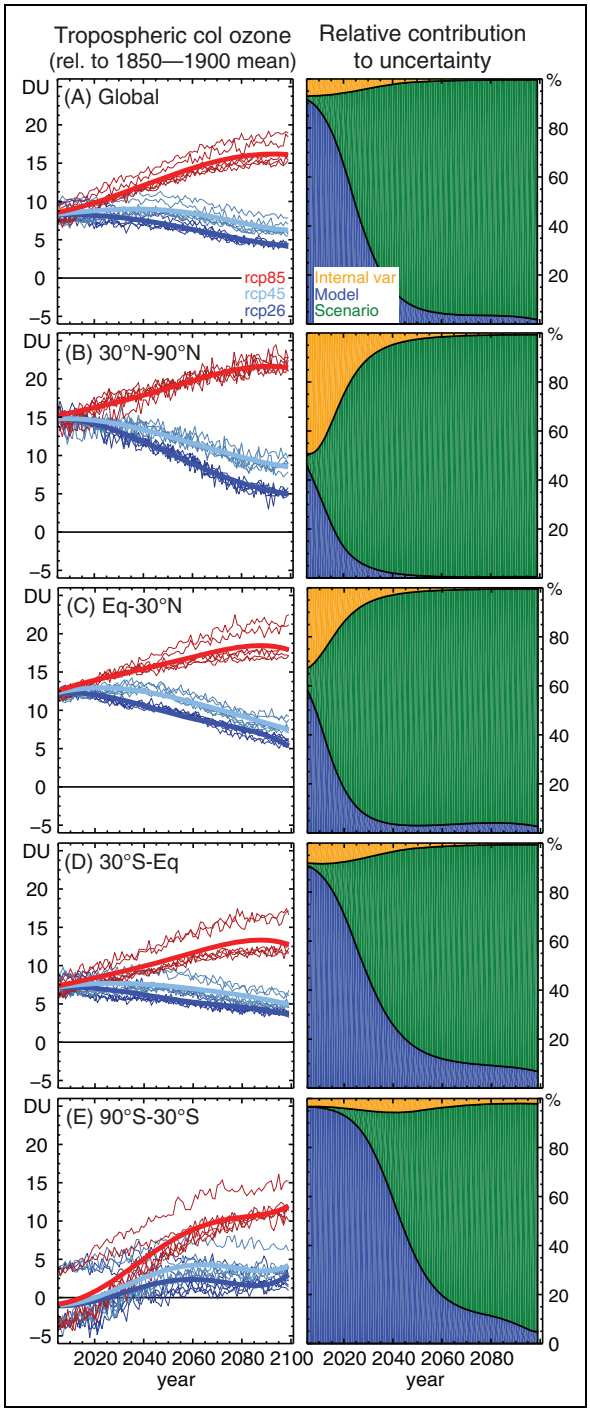

Figure 10. Projected changes in tropospheric column ozone and their uncertainties in CMIP5 models over the 21st century. The left-hand panels show the change in the modeled ozone column, and the right-hand panels show the relative contribution to the uncertainty (variance) in the change in ozone (decomposed into three components). Panel A shows the global change, and Panels B–E show regional changes. The six models (CESM1-WACCM, GFDL-CM3, GISS-E2-H-p2, GISS-E2-H-p3, GISS-E2-R-p2, and GISS-E2-R-p3) represent only three independent modeling centers (NCAR, NOAA GFDL, and NASA GISS), but these are the only models that provided output for more than two scenarios. DOI: https://doi.org/10.1525/elementa.2020.034.f10

(2000–2030) projections of ozone (right-hand side, FIgure 10A), but beyond that time, the largest source of variability comes from which of the three emissions scenarios is followed (i.e., emission scenario uncertainty). Trivially, this term dominates due to the diverging nature of RCP8.5 compared to the other RCPs. For RCP8.5, the increases in ozone are driven by the projected near doubling of methane concentrations relative to the year 2000, with some contribution from an enhanced net stratospheric source (Banerjee et al., 2016). For the RCP2.6 and RCP4.5, precursor emissions reductions drive the long-term decreases.

With respect to near-term projections, even at the global mean scale, the model diversity alone is high enough to prevent us from distinguishing between ozone concentrations produced under the RCP8.5, RCP 4.5, and RCP2.6 emission scenarios during the period 2000–2015, for which we have a plethora of surface, aircraft, and satellite observations. As shown in **Figure 10**, ozone predicted by RCP8.5 is not distinct from the other scenarios until after 2020. Based on this limited set of models and three illustrative scenarios, at least another 5 years of observations is needed before a robust comparison between trends simulated in models and retrieved from observations can be made.

We recognize the shortcomings in this analysis, and a more robust approach will require a larger number of ensemble members from a large number of independent models, spanning a wide range of process complexity to more accurately quantify the role of structural uncertainty in projecting future ozone changes. Furthermore, including additional scenarios that more comprehensively span the range of possible futures, or taking a selective approach to which scenarios are used, would enable a better quantification of the relative role of scenario uncertainty.

5. Challenges to modeling the budget and burden of ozone: Chemical processes

Although model simulations are vital for projecting changes in the ozone budget, they remain incomplete and not without error. **Figure 10** highlights that the intrinsic differences between models (the blue area) is a large source of uncertainty in near-term (the next two to three decades) future projections of the burden of tropospheric ozone. As described in Section 8.2 of *TOAR-Model Performance*, one of the main sources of uncertainty in global models is their limited representation of tropospheric chemistry (Young et al., 2018). Here, we review recent studies describing a range of chemical processes that are believed to be important for tropospheric ozone and are, to date, not included in the types of models we have reviewed in Section 4.

5.1. Nitryl chloride photolysis

The importance of nitryl chloride ($ClNO_2$) for the simulation of ozone formation has only recently been recognized. $ClNO_2$ is formed from the reaction of dinitrogen pentoxide (N_2O_5) with chloride-containing aerosol at night. $ClNO_2$ is an important nocturnal reservoir for NO_x and atomic Cl, particularly in polluted coastal environments. Photolysis of $ClNO_2$ in the early morning

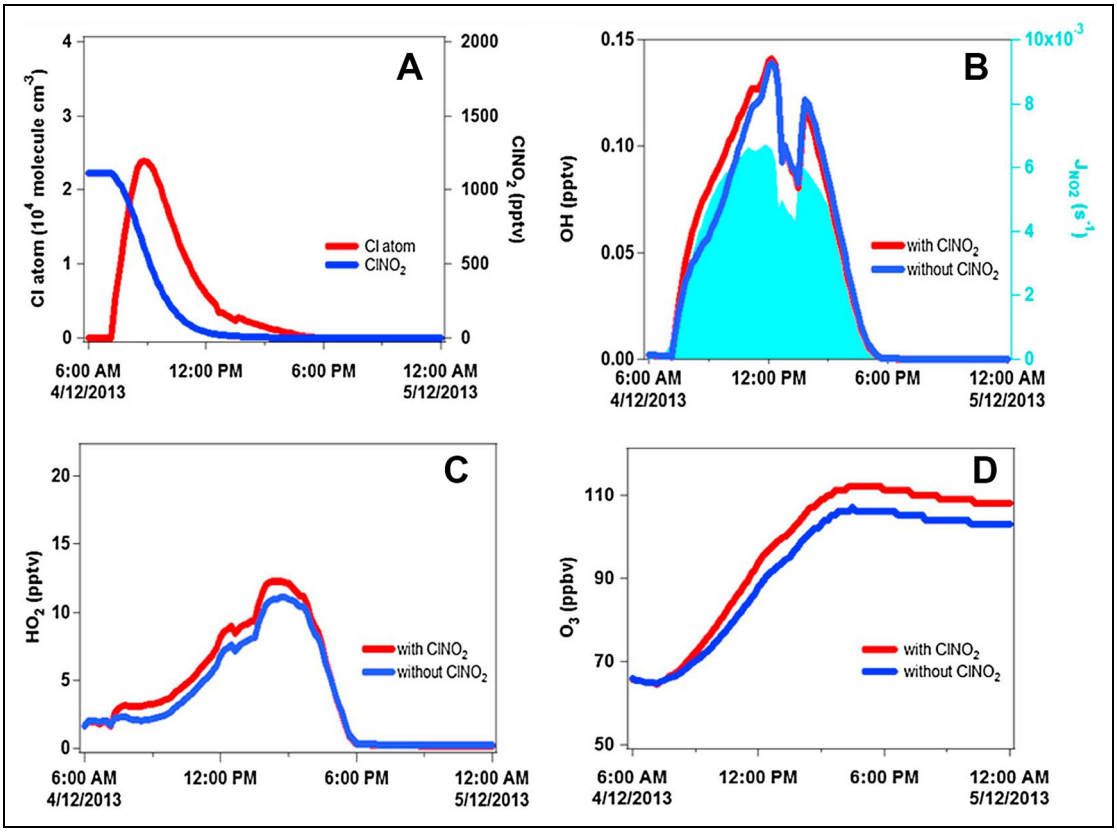

Figure 11. Model-simulated concentrations/mixing ratios of (a) $ClNO_2$ and Cl, (b) OH, (c) HO_2, and (d) ozone during the day following plume sampling from the Mt. Tai Mao Shan site (957 m a.s.l) in Hong Kong, with and without the inclusion of $ClNO_2$ chemistry. The measured photolysis rate constant of NO_2 is shown by the light blue shading. The model was initiated with the measured concentrations of $ClNO_2$ and other relevant chemical constituents at 06:00. Adapted from Wang et al. (2016). DOI: https://doi.org/10.1525/elementa.2020.034.f11

regenerates NO_2 and atomic Cl, which affects oxidant photochemistry and enhances photochemical ozone production, especially in polluted environments where the concentrations of N_2O_5 precursors (nitrogen oxide radicals and ozone) are high (Osthoff et al., 2008; Sarwar et al., 2012). In environments where $ClNO_2$ yields are appreciable, overnight conversion of NO_x to $HONO_2$ (i.e., permanent NO_x loss) would be considerably reduced, leaving more NO_x available for ozone formation the next day. In addition, the reactive chlorine atoms from $ClNO_2$ photolysis can significantly enhance VOC oxidation rates—particularly in VOC-rich areas such as Houston—in the early morning when other common oxidants (e.g., NO_3, OH) are scarce (Osthoff et al., 2008; Mielke et al., 2011).

(R13) $HCl + N_2O_5$ (het)$\rightarrow ClNO_2(g) + HONO_2(aq)$
(R14) $ClNO_2 + h\nu \rightarrow Cl + NO_2$

Recent studies (e.g., Riedel et al., 2012, 2014; Wang et al., 2016) have found that photolysis of $ClNO_2$ increases boundary layer mixing ratios of ozone by 7%–30% (e.g., Riedel et al., 2014).

At a mountain-top (957 m a.s.l) site in Southern China, $ClNO_2$ mixing ratios as high as 4.7 nmol/mol were observed in December 2013 (Wang et al., 2016), suggesting strong production of this compound in highly polluted regions. Wang et al. (2016) estimate that such large amounts of $ClNO_2$ were responsible for up to 40% of daytime production of ozone in the upper boundary layer (**Figure 11**). More effort is required to integrate this process-based understanding of this chemistry into regional and global CCMs.

5.2. HONO photolysis

Nitrous acid (HONO) was first recognized as a morning source of OH radical by Perner and Platt (1979). Recent field studies have found much higher daytime HONO concentrations than those calculated based on the gas-phase reaction of NO + OH in both urban and rural areas, implying a missing source or sources of HONO and thus of OH during daytime (Kleffmann et al., 2005; Elshorbany et al., 2009; Wong et al., 2013; Li et al., 2014b). Kleffmann et al. (2005) showed that HONO measured above a forest canopy close to the Jülich Research Center, Germany, was on average a factor of 10 larger than model predictions.

The search for the source of the "missing" HONO has taken place across the globe, with observations pointing to a pervasive source of HONO that does not appear to be limited to specific geographical regions or times of year. Possible additional sources of daytime HONO include heterogeneous formation on humid surfaces

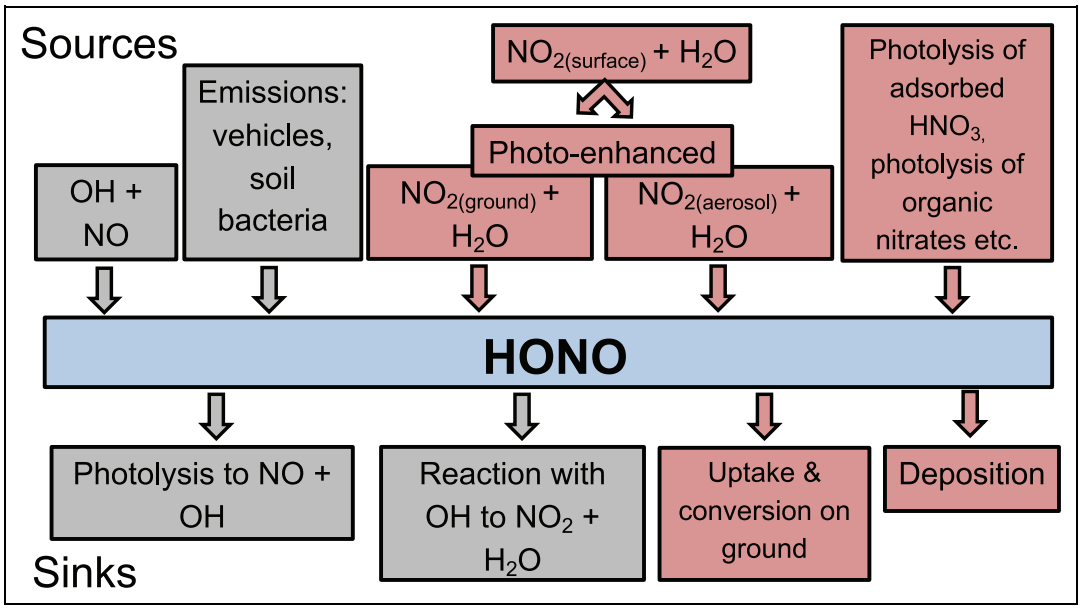

Figure 12. Diagram of major HONO sources and sinks in the troposphere. Boxes in gray represent the traditionally understood sources and sinks, and boxes in red show more recently established processes (see text for references). DOI: https://doi.org/10.1525/elementa.2020.034.f12

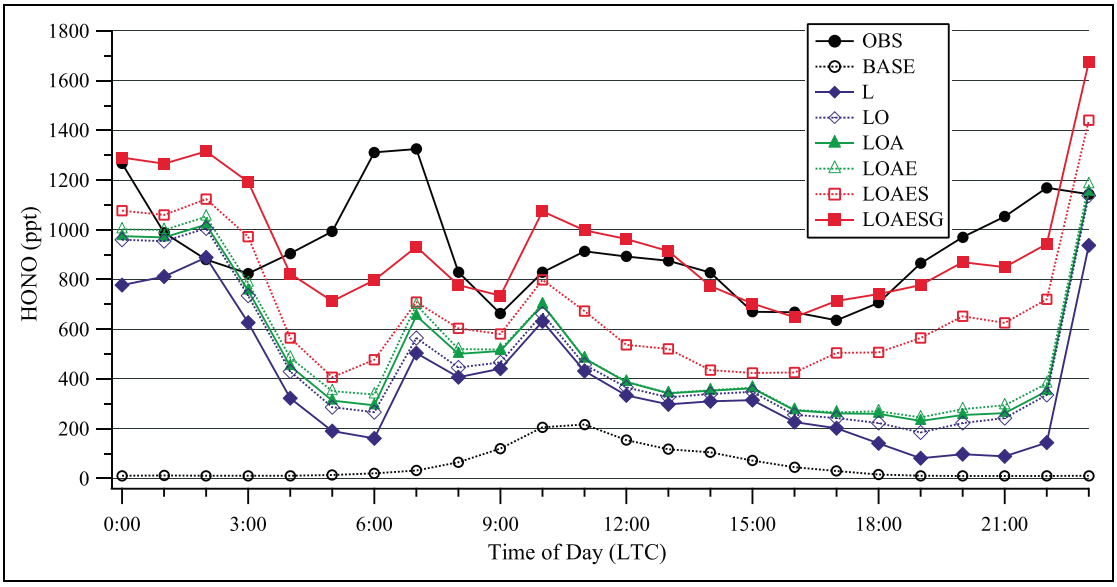

Figure 13. Observed and simulated average diurnal concentration of HONO at Tung Chung, Hong Kong, during the polluted period (August 25–31, 2011). OBS = observed values; BASE = only consider HO + NO; L = heterogeneous source from land surfaces; LO = heterogeneous source from land and ocean surfaces; LOA = heterogeneous source from land, ocean, and aerosol surfaces; LOAE = heterogeneous source from land, ocean, and aerosol surfaces plus traffic emission; LOAES = LOAE plus soil emission; LOAESG = LOAES plus additional gas-phase reactions. Adapted from Zhang et al. (2016a). DOI: https://doi.org/10.1525/elementa.2020.034.f13

(Kleffmann, 2007), traffic emissions (Kurtenbach et al., 2001), gas-phase photolysis of potential precursors such as nitro-aromatic compounds (Bejan et al., 2006; Kleffmann, 2007), and biological sources in soils (Su et al., 2011; Maljanen et al., 2013; Oswald et al., 2013). The presently known sources and sinks of HONO are summarized in **Figure 12.** The search for the missing daytime sources is still an active area of research.

Models that consider only the gas phase homogenous pathways of HONO formation predict low daytime HONO concentrations (Vogel et al., 2003; Li et al., 2010). To improve simulations of the OH radical and its effect on photochemistry, more recent models have attempted to incorporate additional direct and/or secondary HONO sources (e.g., **Figure 13**), which improves simulation of HONO, ozone production, and secondary aerosols in

polluted urban areas (Sarwar et al., 2008; Li et al., 2010; Czader et al., 2012; Zhang et al., 2016a). Nonetheless, uncertainties remain in representing these sources in the current state-of-the-art models due to simplifications in their source parameterizations and to adopting different values of key parameters. For instance, model values for the uptake coefficient on aerosol surfaces range from 10^{-6} to 10^{-4}, leading to different conclusions regarding the importance of atmospheric aerosols in HONO formation (Aumont et al., 2003; Sarwar et al., 2008; Li et al., 2010; An et al., 2013). A recent study incorporated up-to-date HONO sources, including gaseous formation, emissions from soil bacteria, and heterogeneous formation of HONO on ocean, aerosol, urban, and vegetation surfaces into a regional CTM (WRF-Chem; **Figure 13**). The improved model led to improvements in simulated HONO at a suburban site in Hong Kong and increased simulated ground-level ozone by 5%–10% in a multiday photochemical episode in Southern China (Zhang et al., 2016a). This result highlights the importance of accurately representing the additional HONO sources in simulations of ground-level ozone over polluted regions.

Ye et al. (2016) reported trace gas measurements from aircraft flights over the western subtropical North Atlantic Ocean during summer 2013. From these data, they developed a novel mechanism that links particle-bound nitrate (p-NO_3) to the production of HONO via photolysis (Ye et al., 2016). The data from Ye et al. (2016) suggest that the photolysis of p-NO_3 is order of magnitude faster than that of gas-phase $HONO_2$. Kasibhatla et al. (2018) show that inclusion of p-NO_3 photolysis in a global model can lead to increases in ozone of 10%–30% in the tropical and subtropical MBL. They found that using a photolysis rate for p-NO_3 that is 25–100 times that of gas-phase $HONO_2$ provides the best agreement with observations of NO_x and HONO at the Cape Verde Atmospheric Observatory. These values for p-NO_3 photolysis are at the lower end of those determined by Ye et al. (2016). However, Romer et al. (2018) analyzed measurements of NO_x and $HONO_2$ in the Yellow Sea and concluded that these could be reconciled with negligible enhancements in p-NO_3 (1–30 times faster than in the gas phase). Further work is required to quantify and understand the rates of p-NO_3 photolysis under a range of tropospheric conditions and quantify the effect it has on the tropospheric ozone budget and its expected evolution in the future.

5.3. Halogen chemistry

Ozone depletion events (ODEs) were discovered in the troposphere, more specifically in the spring polar boundary layer, about four decades ago. They were first observed in the Arctic at Barrow (now called Utqiaġvik), Alaska (Oltmans, 1981), and Alert, Canada (Bottenheim et al., 1986), and later in the Antarctic (Kreher et al., 1996). During ODEs, surface ozone levels decrease from typical values of approximately 30–40 nmol/mol to levels below the detection limit of ozone sensors, 1–2 nmol/mol. This phenomenon makes the polar regions one of the environments where chemical loss of tropospheric ozone is most efficient.

In the mid-1980s, it was recognized that the loss of polar boundary layer ozone during ODEs was coupled to halogen chemistry—primarily involving bromine and, to a lesser extent, chlorine. This was confirmed in the following decades by a myriad of observations with different measurement techniques, which identified levels of boundary layer BrO in the range of 30–40 pmol mol^{-1} (Simpson et al., 2007; Saiz-Lopez and von Glasow, 2012). To understand chemical sources and sinks of ozone in this unique environment, detailed modeling exercises were performed focusing on HO_x, NO_x, and halogen chemistry (Bloss et al., 2010; see discussion below for details of the ozone loss catalytic cycles). The exact mechanisms of bromine activation in the polar regions remain uncertain, but experimental and modeling studies have shown that gas exchange between the atmosphere and snow/ice surfaces plays a key role (Abbatt et al., 2012). Space-based observations of column BrO enhancements are correlated with modeled sea-salt aerosol generated from blowing snow (Choi et al., 2018). Yang et al. (2010) found that the inclusion of blowing snow as a source of bromine in a global model reduces average modeled high latitude lower tropospheric ozone amounts by as much as 8% in polar spring. Forecasting long-term changes in tropospheric polar ozone is a formidable challenge because of the importance of air–ice exchange processes, which are subject to change as ice-covered areas are modified in a warming climate.

Reactive halogens (Cl, Br, and I) are also present globally in the MBL due to several processes. It is well established that gaseous photolabile compounds (e.g., Br_2, Cl_2, BrCl, $BrNO_2$, and $ClNO_2$; see Section 5.1) are produced from heterogeneous and multiphase reactions in/on chloride- and bromide-containing particles such as sea salt (e.g., Finlayson-Pitts et al., 1989; Fickert et al., 1999; Roberts et al., 2009). Iodine is directly emitted from the ocean as HOI or I_2 (R15 and R16) following the ozonolysis of seawater iodide (Garland and Curtis, 1981; Carpenter et al., 2013).

(R15) $H^+ + I^- + O_3 \rightarrow HOI + O_2$
(R16) $H^+ + HOI + I^- \leftrightarrow I_2 + H_2O$

A number of volatile halocarbons (e.g., CH_2I_2, CH_2IBr, CH_2ICl, CH_3I, and $CHBr_3$), with lifetimes ranging from minutes to approximately 1 month, are also present in the MBL (e.g., Jones et al., 2009). Elevated levels of these biogenic compounds are generally observed in coastal regions due to strong emissions from exposed macroalgae (e.g., Carpenter et al., 1999). In marine air, halogen atoms produced from the photolysis of these halocarbon precursors initiate catalytic ozone loss cycles, for example, R17–R19 and R20–R23 (where $X/Y =$ Br, Cl, or I).

Cycle 1
(R17) $X + O_3 \rightarrow XO + O_2$
(R18) $Y + O_3 \rightarrow YO + O_2$
(R19) $XO + YO \rightarrow X + Y + O_2$
$2\ O_3 \rightarrow 3\ O_2$ Net

Cycle 2
(R20) $X + O_3 \rightarrow XO + O_2$
(R21) $XO + HO_2 \rightarrow HOX + O_2$
(R22) $HOX + h\nu \rightarrow X + OH$
(R23) $OH + CO\ [+ O_2] \rightarrow HO_2 + CO_2$
$CO + O_3 \rightarrow O_2 + CO_2$ Net

Halogen chemistry may also indirectly reduce ozone production by decreasing the $[HO_2]/[OH]$ ratio (R21/R22) and by accelerating NO_x loss via the production and the subsequent hydrolysis of halogen nitrates ($XONO_2$) in aerosol and cloud (R24 and R25). In regions of elevated NO_x, VOC oxidation by Cl atoms can *enhance* ozone production (Section 2.2).

(R24) $XO + NO_2 \rightarrow XONO_2$
(R25) $XONO_2 + H_2O \rightarrow HOX + HONO_2$

Evidence for significant MBL halogen-driven ozone loss is based on a limited, but growing, body of measurements of XO radicals and their precursors, underpinned by numerical modeling on a range of scales. BrO mixing ratios of <1–10 pmol mol^{-1} have been reported using Differential Optical Absorption Spectroscopy in the North Atlantic (Leser et al., 2003; Saiz-Lopez et al., 2004; Mahajan et al., 2009). IO has been detected over the Atlantic (e.g., Allan et al., 2000), East Pacific (e.g., Mahajan et al., 2012), and West Pacific oceans (Großmann et al., 2013) and appears to be fairly ubiquitous in the MBL. A compilation of these and other data suggests typical daytime IO mixing ratios in the range of 0.4–1 pmol mol^{-1} over the open ocean (Prados-Roman et al., 2014). Measurement-constrained box model studies suggest halogen chemistry can cause substantial reductions in MBL ozone (e.g., Saiz-Lopez and Plane, 2004; Mahajan et al., 2010). At Cape Verde, a site characterized by low NO_x and thereby representative of the typical open ocean, the combined presence of BrO and IO is estimated to enhance photochemical ozone destruction by about 50% (Read et al., 2008).

Few assessments of the impact of halogens on global ozone have been performed. Available global model studies estimate that bromine decreases the tropospheric ozone burden by approximately 6%–9% (e.g., Yang et al., 2010; Parrella et al., 2012) and that bromine and iodine combined lower the ozone burden by about 14% (Saiz-Lopez et al., 2014; Sherwen et al., 2016), relative to model simulations without halogens. In the MBL, ozone loss from halogens may be comparable to that from HO_x chemistry alone (**Figure 14**), with iodine making the largest contribution (Saiz-Lopez et al., 2014). Such models are subject to a large range of process and parametric uncertainty, notably with respect to their treatment of halogen recycling on aerosol. A major challenge lies in capturing the effects of complex multiphase halogen processes, given that few models explicitly consider aqueous phase chemistry, while retaining a reasonable degree of computational efficiency (Tost et al., 2006). Laboratory investigations of the photochemistry and fate of higher iodine oxides (I_xO_y), in particular, are needed to better quantify the role of iodine in ozone chemistry. A more comprehensive measurement database of halogen radicals and their precursors is also needed to assess the fidelity of model simulations. Measurements of BrO in the MBL, for example, are extremely sparse outside of polar regions. Finally, we note that emissions of these halogenated compounds are also a major uncertainty at present, although recent work highlights promise in the use of new machine learning–based techniques at overcoming the limitations of sparse observations (Sherwen et al., 2019) for developing emissions estimates.

Cl and ClO measurements are also extremely sparse in the troposphere, but several modeling studies have shown that Cl could be important for the tropospheric ozone budget. Wang et al. (2019) recently reviewed the role of Cl on chemistry in the troposphere and calculated an important role for Cl in enhancing BrO levels through heterogenous chemistry, thereby reducing the ozone burden by 7%. More modeling has focused on the regional impacts of Cl and $ClONO_2$ (see Section 5.1). Accounting for the chemistry associated with these molecules can lead to increases of 3%–5% in surface ozone in the United States (Sarwar et al., 2012) and significant regional enhancements elsewhere in the NH, particularly over China (Sarwar et al., 2014; Li et al., 2020), with smaller increases over Europe (Sherwen et al., 2017b).

Quantitatively, it is largely unknown how halogen sources have changed on decadal timescales. Levels of iodine in the MBL may have increased since the preindustrial era (Prados-Roman et al., 2015) owing to increases in surface ozone (R15 and R16). These increases in iodine can then feedback onto the ozone levels in the troposphere, ultimately changing the ozone radiative forcing (Sherwen et al., 2017a). Further laboratory and field characterisation of air–ocean and air–ice halogen exchange is needed to assess possible future changes to MBL halogen levels (e.g., Hughes et al., 2012) as a consequence of climate change. Overall, understanding of tropospheric halogen processes is a rapidly evolving field. Given the apparent leverage halogens possess over tropospheric ozone concentrations, research focused on addressing the deficiencies of halogen processes in model simulations of current and future ozone would be beneficial. Iglesias-Suarez et al. (2020) suggest that, although at the global scale halogen chemistry may not be enhanced in future warmer climates, increases in regional iodine-driven ozone destruction in the future may help offset the ozone climate penalty and help reduce human exposure to high ozone levels in urban areas.

5.4. Unconventional hydrocarbon extraction

Although intense photochemical production of ozone (often resulting in hourly average ozone concentrations exceeding 150 nmol/mol) near the Earth's surface is considered a summertime, urban phenomenon, rapid diurnal photochemical production of ozone in winter with air temperatures as low as −17 °C has been reported (e.g., Schnell et al., 2009; Ahmadov et al., 2015; Oltmans et al., 2016). Schnell et al. (2009) found that in the vicinity of the Jonah–Pinedale Anticline natural gas field in rural Wyoming, high-pressure systems that promote cold

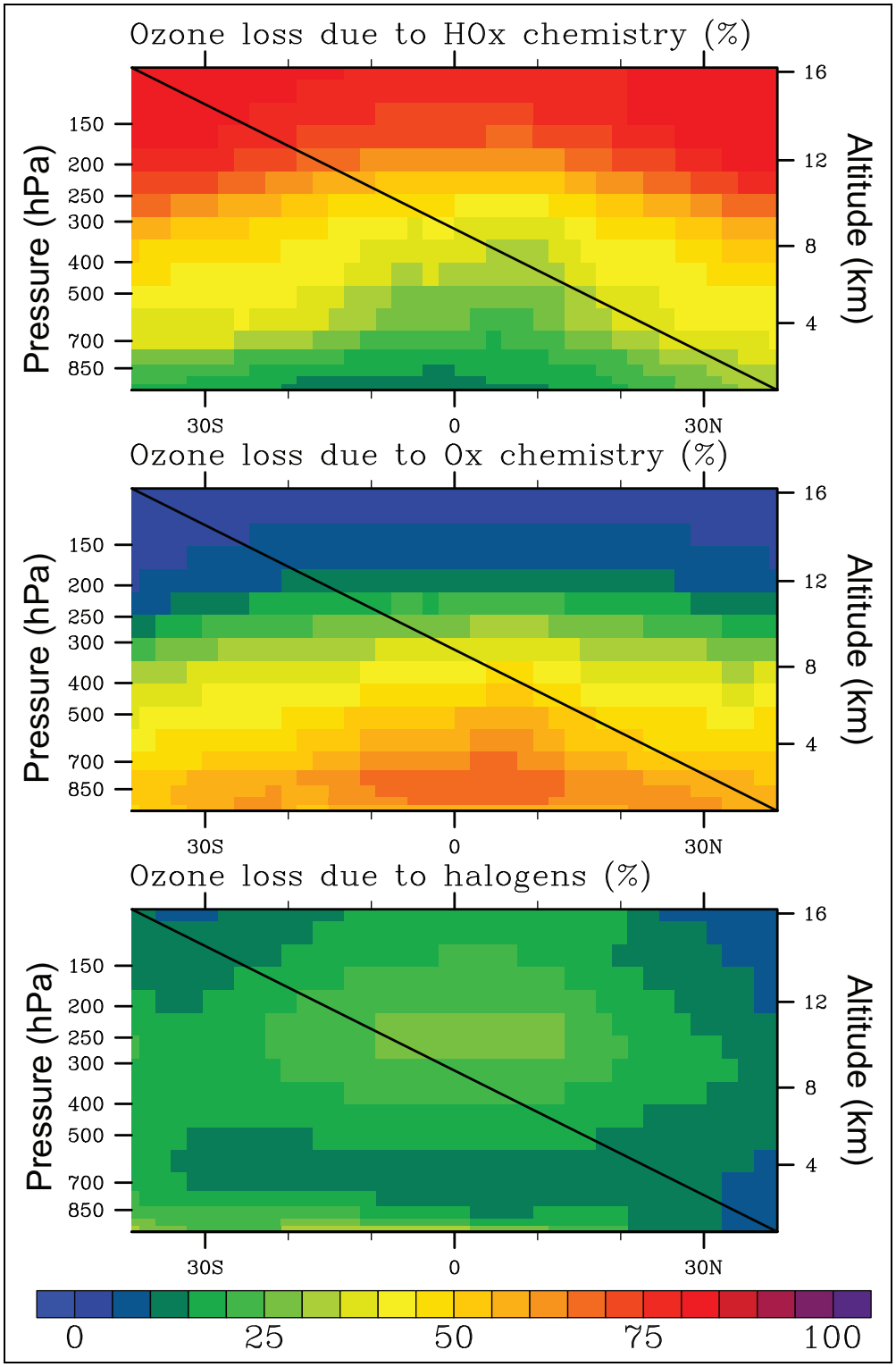

Figure 14. Percentage contribution to chemical ozone loss from HO_x, O_x, and halogen photochemistry between 40°N and 40°S. Approximately 70% of the halogen-mediated ozone loss is calculated to be driven by iodine photochemistry. Adapted from Saiz-Lopez et al. (2012). DOI: https://doi.org/10.1525/elementa.2020.034.f14

temperatures, low wind speeds, and limited cloudiness can cause hourly average ozone concentrations to rise from 10 to 30 nmol/mol at night to more than 140 nmol/mol shortly after solar noon (**Figure 15**). Under these conditions, an intense, shallow temperature inversion develops in the lowest 100 m of the atmosphere during the night, which traps high concentrations of ozone precursors (i.e., VOC and NO_x) associated with the production of natural gas. During daytime, photolytic ozone production then leads to the observed high concentrations. They suggested that similar ozone production during wintertime is probably occurring around the world under comparable industrial and meteorological conditions.

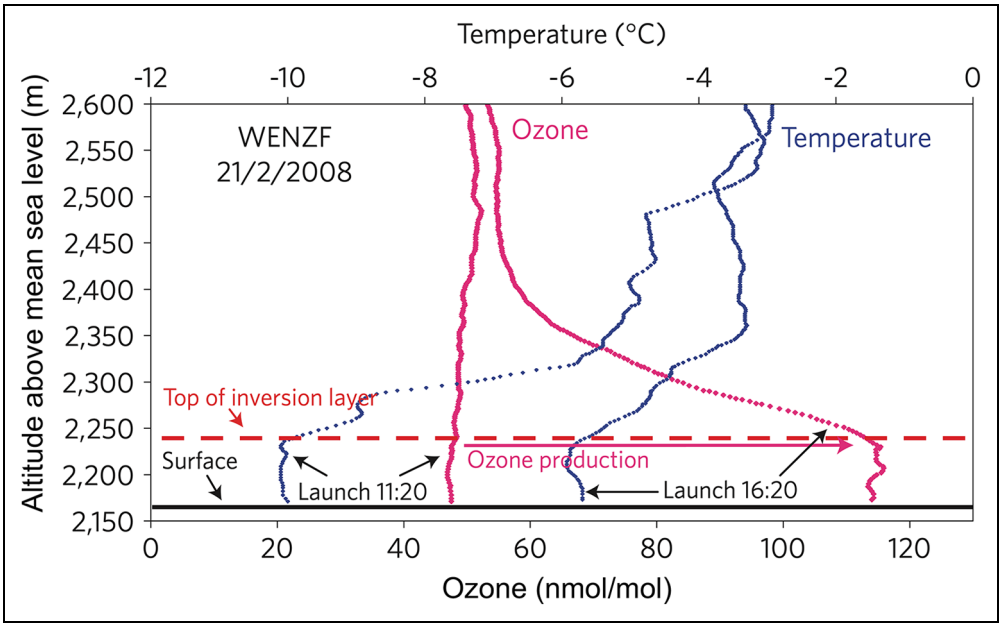

Figure 15. Ozonesonde profile 10 km north of the gas field showing ozone and temperature profiles, surface to 2,600 m, February 21, 2008. Adapted from Schnell et al. (2009). DOI: https://doi.org/10.1525/elementa.2020.034.f15

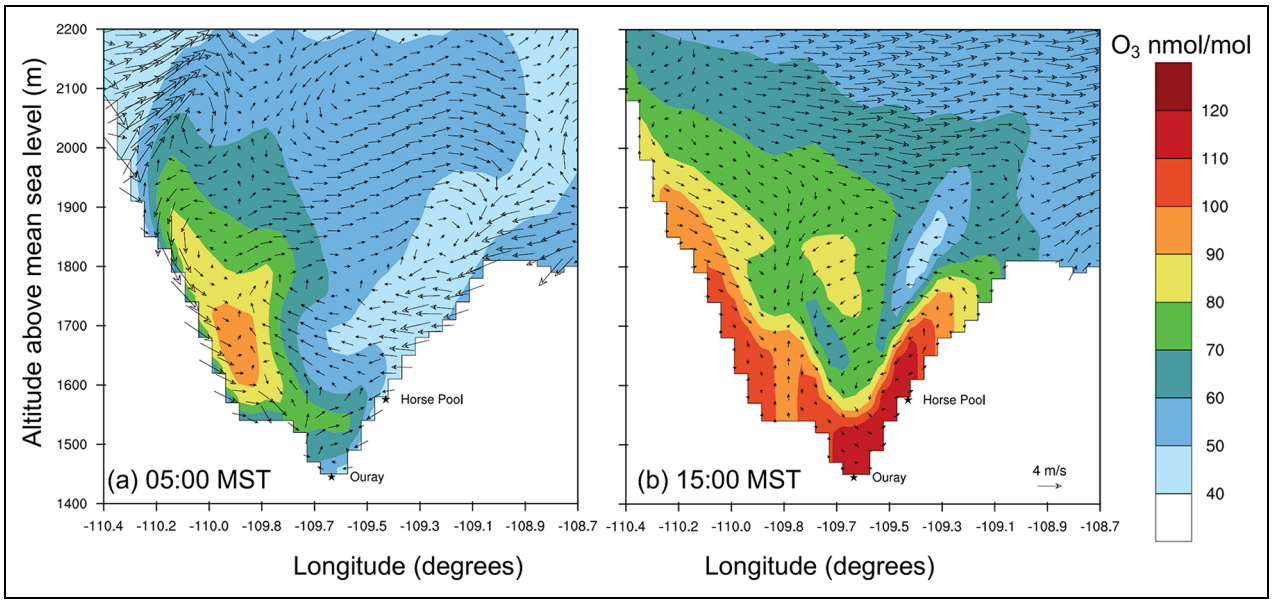

Figure 16. Simulated ozone distribution and wind vectors over the Uinta Basin (west-to-east direction in the WRF grid). The Horse Pool and Ouray surface stations along the cross section are indicated with stars. Panel A shows the data from early morning (05:00 MST) and Panel B the afternoon (15:00 MST) on February 5, 2013. The vertical wind components were multiplied by 100 for illustration of the wind vectors. Adapted from Ahmadov et al. (2015). DOI: https://doi.org/10.1525/elementa.2020.034.f16

Ahmadov et al. (2015) observed this same phenomenon over the Uinta Basin in Northeastern Utah, which is densely populated by thousands of oil and natural gas wells, during winter 2013. They used a regional-scale air quality model (WRF-Chem) and high-resolution meteorological simulations and were able to qualitatively reproduce the wintertime cold pool conditions as well as the observed multiday buildup of atmospheric pollutants and the accompanying rapid photochemical ozone formation in the Uinta Basin (**Figure 16**).

Edwards et al. (2014) concluded that photolysis of oxidized organic compounds (often containing carbonyl functional groups) from unconventional hydrocarbon extraction was the primary driver for producing radicals that lead to ozone production in the Uinta Basin. Archibald et al. (2018) assessed the potential impacts of unconventional hydrocarbon extraction in the United Kingdom

and concluded that there is likely to be only a small impact on ozone, even under the assumption of high levels of VOC emissions similar to those observed in locations like Uinta (Edwards et al., 2014). This disparity in the response of ozone to unconventional hydrocarbon extraction emissions seems to be a result of the geography of the emissions region. Indeed, Edwards et al. (2014) show that the high levels of ozone they simulated in Uinta occur only in episodes when vertical mixing is limited and when the concentrations of the secondary products (which act as catalysts to the production of ozone) accumulate (conditions that Archibald et al., 2018, have shown do not occur in the United Kingdom).

It is worth noting that although the impact of emissions from unconventional hydrocarbon extraction is largely a regional issue, the rapid growth in the industry could see it becoming a more widespread problem in the future if the emissions of VOCs and NO_x from hydrocarbon production are not sufficiently controlled.

5.5. Organic peroxy radicals

Peroxy radicals are formed as intermediates during the atmospheric oxidation of all organic compounds and have an expansive chemistry (Orlando and Tyndall, 2012). HO_2, CH_3O_2, and $CH_3C(O)O_2$ are the most abundant, but peroxy radicals are present in great diversity in the atmosphere (e.g., Khan et al., 2015). They react with NO, NO_2, HO_2, and other peroxy radicals; undergo unimolecular isomerization; and have lifetimes of the order of 1–100 s under typical atmospheric conditions. Atmospheric reactions of peroxy radicals usually proceed via more than one channel, with the different channels having different temperature, and sometimes pressure, dependencies. A large body of work has been performed over the past 30 years to elucidate the complex chemistry of peroxy radicals. Although the general features of peroxy radical chemistry are established, many important details remain unclear.

From the perspective of ozone chemistry, the most important reaction of peroxy radicals is that with NO, which produces NO_2 and is responsible for photochemical ozone formation in the troposphere (see Section 3.1). Organic peroxy radicals react with NO via two pathways to give either an alkoxy radical and NO_2 or an alkyl nitrate (Arey et al., 2001).

(R1a) $RO_2 + NO \rightarrow RO + NO_2$
(R1b) $RO_2 + NO + M \rightarrow RONO_2 + M$

The channel that produces an alkoxy radical and NO_2 leads to radical propagation and promotes photochemical ozone formation. The channel that produces an alkyl nitrate removes radicals and NO_x and hinders local photochemical ozone formation. Alkyl nitrates can be transported and undergo photolysis and reaction with OH, releasing NO_x and promoting ozone formation in downwind locations. Neu et al. (2008) show that matching methyl nitrate (CH_3ONO_2) observations in the western Pacific with the UCI-CTM results in an enhancement of 1 DU to the tropospheric ozone column, emphasizing the importance of even the smallest of organic nitrates.

The organic nitrate yield increases with decreasing temperature, increasing pressure, and size of the peroxy radical (Atkinson et al., 1983, 1987; Carter and Atkinson, 1989; Harris and Kerr, 1989). Organic nitrate yields for substituted peroxy radicals are lower than those for unsubstituted alkylperoxy radicals of a similar size, particularly when the substituent is located close to the peroxy moiety, although the data are limited and the precise effects are unclear (Arey et al., 2001; Lim and Ziemann, 2005; Matsunaga and Ziemann, 2010). Early studies indicated that nitrate yields were higher for secondary radicals (RCH(OO)R') and lower for primary (RCH_2OO) and tertiary RR'R''COO) radicals (Arey et al., 2001). However, several studies (e.g., Espada et al., 2005; Cassanelli et al., 2007) report approximately equal yields from secondary, primary, and tertiary radicals of the same size. As discussed by Calvert et al. (2015), thermal decomposition of tertiary alkyl nitrates at gas chromatogram (GC) injection temperatures may have led to an underestimation of the yields of tertiary nitrates in the early studies using GC analysis.

Data for the organic nitrate yields of peroxy radicals formed in the oxidation of important biogenic VOCs are limited and often contradictory inspite of the significance of these molecules to tropospheric ozone (e.g., Fisher et al., 2016). Reported organic nitrate yields from the oxidation of isoprene lie in the range 4%–15% (Calvert et al., 2015). Data for the organic nitrate yields for the atmospherically relevant monoterpenes and sesquiterpenes are extremely limited and uncertain. As an example, the organic nitrate yield following the HO-initiated oxidation of α-pinene has been reported as $18 \pm 9\%$ by Nozière et al. (1999) and 1% by Aschmann et al. (2002). Clearly, given the importance of well-established branching ratios for organic nitrate formation to atmospheric models of ozone formation, there is an urgent need for further work in this area.

Peroxy radicals have been proposed to form water complexes (e.g., Aloisio and Franscico, 1998; Clark et al., 2008), and it has been estimated that approximately 10%–20% of HO_2 radicals in the atmosphere exist as the $HO_2 \bullet H_2O$ complex (Archibald et al., 2011b) and that approximately 5%–15% of organic peroxy radicals in the atmosphere exist as the $RO_2 \bullet H_2O$ complex (Khan et al., 2015). Water-complexed peroxy radicals may be more reactive and have different product distributions than uncomplexed peroxy radicals and may be important in atmospheric ozone chemistry. An increase of approximately 12%–14% in ozone production has been estimated for a two-fold increase in reactivity of $RO_2 \bullet H_2O$ compared with RO_2 radicals (Khan et al., 2015). Definitive direct experimental studies are required to establish the atmospheric importance of reactions involving water-complexed peroxy radicals.

Finally, we note that much recent attention has focused on isomerization of peroxy radicals, where 1–5 and 1–6 H-atom abstractions can occur rapidly and may switch the peroxy radical from primary to secondary or even tertiary, with concomitant changes in reactivity and possible organic nitrate yields (e.g., Peeters et al., 2009; Praske et

al., 2018). As Praske et al. (2018) highlight, given the significant regional reductions in anthropogenic NO_x that have occurred in recent decades, the fate of the RO_2 in VOC source regions may now change from propagating NO–NO_2 conversion to the formation of highly oxygenated compounds. Further work is needed to clarify the role of peroxy radical isomerization in atmospheric chemistry and integrate this in global model studies to understand the potential implications for the tropospheric ozone budget.

5.6. Heterogeneous processes

The largest potential impact of heterogeneous processes on tropospheric ozone is via removal of N_2O_5 (a NO_x and ozone reservoir) and the hydroperoxyl radical HO_2 (Jacob, 2000). Following on from earlier work by Lelieveld and Crutzen (1990), Dentener and Crutzen (1993) showed that removal of NO_3 and N_2O_5 by aerosol particles caused decreases in ozone at the Earth's surface of up to 25% and global decreases in ozone and OH of 9%. Tie et al. (2001) studied the global impact of HO_2, N_2O_5, and CH_2O uptake on aerosols and found a significant effect of removal of these compounds on ozone. Martin et al. (2003) showed that aerosols have a strong effect not only on chemistry through heterogeneous uptake but also on photolysis rates, with the two processes having approximately equal impacts on OH. However, Holmes et al. (2019) have shown that the way in which these heterogeneous processes are represented in large-scale models has an important influence with respect to their impacts on tropospheric ozone. They have shown that reformulating the way that cloud chemistry is represented in the GEOS-Chem model leads to the conclusion that clouds and aerosols have similar impacts on the global budgets of ozone and OH, reducing them by around 2% each relative to the default treatment.

Our current understanding of the uptake of N_2O_5 from laboratory measurements is based on a large and relatively coherent body of experimental data, which has resulted in a well-validated mechanism. However, there remain significant challenges in parameterizing these results in a reduced form for use in global models, primarily due to the scarcity of data on the temperature dependence of the uptake coefficient and differing determinations of the relative humidity (RH) dependence in the literature. Stavrakou et al. (2013) chose three realistic, but different, parameterizations for N_2O_5 loss onto tropospheric aerosol. **Figure 17** shows the effect of these parameterizations on rate coefficients of N_2O_5 loss, with Brown et al. (2009) representing a lower limit. A wide range of rate coefficients is simulated by the different parameterizations, corresponding to an uncertainty in the lifetime of N_2O_5 of over three orders of magnitude to this process, with implications for simulated ozone. A more robust parameterization is clearly required.

A more significant challenge for modeling is the inclusion of the effect of nitrate aerosol composition on N_2O_5 removal. It is known that nitrate reduces the reactivity of mixed composition aerosols (Mentel et al., 1999), and the observed strong negative dependence of N_2O_5 on nitrate aerosol concentration means that two important

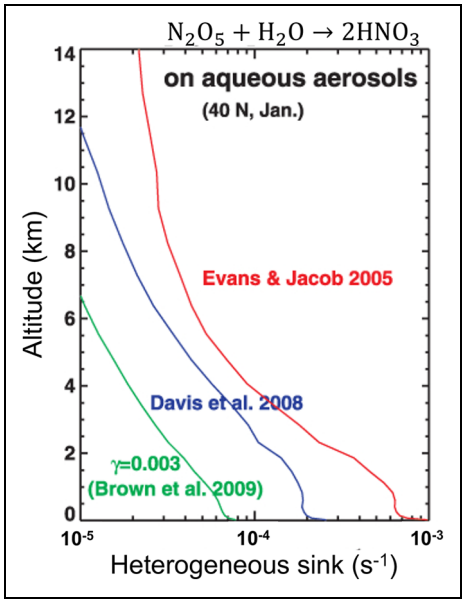

Figure 17. Calculated rate of hydrolysis of N_2O_5 onto tropospheric aerosol (the heterogeneous sink) as a function of altitude, using three different parameterizations widely used in models. The different calculations result in an order of magnitude difference in the rate of heterogeneous sink within the boundary layer. Adapted from Stavrakou et al. (2013). DOI: https://doi.org/10.1525/elementa.2020.034.f17

feedbacks are missing from models. With increasing nitrate levels, (1) the contribution of N_2O_5 hydrolysis to the aerosol nitrate burden is reduced, and (2) less NO_x is removed from the gas phase. At present, an online description of the nitrate aerosol mode is not included in a large number of CCMs. A global study of the aerosol burden by Feng and Penner (2007) highlighted the contribution of N_2O_5 uptake to nitrate levels, but the use of offline (noninteractive) OH and ozone fields means that the feedback of N_2O_5 loss on oxidation rates was missing. Paulot et al. (2016) highlighted the effect of aerosol composition on uptake, noting that decreasing the uptake of N_2O_5 reduced the model bias in nitrate aerosol concentrations at the surface, providing indirect evidence for reduced uptake coefficients onto nitrate aerosol.

The simulation of nitrate aerosol presents a significant challenge, and there are large uncertainties in the expected burden under climate change scenarios. Although higher temperatures decrease the nitrate aerosol burden, Pye et al. (2009) projected increases in NO_x emissions lead to a significant increase in nitrate aerosol burden, both in absolute terms and as a fraction of total aerosol amount, due to simultaneous decreases in SO_2 emission. The combined effect of increasing temperature and emissions is not yet resolved, with studies showing no significant change in nitrate aerosol (Pye et al., 2009) or modest increases (Bauer et al., 2007; Bellouin et al., 2011). At this point, the effect of nitrate aerosol on N_2O_5 has not yet been fully quantified, and, in view of the possibility of increasing nitrate aerosol burden in the future, this should be an area of focus.

The uptake coefficient of HO_2 into aqueous aerosol and the picture from laboratory data are unclear. Initially, uptake of HO_2 was determined to follow first-order kinetics (Cooper and Abbatt, 1996), but subsequent measurements showed pronounced second-order behavior, consistent with uptake controlled by self-reaction of HO_2 in the absence of transition metals (Thornton and Abbatt, 2005). On this basis, Thornton et al. (2008) proposed a parameterization that gave low values of $\gamma < 0.05$ for a surface-weighted uptake coefficient in the lower troposphere. The authors conclude that the effect of temperature on uptake of HO_2 was significant, and this should be included in CCM parameterizations.

More recent measurements, using lower mixing ratios of HO_2, indicate that the reaction under ambient conditions is first order, although the fate of the HO_2 following uptake remains unclear. Taketani et al. (2008, 2009) showed that first-order loss of HO_2 is observed onto aqueous sulfate aerosol, as well as on aerosol regenerated from ambient aerosol filter samples (Taketani et al., 2012). In these experiments, large values of the uptake coefficient, $\gamma > 0.1$, were observed. Uptake by solid mineral dust aerosol has been measured and shown to be less efficient but still significant ($\gamma = 0.03$; George et al., 2013). A self-reaction to form H_2O_2 now appears unlikely to be the dominant atmospheric sink, although it may certainly occur in the lab under higher gas phase HO_2 concentrations than are typically observed in the atmosphere.

Mao et al. (2010) showed that including the loss of HO_2 into aerosol improved the agreement between modeled and observed HO_2 but that including subsequent release of H_2O_2 in the model reduced the level of agreement. Although Mao et al. (2013) assessed the role of transition metals (e.g., iron, manganese, chromium, and copper) in controlling the reactivity of ambient aerosols, the mechanism for other aerosols is unclear. Li et al. (2019) applied the GEOS-Chem CTM with the current knowledge of HO_2 aerosol chemistry and found that the decrease in ambient aerosol has contributed to recent increasing trend of summer surface ozone in China due to slowing down the aerosol-HO_2 sink. However, the lack of mechanistic understanding of the factors controlling uptake of HO_2 limits confident assessment of the impact of this heterogeneous process on ozone.

The role of mineral dust has been highlighted in lab studies as being important. The release of NO and NO_2 from adsorbed nitrate has been observed (Ndour et al., 2009). The release of OH from the photolytic reduction of H_2O adsorbed onto mineral dust seen in the laboratory (Dupart et al., 2012) is indirectly supported by observations of new particle formation following episodes of high mineral dust loading, presumably via enhanced flux of OH + SO_2. Observations of Dust from Thar Desert and WRF-Chem study showed that without including dust aerosols through heterogeneous chemistry and perturbation in photolysis rates, ozone loss of 16 nmol/mol and NO_y loss of about 2 nmol/mol remains unexplained (Kumar et al., 2014). It is also shown that dust could lead to ozone loss by 10%–15% up to 4-km altitude region.

Several recent studies of ozone uptake indicate a significant perturbation to the oxidation pathways within the aerosol, presumably through the formation of reactive oxygen species (Shiraiwa et al., 2011). The impact of direct loss of ozone onto SOA aerosol surfaces should be examined further, as these latter processes are important to our understanding of the largely unexplored oxidative chemistry within the aerosol and to their impact on human health.

6. Challenges to modeling the budget and burden of tropospheric ozone: Emissions and dynamics

As Section 5 highlights, there are numerous chemical processes that have a bearing on our ability to model the tropospheric ozone budget and potentially its trends. Our understanding of these processes is increasing, but they are still poorly represented in models (Young et al., 2018). There are also numerous uncertainties associated with transport of ozone and its precursors and their emissions that provide a challenge for understanding trends in the tropospheric ozone burden and the details of the tropospheric ozone budget from local to global scales.

6.1. Impacts of dynamical variability on the ozone burden and budget

Although the global tropospheric ozone burden is estimated to have increased from 1960 to 2010 (Young et al., 2013a; Parrish et al., 2014; Griffiths et al., 2020), the pattern of changes in ozone is complex, with ozone leveling off after ca. 2000 in some areas but continuing to grow in others (Cooper et al., 2014; Gaudel et al., 2018). Studies have shown that ozone at a given location is strongly influenced not only by emissions changes but also by variability in transport associated with large-scale dynamics. Dynamical variability is generally diagnosed from a constant emission run, while the difference between this "base" simulation and one in which emissions vary realistically with time provides the emissions-driven component. However, these types of experiments tend to be performed ad hoc by modeling groups, and there is little coordinated effort to understand the role of dynamical variability in a multimodel sense. Lin et al. (2014) show that the lack of a springtime increase in ozone levels at Mauna Loa Observatory Hawaii during the 2000s—in sharp contrast to trends at other remote northern midlatitude sites—was driven by a weakening of springtime transport of ozone-rich air from Asia to Hawaii. This occurred as a result of a predominance of La Nina-like conditions associated with the Pacific Decadal Oscillation. Long-range transport from midlatitudes to the Arctic likewise varies strongly with the phase of the North Atlantic Oscillation (Eckhardt et al., 2003), and the cold temperatures mean that PAN formed in midlatitudes acts as a significant source of NO_x, accounting for 50%–90% of Arctic surface ozone production during spring (Walker et al., 2012).

Even in less remote locations, long-range transport confounds attribution of observed ozone changes to changes in local emissions. Asian emissions have been shown to be a major contributor to springtime ozone increases in the Western United States (e.g., Jacob et al., 1999; Zhang et al., 2008; Jaffe et al., 2018). Lin et al. (2017) estimate that transport from Asia has driven as much as 65% of the increase in surface background ozone levels during springtime that has occurred since 1990, despite a 50% reduction in Western U.S. NO_x. Verstraeten et al. (2015) similarly found that from 2005 to 2010, long-range transport of pollution from China offset approximately 40% of the reduction in mid-tropospheric ozone, which should have occurred over the Western United States in response to a 21% decrease in regional NO_x emissions there. Long-range transport from both Asia and North America have likewise been found to reduce the efficacy of European emissions controls (e.g., Jonson et al., 2006). In the SH, large increases (20%–30% decade^{-1} since 1990) in mid-tropospheric ozone in the austral winter over two sites in Southern Africa have been at least preliminarily attributed to increases in anthropogenic NO_x emissions throughout the hemisphere rather than any significant change in biomass burning (Thompson et al., 2014). On the other hand, a more recent study by Lu et al. (2018) found that the increasing tropospheric ozone over 1990–2015 in the extratropical SH is not mainly due to increases of anthropogenic emissions. Instead, they attribute the trend to changes in the meridional circulation driven by the poleward expansion of the SH Hadley circulation, again highlighting the importance of large-scale dynamics to the tropospheric ozone budget.

Variability in STT also plays an important role in tropospheric ozone variability and trends (Hess and Zbinden, 2013), leading to changes in tropospheric ozone levels in the northern midlatitudes of around 2%, approximately half of the interannual variability (Neu et al., 2014). An increase in STE in 2009–2010 associated with a combination of El Niño and easterly shear in the stratospheric QBO was calculated as being responsible for half of the net increase in mid-tropospheric ozone over Eastern China from 2005 to 2010, with the other half driven by local emissions increases (Verstraeten et al., 2015).

As **Figure 10** shows, in the near term at the regional scale, particularly in the southern high latitudes, we can expect that dynamical variability will make the greatest relative contribution to the uncertainty of the tropospheric mean ozone column. But key unresolved questions remain regarding the current generation of CCMs' ability to accurately capture this process and how changes in climate will affect dynamical variability. We suggest further work be performed to better understand these questions from a multimodel perspective.

In addition to the issues described above, outstanding issues around the representation of the transport of ozone in models remain. These issues have been assessed recently in the context of the effect of model grid resolution on simulations that tag ozone production to different sources of ozone precursors (Mertens et al., 2020). Mertens et al. (2020) have shown that contributions from anthropogenic emissions averaged over large scales (1,000 km) are quite robust with respect to model resolution but that contributions from stratospheric ozone transported to the surface differ strongly between models of different resolution. They ascribe the reason for this to differences in the efficiency of mixing in the vertical and emphasize that studies that perform attribution of ozone to source sectors should account for the stratospheric ozone source explicitly in order to better understand intermodel differences. In addition, we suggest that model intercomparison exercises encourage modeling groups to produce idealized stratospheric ozone tracers (Roelofs and Lelieveld, 1997) to help better understand the role of stratospheric ozone on the future evolution of the ozone burden and budget.

6.2. Impacts of emission uncertainty on the ozone budget and burden

Although projects like ACCMIP, CCMI, and AerChemMIP coordinate modeling efforts by providing common sets of emissions data for groups to use, these activities represent an ensemble of opportunity. As a result, modeling groups often make pragmatic decisions that result in teams using different emissions data sets within each model (Young et al., 2013a, 2018). Differences in emissions in models may be a key reason for differences in the modeled simulations of the historic changes in the ozone budget and burden (**Figures 5**–7) and its future evolution (**Figure 10**).

Although our focus in the rest of this section is on the role of uncertainty in anthropogenic emissions, there exists significant uncertainty in natural emissions that are important to highlight briefly. The most important natural emission sources for tropospheric ozone are BVOCs (e.g., Guenther et al., 1995, 2006) and soil (e.g., Vinken et al., 2014) and lightning NO_x. Uncertainty in BVOC emissions is significant for the monoterpenes but less so for isoprene; although there is debate about the reasons for this with some suggestions that this is driven by too few independent formulations of the algorithms to simulate isoprene emissions (e.g., Arneth et al., 2008). Uncertainty in the impacts of BVOCs on ozone is not only limited to the uncertainty in the BVOC emissions themselves (e.g., Williams et al., 2013) but also in the representation of their oxidation chemistry in models (e.g., Archibald et al., 2010; Squire et al., 2015; Bates and Jacob, 2019a).

Soil NO_x emissions currently account for approximately 25% of total NO_x emissions and are subject to variability driven by changes in weather and agricultural practices (Hudman et al., 2010). As anthropogenic NO_x emissions decrease over time, soil NO_x is likely to become a much more important factor in the ozone budget, and there is urgent need for a better representation of these emissions in models.

Lightning NO_x tends to have the highest OPE of all precursors of tropospheric ozone (e.g., Finney et al., 2016) and acts as the major source of NO_x in the SH and the free troposphere (e.g., Grewe, 2007). The representation of lightning NO_x in models is most commonly based on the scheme of Price and Rind (1992). Gordillo-Vazquez

et al. (2019) recently compared the effects of six different parameterizations of lightning NO_x on ozone under "present-day" conditions (ca. year 2000). They found that an ice flux–based scheme provided best agreement with ozonesonde measurements and observations of lightning flashes using the LIS/OTD satellite products. Finney et al. (2018) showed that using their ice flux–based scheme resulted in a decrease of 15% in lightning flashes when comparing year 2000 to 2100, whereas a cloud top height-based scheme (Price and Rind, 1992) resulted in an increase of 43% in lightning flashes. This uncertainty in the sign of the response of lightning flashes, and as a consequence lightning NO_x emissions, is a critical area for future research given the importance of lightning to the global ozone background (Grewe, 2007).

Finally, biomass burning encompasses both natural- and human-induced fires, and there remains significant uncertainty in the global estimates of emission factors of VOCs and NO_x from these sources (e.g., Akagi et al., 2011) and in the trends of these emissions over time (Granier et al., 2011). Rowlinson et al. (2020) show that the change in tropospheric ozone radiative forcing from the preindustrial to the present day is very sensitive to uncertainty in preindustrial biomass burning emissions, and in their calculations, tropospheric ozone radiative forcing is reduced by 34% when using more realistic biomass burning and BVOC emissions for the preindustrial. For a comprehensive review on the effects of biomass burning emissions on ozone, we direct the reader to Jaffe and Wigder (2012).

A key issue with emission inventories is the assessment of their uncertainty. Despite the complexity of inventories, systematic uncertainty estimates on these data sets are often not reported. Inventory developers have begun to report uncertainty estimates, and this has become good practice for national greenhouse gas inventories (Penman et al., 2000). Other approaches, including comparisons of different inventories and comparisons of inventory emission ratios with ambient enhancement ratios, have been used for estimating emissions uncertainty (e.g., Hassler et al., 2016). Similarly, comparisons between independent approaches to determining emissions (e.g., using remote sensing, Streets et al., 2013; Stavrakou et al., 2015; aircraft, Pitt et al., 2019; or flux towers, Lee et al., 2015) can provide an estimate of uncertainty. Here, we consider some examples of these different types of emissions uncertainty estimates, along with a discussion of the possible impacts on ozone simulations. We emphasize that there is no single definitive evaluation method regarding uncertainties on emissions of ozone precursors on a global or national scale. We recommend that the development of such a method be a key component of future MIPs.

Hoesly et al. (2018) summarize a number of existing studies that assess uncertainty on ozone precursors in global and regional inventories that inform the CMIP6 historical (1750–2014) inventory data set produced by the Community Emissions Database System. From their analysis, a few general statements can be made: (1) Uncertainties in NO_x, CO, and VOC emissions are higher than those in CO_2 from fossil fuel combustion; (2) uncertainties on ozone precursor emissions from specific sectors such as mobile sources can be as high as a factor of two, even in industrialized nations with sophisticated inventory development efforts; (3) uncertainties vary across sectors, with some sectors having much higher uncertainties due to the manner in which estimates are derived and the lack of independent estimates; (4) global emissions estimates tend to be less uncertain than those of any particular region; and (5) more recent estimates (e.g., in the past two decades) are generally less uncertain than those from earlier periods.

Emissions inventories are always a few years out of date. Present-day emissions are very difficult to estimate because the main drivers in such estimates, that is, fuel use, energy production and consumption, and so on, are generally available with delays of up to 3 years at the global scale and of at least 2 years for country-level data, and emission factors that may be derived for a specific country or city are often used in other regions with missing data. It is therefore very difficult to estimate the most recent trends in emissions and to provide accurate scenarios for future years.

For example, as a result of the rapid industrial growth of China and the development of several densely populated areas, several studies have shown that the emissions of all ozone precursors significantly increased in China over the past four to five decades (Zhang et al., 2007; Kurokawa et al., 2013; Granier et al., n.d.) but have recently started to decrease (de Foy et al., 2016; Krotkov et al., 2016). **Figure 18** shows the evolution of the emissions of NO_x between 1960 and 2014 in China from different global and regional emission inventories, with all inventories showing the emissions of NO_x constantly, and fairly consistently, increasing up to 2012. However, the more recent observations of decreases in NO_x are not yet available in a multiinventory sense and highlight the challenge of developing an inventory for a region undergoing rapid change in emissions.

A further uncertainty in the modeling of ozone chemistry is introduced from partitioning of VOC emissions into individual species. This is a complex task that is likely to have particularly large impacts on understanding trends in ozone at the regional scale. von Schneidemesser et al. (2015) highlighted how simulated tropospheric ozone depends on the precise VOC speciation in different inventories and found that modeled ozone had a greater sensitivity to VOC emissions speciation than to the choice of chemical mechanism used in the simulation. Further research using more realistic CTMs is needed to understand the importance of VOC emissions speciation for determining global and regional budgets of tropospheric ozone.

7. Conclusions and outlook

TOAR has provided an unprecedented review of our understanding of the recent trends in tropospheric ozone and enabled a legacy of new research that will maximize the potential of the TOAR database (Schultz et al., 2017). Furthermore, the insight gained from understanding contemporary (Gaudel et al., 2018) and historic (Tarasick et al., 2019b) measurements of

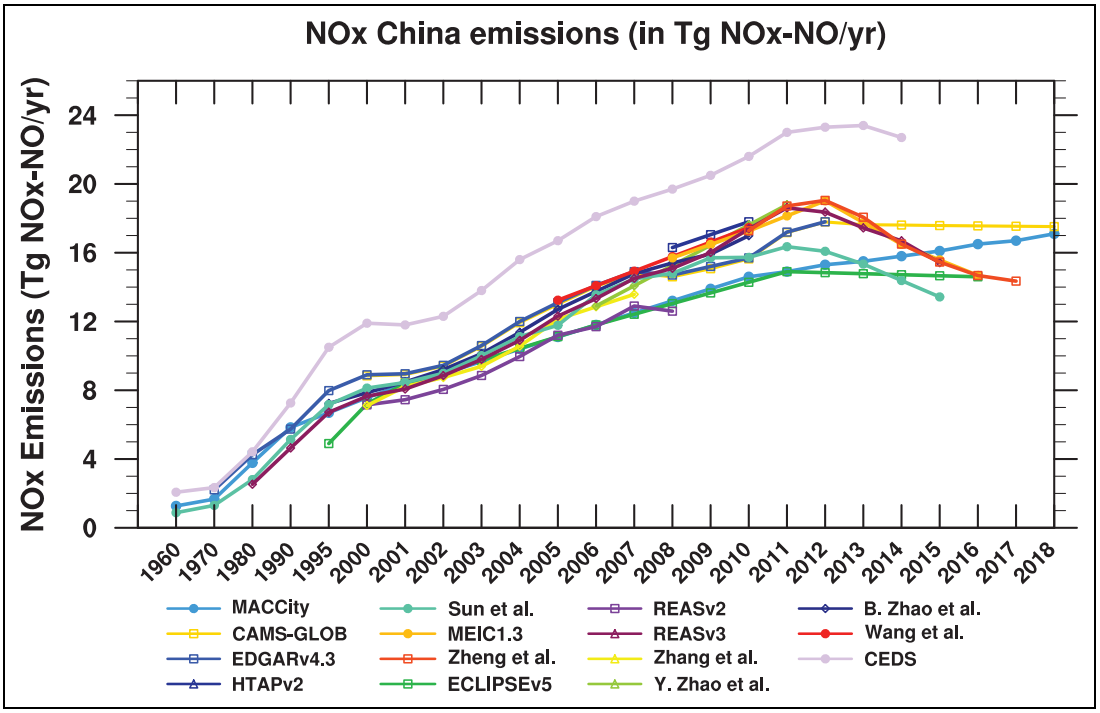

Figure 18. Evolution of the NO_x emissions in China from 1960 from different inventories. Data from Granier et al. (n.d.), an update from Granier et al. (2011). DOI: https://doi.org/10.1525/elementa.2020.034.f18

tropospheric ozone will enable improved evaluation of model performance (Young et al., 2018).

In addition, TOAR has provided a timely opportunity to reflect on what we've learned since the publication of the 2003 IGAC atmospheric chemistry review (Brasseur et al., 2003) and what we still don't know. In the following sections, we review where we have made progress, where uncertainty still remains, and some recommendations for future research areas.

7.1. Outlook for global ozone monitoring

Monitoring surface and free tropospheric ozone on the global scale is challenging due to its high spatial and temporal variability and the wide range of ozone precursor sources. Furthermore, there have been major changes in the locations of anthropogenic ozone precursor emissions, with big reductions in Organization for Economic Cooperation and Development (OECD) countries counteracted by large increases in non-OECD countries. This is especially true of Asia but also in Africa and South and Central America. The impact of this shift in emissions has been shown to be a key driver for increases in the total burden of ozone (Zhang et al., 2016b). If emissions of NO_x continue to increase in the tropics and subtropics over the next few decades, as technological development and population increases (Jones and O'Neil, 2016), we can expect an increase in the tropospheric ozone burden (Kumar et al., 2018). We still don't fully understand the impacts of the uncertainty in emissions, and future work should systematically target this knowledge gap.

Through the reassessment of historical surface ozone trends (Tarasick et al., 2019b) and very recent isotopic constraints (Yeung et al., 2019), we are in a strong position to challenge the validity of some of the early measurements of ozone that would suggest ozone more than doubled between the late 19th century and present day (i.e., those made at Montsouris, France). Replicating these very low ozone values was a huge challenge to modelers, but it now appears that the modeled increase in the burden of tropospheric ozone of around 30% since the preindustrial (**Figure 5**) is consistent with observational estimates over shorter time periods.

In addition to our improved understanding of historical ozone observations, major advances have been made over the past 30 years in our ability to monitor tropospheric ozone from space. The earliest satellite observations of global-scale tropospheric column ozone date back to 1979, based on the difference between TOMS total ozone and SAGE stratospheric column ozone (Fishman et al., 1990, 2008). These early observations were followed by the next generation of instruments in the 1990s and early 2000s, based on thermal infrared spectra (TES and IASI) or ultraviolet wavelengths (GOME, SCHIAMCHY, and OMI; Burrows et al., 1995, 1999; Ziemke et al., 2005; Bowman, 2013; Verstraeten et al., 2015; Ebojie et al., 2016; Gaudel et al., 2018). TOAR-climate conducted the first intercomparison of a range of satellite ozone products and found a high level of agreement regarding the tropospheric ozone burden (Gaudel et al., 2018). However, the products did not agree regarding short-term trends (2008–2016), and future research led by TOAR will explore the reasons for this discrepancy. Current research on long-term ozone trends has highlighted the power of combining satellite data sets to quantify ozone trends, including those since the late 1970s (Ziemke et al., 2019) and the mid-1990s (Heue et al., 2016; Leventidou et al., 2018).

In the next decade, planned satellite measurements of ozone and ozone precursors will be acquired from both low earth orbit (LEO) and geostationary orbit (GEO). LEO observations such as TropOMI on ESA/Sentinel 5P (Beirle et al., 2019) and IASI-NG on Eumetsat/MetOP and CrIS on the Joint Polar Satellite System will continue the global monitoring of the atmosphere obtained by existing LEO satellites, while the GEO perspective will provide temporal coverage that is not possible from LEO over continental-scale observing domains. The new GEO satellite instruments such as NASA/TEMPO (North America; Zoogman et al., 2017), ESA/Sentinel-4 (Europe; Ingmann et al., 2012), and the Korean GEMS (East Asia; Kim et al., 2020) should be able to help us quantify diurnal changes in precursor emissions and chemical production of ozone. Both LEO and GEO observations will have finer spatial resolution (<10 km) than existing assets to aid in distinguishing emissions, chemistry, and transport processes. These new measurements will help enable substantial improvements in air quality prediction along with our understanding of atmospheric composition when used in conjunction with models and other observational platforms (such as ozonesondes). There is great scope in the future for combining models and satellite measurements (i.e., through data assimilation) to improve understanding of global-scale tropospheric ozone trends and distribution that would not be possible with the relatively limited availability of in situ ozone profiles (Tarasick et al., 2019a, 2019b).

7.2. Outstanding science questions related to understanding the ozone budget

Although this is not a major focus of TOAR, as we highlighted in Section 6.1 and Young et al. (2018) discussed, there is a strong body of evidence which highlights that over the last 15 years we have made great progress in understanding the role of natural climate variability and climate change in tropospheric ozone (e.g., Fiore et al., 2012; Doherty et al., 2013). CCMs provide a great opportunity for us to explore these interactions, and the new AerChemMIP and CMIP6 projects (Collins et al., 2017) will provide the community with larger volumes of data to analyze than ever before.

The discovery of $ClNO_2$ as a ubiquitous reservoir of chlorine and NO_x (Mielke et al., 2011) has potential to change our current understanding of the role of N_2O_5 chemistry in the troposphere. Few global modeling studies have been performed to understand the impacts on trends in tropospheric ozone with or without this chemistry, and further studies are necessary. More generally, the role of halogens on tropospheric composition is still highly uncertain, but their influence on concentrations and trends may be profound.

The discovery of a significant role for peroxy radical isomerization reactions has also been a breakthrough in the last few decades. It is now widely recognized that the fate of peroxy radicals in the troposphere is not limited to bimolecular reactions. Indeed, for many peroxy radicals, these unimolecular H-shifts may outcompete bimolecular reactions in the troposphere. But what role this chemistry plays on the ozone budget and burden is still not completely understood. The most recent isoprene chemistry schemes all include H-shifts (Archibald et al., 2011a; Bates and Jacob, 2019a) and suggest that these reactions result in large increases in OH and decreases in ozone in the tropical lower troposphere (Squire et al., 2015; Bates and Jacob, 2019a).

The formation of $HONO_2$ as a product from the reaction between $HO_2 + NO$ (Butkovskaya et al., 2005, 2007, 2009) has been shown in modeling studies to have a potentially significant impact on the tropospheric ozone burden (Søvde et al., 2011; Gottschaldt et al., 2013; Archibald et al., 2020). Independent laboratory studies are required to verify this channel in the reaction and to better understand the role of water vapour in this and other peroxy radical reactions.

In spite of the huge role it plays on the ozone budget, relatively little work has focused on the deposition sink of ozone in recent years. As we have reviewed in Section 2.1, changes in the deposition of ozone are likely to have significantly impacted historic trends and are likely to continue to do so at the regional scale (Lin et al., 2019) and in particular as land use is altered in the wake of the impacts of climate change and the drive to net zero emissions.

7.3. Recommendations for the future

In TOAR-Ozone Budget, we have reviewed the literature and have highlighted the significant progress in modeling the processes that control the ozone budget. However, progress in constraining these processes has been poorer. We still don't know whether a model with an NCP of 500 Tg is more accurate than a model with an NCP of 100 Tg. A huge focus continues to be on the evaluation of simulations around observational campaigns fixed in time. Less work has focused on evaluating the interannual variability and trends in ozone over time—in part owing to limited data on ozone trends in the troposphere. We see two opportunities for work supported by TOAR in this area, first by helping to focus efforts on understanding trends and model sensitivities and second in encouraging wider use of new constraints when evaluating ozone. For example, the work of Yeung et al. (2019) on oxygen isotopes highlights novel approaches to constraining changes in ozone since the preindustrial, which other modeling teams and observational teams can take forward. Similarly, the paradigm for field measurements achieved in the NASA ATom campaign is beginning to enable not only new approaches to the analysis of the distribution of ozone and other short-lived climate forcers in the troposphere (Prather et al., 2017) but also improved insight into the processes that control them (e.g., Travis et al., 2020).

Do we have sufficient data for understanding trends in the ozone burden and budget? As we've shown here and in *TOAR-Model Performance* (Young et al., 2018), there have been a large number of model simulations performed by the community, especially through MIPs. But much less of the data generated has been made available to the community, particularly in the area of enabling process-oriented model evaluation and quantification of

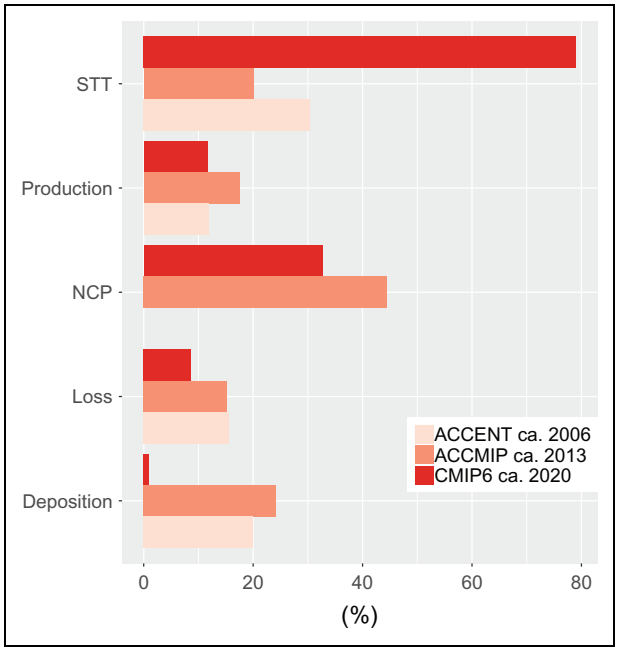

Figure 19. Comparison of the spread in the terms of the ozone budget from recent multimodel assessments (data from Stevenson et al., 2006, Young et al., 2013a, and Griffiths et al., 2020). Each bar shows the relevant multimodel standard deviation divided by the multimodel mean expressed as a percentage. Data shown are for the same time period (1995–2005) but with different models and different emissions. DOI: https://doi.org/10.1525/elementa.2020.034.f19

the ozone budget and its changes. In CCMI and ACCMIP, many more models provided output on their simulated tropospheric ozone trends but less data on what drives them. Excellent work has been performed to understand individual models, but with such large spread in the few model budgets available, what can we tell from these individual studies? How do we increase the accessibility and interoperability of ozone process data? The new ideas around definitions of the ozone budget (Edwards and Evans, 2017; Bates and Jacob, 2019b) provide new opportunities to better understand the role of emissions and the stratosphere, but at a potentially large cost in having to output more data. **Figure 19** highlights that over the last 14 years, the spread in the terms of the ozone budget simulated by multimodel studies has not reduced. For some of the budget terms, there is large variability between the multimodel studies. **Figure 19** suggests a large increase in spread in STT in the most recent CMIP6 models, but it should be noted that oly three models were used in the most recent multimodel assessment (Griffiths et al., 2020). What is clear is that the spread in the gross chemical terms (*P* and *L*) has remained fairly consistent and modest (<15%) but that the NCP of ozone has remained an area with significant variability across models (>30%) as has the deposition flux (≥20%; excluding the data point from the recent CMIP6 study, Grifftiths et al., 2020).

So far, we have spent a huge amount of resources on increasing the detail in the representation of processes in models and their resolution. However, the biases against observations of tropospheric ozone have not changed significantly over the last two decades. There remain open questions still on the exchange of material with the surface and between the troposphere and the stratosphere. Progress is needed in these areas as well as in areas focused on elucidating the emissions and chemistry. Moreover, formal assessments of model uncertainty are difficult, but when performed even on a small part of the model (e.g., on the impact of rate constant uncertainty, see Section 4.1), these are often large (e.g., Newsome and Evans, 2017; Archibald et al., 2020). Some of these uncertainties could be reduced by further focused laboratory studies, improved emission inventories, and so on. However, there may also be a need for new measures of success. Such a new measure of success could be as simple as identifying what new science has been included, such as enabling chemical interactions with strong feedbacks on the Earth system (i.e., through improved coupling of the reactive nitrogen inventory in the atmosphere with the terrestrial biosphere). There are separate, but related, questions around measures of success in the climate community. But could the TOAR community adopt some of these, such as an ozone equivalent of equilibrium climate sensitivity that can be used to summarize performance in a single metric?

One can argue that in general more research is needed to characterize how our understanding of the budget of ozone simulated in models is evolving over time. Are we getting any better at modeling tropospheric ozone? One suggestion is the adoption of a core tropospheric ozone simulation with prescribed emissions of ozone precursors and meteorology that will enable modeling groups to more precisely identify the role of changes in the chemistry of ozone included in models. This methodology builds upon and aspires to emulate the success of the Diagnostic, Evaluation and Characterization of Klima (DECK) experiments, which are used in the CMIP (Eyring et al., 2016). The DECK experiments enable the climate modeling community to understand how changes to climate models impact metrics such as climate sensitivity and include, for example, a 100-year simulation with increasing CO_2 at 1% yr^{-1}. A tropospheric ozone "DECK" experiment would require sufficient buy-in from the community but could be used to resolve some of these outstanding questions.

We have made a lot of progress in understanding the burden and budget of ozone in the troposphere, and with the advent of the new generation of GEO and LEO satellites, the availability of more model simulations from CMIP6 than ever before, and an improved understanding of recent and historic trends in ozone observations, enabled by *TOAR*, we are in a great position to close out some of the remaining questions and reduce the uncertainty in predictions of future tropospheric ozone.

Data accessability statement

All data analyzed are available from the primary citing literature. The CCMI model data are available open access

via the Centre for Environmental Data Archive (https://www.ceda.ac.uk/).

Supplemental files

Tables S1 and S2. Docx.

Authors' note

I. Shahid now at Environmental Science Centre, Qatar University, Doha, Qatar.

P. Saxena now at Department of Environmental Sciences, Hindu College, University of Delhi, Delhi110007, India.

Acknowledgments

ATA and PJY would like to acknowledge the International Global Atmospheric Chemistry Chemistry Climate Model Initiative project, Atmospheric Chemistry and Climate Model Intercomparison Project, and CMIP5 for providing simulations that underpinned the analysis in Section 4. VN would like to acknowledge the Community Emissions Database System emissions inventory developed in support of the CMIP6 shown in **Figure 8.**

Funding

ATA and PTG would like to acknowledge support from National Centre for Atmospheric Science. YE would like to acknowledge support from the National Science Foundation Atmospheric and Geospace Sciences awards # 1900795 and 1929368. TW acknowledges support from the Hong Kong Research Grants Council (T24-504/17-N) and the National Natural Science Foundation of China (91844301). ASL thanks European Executive Agency under the European Union's Horizon 2020 Research Innovation programme (Project "ERC-2016-COG 726349 CLIMAHAL"). RH is supported by an NERC Independent Research Fellowship (NE/N014375/1). YMS is supported by an NERC PhD studentship. Part of this research was carried out at the Jet Propulsion Laboratory, California Institute of Technology, under a contract with the National Aeronautics and Space Administration.

Competing interests

The authors have declared that no competing interests exist.

Author contributions

ATA and JN lead the manuscript. ATA, JN, and YE lead the writing and editing of the paper with significant contributions from ORC, TJW, VN, and PJY. All co-authors contributed to reviewing and editing this article and leading specific areas.

Contributed to conception and design: ATA, JN, YE, ORC.

Contributed to acquisition of data: BJ, PTG, YMS, ATA, PJY, VN.

Contributed to analysis and interpretation of data: ATA, JN, ORC, ASL.

Drafted and/or revised the article: All co-authors contributed to the drafting and revision of this article.

References

Abbatt, JPD, Thomas, JL, Abrahamsson, K, Boxe, C, Granfors, A, Jones, AE, King, MD, Saiz-Lopez, A, Shepson, PB, Sodeau, J, Toohey, DW, Toubin, C, von Glasow, R, Wren, SN, Yang, X. 2012. Halogen activation via interactions with environmental ice and snow in the polar lower troposphere and other regions. *Atmos Chem Phys* **12**: 6237–6271. DOI: http://dx.doi.org/10.5194/acp-12-6237-2012.

Ahmadov, R, McKeen, S, Trainer, M, Banta, R, Brewer, A, Brown, S, Edwards, PM, de Gouw, JA, Frost, GJ, Gilman, J, Helmig, D, Johnson, B, Karion, A, Koss, A, Langford, A, Lerner, B, Olson, J, Oltmans, S, Peischl, J, Pétron, G, Pichugina, Y, Roberts, JM, Ryerson, T, Schnell, R, Senff, C, Sweeney, C, Thompson, C, Veres, PR, Warneke, C, Wild, R, Williams, EJ, Yuan, B, Zamora, R. 2015. Understanding high wintertime ozone pollution events in an oil- and natural gas-producing region of the western US. *Atmos Chem Phys* **15**: 411–429. DOI: http://dx.doi.org/10.5194/acp-15-411-2015.

Akagi, SK, Yokelson, RJ, Wiedinmyer, C, Alvarado, M, Reid, JS, Karl, T, Crounse, JD, Wennberg, PO. 2011. Emission factors for open and domestic biomass burning for use in atmospheric models. *Atmos Chem Phys* **11**(9): 4039.

Allan, BJ, McFiggans, G, Plane, JM, Coe, H. 2000. Observations of iodine monoxide in the remote marine boundary layer. *J Geophys Res Atmos* **105**(D11): 14363–14369.

Aloisio, S, Francisco, JS. 1998. Existence of a hydroperoxy and water ($HO_2 \bullet H_2O$) radical complex. *J Phys Chem A* **102**: 1899–1902.

An, J, Li, Y, Chen, Y, Li, J, Qu, Y, Tang, Y. 2013. Enhancements of major aerosol components due to additional HONO sources in the North China Plain and implications for visibility and haze. *Advances Atmos Sci* **30**(1): 57–66.

Andersson, C, Engardt, M. 2010. European ozone in a future climate: Importance of changes in dry deposition and isoprene emissions. *J Geophys Res Atmos* **115**(D2): 1–13.

Anet, JG, Steinbacher, M, Gallardo, L, Velásquez Álvarez, PA, Emmenegger, L, Buchmann, B. 2017. Surface ozone in the Southern Hemisphere: 20 years of data from a site with a unique setting in El Tololo, Chile. *Atmos Chem Phys* **17**: 6477–6492. DOI: http://dx.doi.org/10.5194/acp-17-6477-2017.

Appenzeller, CH, Davies, HC, Norton, WA. 1996. Fragmentation of stratospheric intrusions. *J Geophys Res Atmos* **101**(D1): 1435–1456.

Archibald, AT, Jenkin, ME, Shallcross, DE. 2010. An isoprene mechanism intercomparison. *Atmos Environ* **44**(40): 5356–5364.

Archibald, AT, Levine, JG, Abraham, NL, Cooke, MC, Edwards, PM, Heard, DE, Jenkin, ME, Karunaharan, A, Pike, RC, Monks, PS, Shallcross, DE. 2011a. Impacts of HOx regeneration and recycling in the oxidation of isoprene: Consequences for the

composition of past, present and future atmospheres. *Geophys Res Lett* **38**(5). DOI: http://dx.doi.org/10.1029/2010GL046520.

Archibald, AT, O'Connor, FM, Abraham, NL, Archer-Nicholls, S, Chipperfield, MP, Dalvi, M, Folberth, GA, Dennison, F, Dhomse, SS, Griffiths, PT, Hardacre, C, Hewitt, AJ, Hill, RS, Johnson, CE, Keeble, J, Köhler, MO, Morgenstern, O, Mulcahy, JP, Ordóñez, C, Pope, RJ, Rumbold, ST, Russo, MR, Savage, NH, Sellar, A, Stringer, M, Turnock, ST, Wild, O, Zeng, G. 2020. Description and evaluation of the UKCA stratosphere–troposphere chemistry scheme (StratTrop vn 1.0) implemented in UKESM1. *Geosci Model Dev* **13**: 1223–1266. DOI: http://dx.doi.org/10.5194/gmd-13-1223-2020.

Archibald, AT, Tonokura, K, Kawasaki, M, Percival, CJ, Shallcross, DE. 2011b. On the impact of HO_2–H_2O complexes in the marine boundary layer: A possible sink for HO_2. TAO: Terrestrial. *Atmos Ocean Sci* **22**(1): 7.

Archibald, AT, Ordóñez, C, Brent, E, Williams, ML. 2018. Potential impacts of emissions associated with unconventional hydrocarbon extraction on UK air quality and human health. *Air Quality, Atmosphere & Health* **11**(6): 627–637.

Arey, J, Aschmann, SM, Kwok, ESC, Atkinson, R. 2001. Alkyl nitrate, hydroxyalkyl nitrate, and hydroxycarbonyl formation from the NOx-air photooxidations of C5-C8 n-alkanes. *J Phys Chem A* **105**: 1020–1027.

Arneth, A, Monson, RK, Schurgers, G, Niinemets, Ü, Palmer, PI. 2008. Why are estimates of global terrestrial isoprene emissions so similar (and why is this not so for monoterpenes)? *Atmos Chem Phys* **8**: 4605–4620. DOI: http://dx.doi.org/10.5194/acp-8-4605-2008.

Aschmann, SM, Atkinson, R, Arey, J. 2002. Products of reaction of hydroxyl radicals with alpha-pinene. *J Geophys Res* 107. DOI: http://dx.doi.org/10.1029/2001JD001098.

Atkinson, R, Aschmann, SM, Winer, AM. 1987. Alkyl nitrate formation from the reaction of a series of branched RO_2 Radicals with NO as a function of temperature and pressure. *J Atmos Chem* **5**: 91–102.

Atkinson, R, Carter, WPL, Winer, AM. 1983. Effects of temperature and pressure on alkyl nitrate yields in the NOx photooxidation of n-pentane and n-hexane. *J Phys Chem* **87**: 2012–2018.

Atlas, E, Ridley, BA. 1996. The manuna loa observatory photochemistry experiment: Introduction. *J Geophys Res* **101**: 14531–14541.

Auer, R. 1939. Über den Faglichen Gang des Ozongehalts der bodennahen Luft. *Beitraege Zur Geschichte Der Geophysik and Kosmischen Physik* **54**: 137–145.

Ayers, GP, Penkett, SA, Gillett, RW, Bandy, B, Galbally, IE Meyer, CP, Elsworth, CM, Bentley, ST, Forgan, BW. 1992. Evidence for photochemical control of ozone concentrations in unpolluted marine air. *Nature* **360**: 446–448.

Banerjee, A, Archibald, AT, Maycock, AC, Telford, P, Abraham, NL, Yang, X, Braesicke, P, Pyle, JA. 2014. Lightning NOx, a key chemistry–climate interaction: Impacts of future climate change and consequences for tropospheric oxidising capacity. *Atmos Chem Phys* **14**: 9871–9881. DOI: http://dx.doi.org/10.5194/acp-14-9871-2014.

Banerjee, A, Maycock, AC, Archibald, AT, Abraham, NL, Telford, P, Braesicke, P, Pyle, JA. 2016. Drivers of changes in stratospheric and tropospheric ozone between year 2000 and 2100. *Atmos Chem Phys* **14**: 9871–9881. DOI: http://dx.doi.org/10.5194/acp-16-2727-2016.

Baray, J-L, Duflot, V, Posny, F, Cammas, J-P, Thompson, AM, Gabarrot, F, Bonne, J-L, Zeng, G. 2012. One year ozonesonde measurements at Kerguelen Island (49.2°S, 70.1°E): Influence of stratosphere-to-troposphere exchange and long-range transport of biomass burning plumes. *J Geophys Res* **117**: D06305. DOI: http://dx.doi.org/10.1029/2011JD016717.

Barnes, EA, Fiore, AM, Horowitz, LW. 2016. Detection of trends in surface ozone in the presence of climate variability. *J Geophys Res Atmos* **121**: 6112–6129. DOI: http://dx.doi.org/10.1002/2015JD024397.

Bates, KH, Jacob, DJ. 2019a. A new model mechanism for atmospheric oxidation of isoprene: Global effects on oxidants, nitrogen oxides, organic products, and secondary organic aerosol. *Atmos Chem Phys* **19**: 9613–9640. DOI: http://dx.doi.org/10.5194/acp-19-9613-2019.

Bates, KH, Jacob, DJ. 2019b. An expanded definition of the odd oxygen family for tropospheric ozone budgets: Implications for ozone lifetime and stratospheric influence. *Geophys Res Lett* **46**. DOI: http://dx.doi.org/10.1029/2019GL084486.

Bauer, SE, Koch, D, Unger, N, Metzger, SM, Shindell, DT, Streets, DG. 2007. Nitrate aerosols today and in 2030: a global simulation including aerosols and tropospheric ozone. *Atmos Chem Phys* **7**: 5043–5059.

Beekmann, M, Ancellet, G, Blonsky, S, De Muer, D, Ebel, A, Elbern, H, Hendricks, J, Kowol, J, Mancier, C, Sladkovic, R, Smit, HGJ, Speth, P, Trickl, T, Van Haver, P. 1997. Regional and global tropopause fold occurrence and related ozone flux across the tropopause. *J Atmos Chem* **28**: 29–44.

Beirle, S, Borger, C, Dörner, S, Li, A, Hu, Z, Liu, F, Wang, Y, Wagner, T. 2019. Pinpointing nitrogen oxide emissions from space. *Sci Adv* **5**(11). DOI: http://dx.doi.org/10.1126/sciadv.aax9800.

Bejan, I, Abd El Aal, Y, Barnes, I, Benter, T, Bohn, B, Wiesen, P, Kleffmann, J. 2006. The photolysis of ortho-nitrophenols: A new gas phase source of HONO. *Physical Chemistry Chemical Physics* **8**(17): 2028–2035.

Bellouin, N, Rae, J, Jones, A, Johnson, C, Haywood, J, Boucher, O. 2011. Aerosol forcing in the Climate Model Intercomparison Project (CMIP5) simulations by HadGEM2-ES and the role of ammonium nitrate. *J Geophys Res* **116**: D20206. DOI: http://dx.doi.org/10.1029/2011JD016074.

Bloomer, BJ, Stehr, JW, Piety, CA, Salawitch, RJ, Dickerson, RR. 2009. Observed relationships of ozone air pollution with temperature and emissions. *Geophys Res Lett* **36**: L09803. DOI: http://dx.doi.org/10.1029/2009GL037308.

Bloss, WJ, Camredon, M, Lee, JD, Heard, DE, Plane, JMC, Saiz-Lopez, A, Bauguitte, SJ-B, Salmon, RA, Jones, AE. 2010. Coupling of HOx, NOx and halogen chemistry in the antarctic boundary layer. *Atmos Chem Phys* **10**: 10187–10209. DOI: http://dx.doi.org/10.5194/acp-10-10187-2010.

Bottenheim, JW, Gallant, AG, Brice, KA. 1986. Measurements of NOy species and O_3 at 82 N latitude. *Geophys Res Lett* **13**(2): 113–116.

Bowman, KW. 2013. Toward the next generation of air quality monitoring: Ozone. *Atmos Environ* **80**: 571–583.

Brasseur, GP, Hauglustaine, DA, Walters, S. 1996. Chemical compounds in the remote Pacific troposphere: Comparison between MLOPEX measurements and chemical transport model calculations. *J Geophys Res* **101**: 14795–14813.

Brasseur, GP, Prinn, RG, Pszenny AAP eds. 2003. *Atmospheric chemistry in a changing world*. Heidelberg, Germany: Springer: 300. IBSN: 978-3-642-62396-7.

Brewer, AM. 1949. Evidence for a world circulation provided by the measurements of helium and water vapor distribution in the stratosphere. *Q J R Meteorol Soc* **75**: 351–363.

Brioude, J, Cooper, OR, Trainer, M, Ryerson, TB, Holloway, JS, Baynard, T, Peischl, J, Warneke, C, Neuman, JA, De Gouw, J, Stohl, A. 2007. Mixing between a stratospheric intrusion and a biomass burning plume. *Atmos Chem Phys* **7**: 4229–4235.

Brown, SS, Dubé, WP, Fuchs, H, Ryerson, TB, Wollny, AG, Brock, CA, Bahreini, R, Middlebrook, AM, Neuman, JA, Atlas, E, Roberts, JM. 2009. Reactive uptake coefficients for N_2O_5 determined from aircraft measurements during the Second Texas Air Quality Study: Comparison to current model parameterizations. *J Geophys Res Atmos* **114**(D7): 1–16.

Brown-Steiner, B, Selin, NE, Prinn, RG, Monier, E, Tilmes, S, Emmons, L, Garcia-Menendez, F. 2018. Maximizing ozone signals among chemical, meteorological, and climatological variability. *Atmos Chem Phys* **18**: 8373–8388. DOI: http://dx.doi.org/10.5194/acp-18-8373-2018.

Burrows, JP, Hölzle, E, Goede, A, Visser, H, Fricke, W. 1995. SCIAMACHY–scanning imaging absorption spectrometer for atmospheric chartography. *Acta Astronaut* **35**: 445–451. DOI: http://dx.doi.org/10.1016/0094-5765(94)00278-T

Burrows, JP, Weber, M, Buchwitz, M, Rozanov, V, Ladstätter-Weißenmayer, A, Richter, A, DeBeek, R, Hoogen, R, Bramstedt, K, Eichmann, KU, Eisinger, M. 1999. The global ozone monitoring experiment (GOME): Mission concept and first scientific results. *JAS* **56**(2): 151–175.

Butkovskaya, NI, Kukui, A, Le Bras, G. 2007. HNO_3 forming channel of the HO_2+ NO reaction as a function of pressure and temperature in the ranges of 72–600 Torr and 223– 323 K. *J Phys Chem A* **111**: 9047–9053.

Butkovskaya, NI, Kukui, A, Pouvesle, N, Le Bras, G. 2005. Formation of nitric acid in the gas-phase HO_2+NO reaction: Effects of temperature and water vapor. *J Phys Chem A* **109**: 6509.

Butkovskaya, NI, Rayez, M-T, Rayez, J-C, Kukui, A, Le Bras, G. 2009. Water vapor effect on the HNO_3 yield in the HO_2+NO reaction: experimental and theoretical evidence. *J Phys Chem A* **113**: 11327–11342.

Calvert, JG, Orlando, JJ, Stockwell, WR, Wallington, TJ. 2015. *The mechanisms of reactions influencing atmospheric ozone*. Oxford, UK: Oxford University Press. ISBN 978-0-19-023302-0.

Carpenter, LJ, Sturges, WT, Penkett, SA, Liss, PS, Alicke, B, Hebestreit, K, Platt, U. 1999. Short-lived alkyl iodides and bromides at Mace Head, Ireland: Links to biogenic sources and halogen oxide production. *J Geophys Res Atmos* **104**(D1): 1679–1689.

Carpenter, L, MacDonald, S, Shaw, M, Kumar, R, Saunders, RW, Parthipan, R, Wilson, J, Plane, JMC. 2013. Atmospheric iodine levels influenced by sea surface emissions of inorganic iodine. *Nature Geosci* **6**: 108–111. DOI: http://dx.doi.org/10.1038/ngeo1687

Carpenter, LJ, Monks, PS, Galbally, IE, Meyer, CP, Bandy, BJ, Penkett, SA. 1997. A study of peroxy radicals and ozone photochemistry at coastal sites in the northern and southern hemispheres. *J Geophys Res* **102**: 25417–25427.

Carter, WPL, Atkinson, R. 1989. Alkyl nitrate formation from the atmospheric photooxidation of alkanes; a revised estimation method. *J Atmos Chem* **8**: 165–173.

Cassanelli, P, Fox, DJ, Cox, RA. 2007. Temperature dependence of pentyl nitrate formation from the reaction of pentyl peroxy radicals with NO. *Phys Chem Chem Phys* 9: 4332–4347.

Chamberlain, AC. 1966. Transport of gases to and from grass and grass-like surfaces. *Proceedings of the Royal Society of London. Series A. Mathematical and Physical Sciences* **290**(1421): 236–265.

Chameides, WL, Walker, JCG. 1973. A photochemical theory for tropospheric ozone. *J Geophys Res* **78**: 8751–8760.

Chapman, S. 1942. The photochemistry of atmospheric oxygen. *Reports on Progress in Physics* **9**(1): 92–100.

Chen, XL, Ma, YM, Kelder, H, Yang, K. 2011. On the behaviour of the tropopause folding events over the Tibetan Plateau. *Atmos Chem Phys* **11**: 5113–5122.

Chen, X, Anel, JA, Su, Z, de la Torre, L, Kelder, H, van Peet, J, Ma, Y. 2013. The deep atmospheric boundary layer and its significance to the stratosphere and troposphere exchange over the Tibetan Plateau. *PloS One* **8**(2): e56909.

Choi, S, Theys, N, Salawitch, RJ, Wales, PA, Joiner, J, Canty, TP, Chance, K, Suleiman, RM, Palm, SP, Cullather, RI, Darmenov, AS. 2018. Link between Arctic tropospheric BrO explosion observed from

space and sea-salt aerosols from blowing snow investigated using Ozone Monitoring Instrument BrO Data and GEOS-5 data assimilation system. *J Geophys Res Atmos* **123**(13): 6954–6983.

Clain, G, Baray, JL, Delmas, R, Keckhut, P, Cammas, J-P. 2010. A Lagrangian approach to analyse the tropospheric ozone climatology in the tropics: Climatology of stratosphere–troposphere exchange at Reunion Island. *Atmos Env* **44**: 968–975.

Clark, J, English, AM, Hansen, JC, Francisco, JS. 2008. Computational study of the existence of organic peroxy radical-water complexes ($RO_2 \bullet H_2O$). *J Phys Chem A* **112**: 1587–1595.

Clark, SK, Ward, DS, Mahowald, NM. 2017. Parameterization-based uncertainty in future lightning flash density. *Geophys Res Lett* **44**(6): 2893–2901.

Clifton, OE, Fiore, AM, Munger, JW, Malyshev, S, Horowitz, LW, Shevliakova, E, Paulot, F, Murray, LT, Griffin, KL. 2017. Interannual variability in ozone removal by a temperate deciduous forest. *Geophys Res Lett* **44**(1): 542–552.

Colange, G, Lepape, A. 1929. Relation entre les titres en ozone de l'air du sol et de l'air de la haute atmosphere. *Comptes Rendus* **189**: 53–54.

Colette, A, Ancellet, G. 2005. Impact of vertical transport processes on the tropospheric ozone layering above Europe. Part II: Climatological analysis of the past 30 years. *Atmos Environ* **39**: 5423–5435.

Collins, WJ, Lamarque, J.-F, Schulz, M, Boucher, O, Eyring, V, Hegglin, MI, Maycock, A, Myhre, G, Prather, M, Shindell, D, Smith, SJ. 2017. AerChemMIP: Quantifying the effects of chemistry and aerosols in CMIP6. *Geosci Model Dev* **10**: 585–607. DOI: http://dx.doi.org/10.5194/gmd-10-585-2017.

Cooper, OR, Forster, C, Parrish, D, Dunlea, E, Hübler, G, Fehsenfeld, F, Holloway, J, Oltmans, S, Johnson, B, Wimmers, A, Horowitz, L. 2004a. On the life cycle of a stratospheric intrusion and its dispersion into polluted warm conveyor belts. *J Geophys Res* **109**: 18. D23S09. DOI: http://dx.doi.org/10.1029/2003JD004006.

Cooper, OR, Forster, C, Parrish, D, Trainer, M, Dunlea, E, Ryerson, T, Hübler, G, Fehsenfeld, F, Nicks, D, Holloway, J, de Gouw, J, Warneke, C, Roberts, JM, Flocke, F, Moody, J. 2004b. A case study of transpacific warm conveyor belt transport: Influence of merging airstreams on trace gas import to North America. *J Geophys Res* **109**: 17. D23508. DOI: http://dx.doi.org/10.1019/2003JD003624.

Cooper, OR, Oltmans, SJ, Johnson, BJ, Brioude, J, Angevine, W, Trainer, M, Parrish, DD, Ryerson, TR, Pollack, I, Cullis, PD, Ives, MA. 2011. Measurement of western US baseline ozone from the surface to the tropopause and assessment of downwind impact regions. *J Geophys Res Atmos* **116**(D21).

Cooper, OR, Parrish, DD, Ziemke, J, Balashov, NV, Cupeiro, M, Galbally, IE, Gilge, S, Horowitz, L, Jensen, NR, Lamarque, J-F, Naik, V, Oltmans, SJ, Schwab, J, Shindell, DT, Thompson, AM, Thouret, V, Wang, Y, Zbinden, RM. 2014. Global distribution and trends of tropospheric ozone: An observation-based review. *Elem Sci Anth* **2**: 000029. DOI: http://dx.doi.org/10.12952/journal.elementa.000029.

Cooper, OR, Stohl, A, Hübler, G, Hsie, EY, Parrish, DD, Tuck, AF, Kiladis, GN, Oltmans, SJ, Johnson, BJ, Shapiro, M, Moody, JL, Lefohn, AS. 2005. Direct transport of midlatitude stratospheric ozone into the lower troposphere and marine boundary layer of the tropical Pacific Ocean. *J Geophys Res* **110**: 15. D23310. DOI: http://dx.doi.org/10.1029JD005783.

Cooper, OR, Stohl, A, Trainer, M, Thompson, AM, Witte, JC, Oltmans, SJ, Johnson, BJ, Merrill, J, Moody, JL, Morris, G, Tarasick, D, Forbes, G, Nédélec, P, Fehsenfeld, FC, Meagher, J, Newchurch, MJ, Schmidlin, FJ, Turquety, S, Crawford, JH, Pickering, KE, Baughcum, SL, Brune, WH, Brown, CC. 2006. Large upper tropospheric ozone enhancements above mid-latitude North America during summer: In situ evidence from the IONS and MOZAIC ozone monitoring network. *J Geophys Res* **111**(D24S05). DOI: http://dx.doi.org/10.1029/2006JD007306.

Cooper, PL, Abbatt, JPD. 1996. Heterogeneous interactions of OH and HO_2 radicals with surfaces characteristic of atmospheric particulate matter. *J Phys Chem* **100**(6): 2249–2254.

Cox, RA, Eggleton, AEJ. 1975. Long-range transport of photochemical ozone in north-western Europe. *Nature* **255**(5504): 118–121.

Cristofanelli, P, Bracci, A, Sprenger, M, Marinoni, A, Bonafè, U, Cazolari, F, Duchi, R, Laj, P, Pichon, JM, Roccato, F, Venzac, H, Vuillermoz, E, Bonasoni, P. 2010. Tropospheric ozone variations at the Nepal Climate Observatory-Pyramid (Himalayas, 5079 a.s.l.) and influence of deep stratospheric intrusion events. *Atmos Chem Phys* **10**: 6537–6549.

Cristofanelli, P, Putero, D, Bonasoni, P, Busetto, M, Calzolari, F, Camporeale, G, Grigioni, P, Lupi, A, Petkov, B, Traversi, R, Udisti, R. 2018. Analysis of multi-year near-surface ozone observations at the WMO/GAW "Concordia" station (75 06′ S, 123 20′ E, 3280 m asl–Antarctica). *Atmos Environ* **177**: 54–63.

Crutzen, PJ. 1973. Photochemical reactions initiated by and influencing ozone in unpolluted tropospheric air. *Tellus* **26**: 47–57.

Czader, BH, Rappenglück, B, Percell, P, Byun, DW, Ngan, F, Kim, S. 2012. Modeling nitrous acid and its impact on ozone and hydroxyl radical during the Texas Air Quality Study 2006. *Atmos Chem Phys* **12**: 6939–6951. DOI: http://dx.doi.org/10.5194/acp-12-6939-2012.

Danielsen, EF. 1968. Stratospheric-tropospheric exchange based on radioactivity, ozone and potential vorticity. J Atmos Sci **25**: 502–518.

Danielsen, EF, Mohnen, VA. 1977. Project dustorm report: Ozone transport, in situ measurements, and meteorological analyses of tropopause folding. *J Geophys Res* **82**: 5867–5877.

Davidson, EA, Kingerlee, W. 1997. A global inventory of nitric oxide emissions from soils. *Nutr Cycling Agroecosyst* **48**: 37–50.

DeCaria, AJ, Pickering, KE, Stenchikov, GL, Ott, LE. 2005. Lightning-generated NOx and its impact on tropospheric ozone production: A three-dimensional modeling study of a Stratosphere-Troposphere Experiment: Radiation, Aerosols and Ozone (STERAO-A) thunderstorm. *J Geophys Res* **110**: 1–13. DOI: http://dx.doi.org/10.1029/2004JD005556.

de la Torre, D. 2008. Quantification of mesophyll resistance and apoplastic ascorbic acid as an antioxidant for tropospheric ozone in durum wheat (Triticum durum Desf. cv. Camacho). *Sci World J* **8**: 1197–1209.

De Foy, B, Lu, Z, Streets, DG. 2016. Satellite NO_2 retrievals suggest China has exceeded its NO_x reduction goals from the twelfth Five-Year Plan. *Scientific Reports* **6**: 35912.

Dentener, FJ, Crutzen, PJ. 1993. Reaction of N_2O_5 on tropospheric aerosols: Impact on the global distributions of NO_x, O_3, and OH. *J Geophys Res Atmos* **98**(D4): 7149–7163.

Ding, A, Wang, T. 2006. Influence of stratosphere-to-troposphere exchange on the seasonal cycle of surface ozone at Mount Waliguan in western China. *Geophys Res Lett* **33**(3): L03803.

Doherty, RM, Wild, O, Shindell, DT, Zeng, D, MacKenzie, IA, Collins, WJ, Fiore, AM, Stevenson, DS, Schultz, MG, Hess, P, Derwent, RG, Keating, T. 2013. Impacts of climate change on surface ozone and intercontinental ozone pollution: A multi-model study. *J Geophys Res* **118**: 3744–3763. DOI: http://dx.doi.org/10.1002/jgrd.50266.

Dolwick, P, Akhtar, F, Baker, K, Possiel, N, Simon, H, Tonnesen, G. 2015. Comparison of background ozone estimates over the western United States based on two separate model methodologies. *Atmos Environ* **109**: 282–296. DOI: http://dx.doi.org/10.1016/j.atmosenv.2015.01.005.

Dupart, Y, King, SM, Nekat, B, Nowak, A, Wiedensohler, A, Herrmann, H, David, G, Thomas, B, Miffre, A, Rairoux, P, D'Anna, B. 2012. Mineral dust photochemistry induces nucleation events in the presence of SO_2. *PNAS* **109**(51): 20842–20847.

Dusanter, S, Vimal, D, Stevens, PS, Volkamer, R, Molina, LT. 2009. Measurements of OH and HO_2 concentrations during the MCMA-2006 field campaign–Part 1: Deployment of the Indiana University laser-induced fluorescence instrument. *Atmos Chem Phys* **9**: 1665–1685.

Ebojie, F, Burrows, JP, Gebhardt, C, Ladstätter-Weißenmayer, A, von Savigny, C, Rozanov, A, Weber, M, Bovensmann, H. 2016. Global tropospheric ozone variations from 2003 to 2011 as seen by SCIAMACHY. *Atmos Chem Phys* **16**: 417–436. DOI: http://dx.doi.org/10.5194/acp-16-417-2016.

Eckhardt, S, Stohl, A, Beirle, S, Spichtinger, N, James, P, Forster, C, Junker, C, Wagner, T, Platt, U, Jennings, SG. 2003. The North Atlantic Oscillation controls air pollution transport to the Arctic. *Atmos Chem Phys* **3**: 1769–1778.

Edwards, PM, Brown, SS, Roberts, JM, Ahmadov, R, Banta, RM, Degouw, JA, Dube, WP, Field, RA, Flynn, JH, Gilman, JB, Graus, M. 2014. High winter ozone pollution from carbonyl photolysis in an oil and gas basin. *Nature* **514**(7522): 351–354.

Edwards, PM, Evans, MJ. 2017. A new diagnostic for tropospheric ozone production. *Atmos Chem Phys* **17**: 13669–13680. DOI: http://dx.doi.org/10.5194/acp-17-13669-2017.

Elshorbany, YF, Kurtenbach, R, Wiesen, P, Lissi, E, Rubio, M, Villena, G, Gramsch, E, Rickard, AR, Pilling, MJ, Kleffmann, J. 2009. Oxidation capacity of the city air of Santiago, Chile. *Atmos Chem Phys* **9**: 2257–2273. DOI: http://dx.doi.org/10.5194/acp-9-2257-2009.

Elshorbany, Y, Barnes, I, Becker, KH, Kleffmann, J, Wiesen, P. 2010. Sources and cycling of tropospheric hydroxyl radicals–an overview. *Zeitschrift für Physikalische Chemie* **224**(7–8): 967–987.

Elshorbany, YF, Steil, B, Brühl, C, Lelieveld, J. 2012a. Impact of HONO on global atmospheric chemistry calculated with an empirical parameterization in the EMAC model. *Atmos Chem Phys* **12**(20): 9977–10000.

Elshorbany, YF, Kleffmann, J, Hofzumahaus, A, Kurtenbach, R, Wiesen, P, Brauers, T, Bohn, B, Dorn, HP, Fuchs, H, Holland, F, Rohrer, F. 2012b. HOx budgets during HOxComp: A case study of HOx chemistry under NOx-limited conditions. *J Geophys Res Atmos* **117**(D3).

Emmerson, KM, Galbally, IE, Guenther, AB, Paton-Walsh, C, Guerette, E.-A, Cope, ME, Keywood, MD, Lawson, SJ, Molloy, SB, Dunne, E, Thatcher, M, Karl, T, Maleknia, SD. 2016. Current estimates of biogenic emissions from eucalypts uncertain for southeast Australia. *Atmos Chem Phys* **16**: 6997–7011. DOI: http://dx.doi.org/10.5194/acp-16-6997-2016.

Esler, JG, Tan, DG, Haynes, PH, Evans, MJ, Law, KS, Plantevin, PH, Pyle, JA. 2001. Stratosphere-troposphere exchange: Chemical sensitivity to mixing. *J Geophys Res Atmos* **106**(D5): 4717–4731.

Espada, C, Grossenbacher, J, Ford, K, Couch, T, Shepson, PB. 2005. The production of organic nitrates from various anthropogenic volatile organic compounds. *Int J Chem Kinet* **37**: 675–685.

Eyring, V, Arblaster, JM, Cionni, I, Sedláček, J, Perlwitz, J, Young, PJ, Bekki, S, Bergmann, D, Cameron-Smith, P, Collins, WJ, Faluvegi, G. 2013. Long-term ozone changes and associated climate impacts in CMIP5 simulations. *J Geophys Res Atmos* **118**(10): 5029–5060.

Eyring, V, Bony, S, Meehl, GA, Senior, CA, Stevens, B, Stouffer, RJ, Taylor, KE. 2016. Overview of the Coupled Model Intercomparison Project Phase 6 (CMIP6) experimental design and organization. *Geosci. Model Dev* **9**(5): 1937–1958.

Fabry, C, Buisson, H. 1913. L'absorption de l'ultra-violet par l'ozone et la limite du spectre solaire. *J Phys Theor Appl* **3**: 196–206. DOI: http://dx.doi.org/10.1051/jphystap:019130030019601.

Fares, S, McKay, M, Holzinger, R, Goldstein, AH. 2010. Ozone fluxes in a Pinus ponderosa ecosystem are dominated by non-stomatal processes: Evidence from long-term continuous measurements. *Agric For Meteorol* **150**(3): 420–431. DOI: http://dx.doi.org/10.1016/j.agrformet.2010.01.007.

Feng, Y, Penner, JE. 2007. Global modeling of nitrate and ammonium: Interaction of aerosols and tropospheric chemistry. *J Geophys Res* **112**(D01304). DOI: http://dx.doi.org/10.1029/2005JD006404.

Fickert, S, Adams, JW, Crowley, JN. 1999. Activation of Br_2 and BrCl via uptake of HOBr onto aqueous salt solutions. *J GeophysiRes Atmos* **104**(D19): 23719–23727.

Finlayson-Pitts, BJ, Livingston, FE, Berko, HN. 1989. Synthesis and identification by infrared spectroscopy of gaseous nitryl bromide, $BrNO_2$. *J Phys Chem* **93**(11): 4397–4400.

Finney, DL, Doherty, RM, Wild, O, Stevenson, DS, MacKenzie, IA, Blyth, AM. 2018. A projected decrease in lightning under climate change. *Nat Clim Change* **8**(3): 210–213.

Finney, DL, Doherty, RM, Wild, O, Young, PJ, Butler, A. 2016. Response of lightning NO_x emissions and ozone production to climate change: Insights from the Atmospheric Chemistry and Climate Model Intercomparison Project. *Geophys Res Lett* **43**(10): 5492–5500.

Fiore, AM, Dentener, FJ, Wild, O, Cuvelier, C, Schultz, MG, Hess, P, Textor, C, Schulz, M, Doherty, RM, Horowitz, LW, MacKenzie, IA, Sanderson, MG, Shindell, DT, Stevenson, DS, Szopa, S, Van Dingenen, R, Zeng, G, Atherton, C, Bergmann, D, Bey, I, Carmichael, G, Collins, WJ, Duncan, BN, Faluwegi, G, Folberth, G, Gaus, M, Gong, S, Hauglustaine, D, Holloway, T, Isaksen, ISA, Jacob, DJ, Jonson, JE, Kaminski, JW, Keating, TJ, Lupu, A, Marmer, E, Montanaro, V, Park, RJ, Pitari, G, Pitari, G, Pringle, KJ, Pyle, JA, Schroeder, S, Vivanco, MG, Wind, P, Woijcik, G, Wu, S, Zuber, A. 2009. Multimodel estimates of intercontinental source-receptor relationships for ozone pollution. *J Geophys Res* **114**: 21. D04301. DOI: http://dx.doi.org/10.1029/2008JD010816.

Fiore, AM, Naik, V, Spracklen, D, Steiner, A, Unger, N, Prather, M, Bergmann, D, Cameron-Smith, PJ, Collins, B, Dalsøren, S, Folberth, G, Ginoux, P, Horowitz, LW, Josse, B, Lamarque, J-F, Nagashima, T, O'Connor, F, Rumbold, S, Shindell, DT, Skeie, RB, Sudo, K, Takemura, T, Zeng, G. 2012. Global air quality and climate. *Chem Soc Rev* **41**: 6663–6683.

Fisher, JA, Jacob, DJ, Travis, KR, Kim, PS, Marais, EA, Miller, CC, Yu, K, Zhu, L, Yantosca, RM, Sulprizio, MP, Mao, J. 2016. Organic nitrate chemistry and its implications for nitrogen budgets in an isoprene- and monoterpene-rich atmosphere: Constraints from aircraft (SEAC4RS) and ground-based (SOAS) observations in the Southeast US. *Atmos Chem Phys* **16**(9): 5969–5991.

Fishman, J, Bowman, KW, Burrows, JP, Richter, A, Chance, KV, Edwards, DP, Martin, RV, Morris, GA, Pierce, RB, Ziemke, JR, Al-Saadi, JA. 2008. Remote sensing of tropospheric pollution from space. *Bull Amer Meteor* **89**(6): 805–822.

Fishman, J, Seiler, W. 1983. Correlative nature of ozone and carbon monoxide in the troposphere: Implications for the tropospheric ozone budget. *J Geophys Res* **88**: 3662–3670.

Fishman, J, Solomon, S, Crutzen, PJ. 1979. Observational and theoretical evidence in support of a significant in-situ photochemical source of tropospheric ozone. *Tellus* **31**: 432–446.

Fishman, J, Watson, CE, Larsen, JC, Logan, JA. 1990. Distribution of tropospheric ozone determined from satellite data. *Geophys Res* **95**: 3599–3617.

Fowler, D, Flechard, C, Cape, JN, Storeton-West, RL, Coyle, M. 2001. Measurements of ozone deposition to vegetation quantifying the flux, the stomatal and non-stomatal components. *Water Air Soil Pollut* **130**: 63–74. DOI: http://dx.doi.org/10.1023/A:1012243317471.

Fowler, D, Pilegaard, K, Sutton, MA, Ambus, P, Raivonen, M, Duyzer, J, Simpson, D, Fagerli, H, Fuzzi, S, Schjoerring, JK, Granier, C, Neftel, A, Isaksen, ISA, Laj, P, Maione, M, Monks, PS, Burkhardt, J, Daemmgen, U, Neirynck, J, Personne, E, Wichink Kruit, RJ, Butterbach-Bahl, K, Flechard, C, Tuovinen, JP, Coyle, M, Gerosa, G, Loubet, B, Altimir, N, Gruenhage, L, Ammann, C, Cieslik, S, Paoletti, E, Mikkelsen, TN, Ro-Poulsen, H, Cellier, P, Cape, JN, Horvath, L, Loreto, F, Niinemets, U, Palmer, PI, Rinne, J, Misztal, P, Nemitz, E, Nilsson, D, Pryor, S, Gallagher, MW, Vesala, T, Skiba, U, Brueggemann, N, Zechmeister-Boltenstern, S, Williams, J, O'Dowd, C, Facchini, MC, de Leeuw, G, Flossman, A, Chaumerliac, N, Erisman, JW. 2009. Atmospheric composition change: Ecosystems–Atmosphere interactions. *Atmos Environ* **43**: 5193–5267.

Franz, M, Simpson, D, Arneth, A, Zaehle, S. 2017. Development and evaluation of an ozone deposition scheme for coupling to a terrestrial biosphere model. *Biogeosciences* **14**: 45–71. DOI: http://dx.doi.org/10.5194/bg-14-45-2017.

Galbally, IE. 1971. Ozone profiles and ozone fluxes in the atmospheric surface layer. *Q J R Meteorol Soc* **97**(411): 18–29.

Galbally, IE. 1974. Gas transfer near the earth's surface. *Adv Geophys* **18B**: 329–339.

Galbally, IE, Bentley, ST, Meyer, CP. 2000. Mid-latitude marine boundary-layer ozone destruction at visible sunrise observed at Cape Grim, Tasmania, 41°S. *Geophys Res Lett* **27**(23): 3841–3844.

Galbally, IE, Roy, CR. 1978. Loss of fixed nitrogen from soils by nitric oxide exhalation. *Nature* **275**: 734–735.

Galbally, IE, Roy, CR. 1980. Destruction of ozone at the Earth's surface. *Q J R Meteorol Soc* **106**(449): 599–620.

Ganzeveld, L, Helmig, D, Fairall, CW, Hare, J, Pozzer, A. 2009. Atmosphere-ocean ozone exchange: A global modeling study of biogeochemical, atmospheric, and waterside turbulence dependencies. *Global Biogeochem Cy* **23**: GB4021. DOI: http://dx.doi.org/10.1029/2008GB003301.

Garland, JA, Curtis, H. 1981. Emission of iodine from the sea surface in the presence of ozone. *J Geophys Res* **86**(C4): 3183–3186.

Garland, JA, Elzerman, AW, Penkett, SA. 1980. The mechanism for dry deposition of ozone to seawater surfaces. *J Geophys Res* **85**(C12): 7488–7492.

Gaudel, A, Cooper, OR, Ancellet, G, Barret, B, Boynard, A, Burrows, JP, Clerbaux, C, Coheur, P-F, Cuesta, J, Cuevas, E, Doniki, S, Dufour, G, Ebojie, F, Foret, G, Garcia, O, Granados-Muñoz, MJ, Hannigan, JW, Hase, F, Hassler, B, Huang, G, Hurtmans, D, Jaffe, D, Jones, N, Kalabokas, P, Kerridge, B, Kulawik, S, Latter, B, Leblanc, T, Le Flochmoën, E, Lin, W, Liu, J, Liu, X, Mahieu, E, McClure-Begley, A, Neu, JL, Osman, M, Palm, M, Petetin, H, Petropavlovskikh, I, Querel, R, Rahpoe, N, Rozanov, A, Schultz, MG, Schwab, J, Siddans, R, Smale, D, Steinbacher, M, Tanimoto, H, Tarasick, DW, Thouret, V, Thompson, AM, Trickl, T, Weatherhead, E, Wespes, C, Worden, HM, Vigouroux, C, Xu, X, Zeng, G, Ziemke, J. 2018. Tropospheric Ozone Assessment Report: Present-day distribution and trends of tropospheric ozone relevant to climate and global atmospheric chemistry model evaluation. *Elem Sci Anth* **6**(1): 39. DOI: http://dx.doi.org/10.1525/elementa.291.

George, IJ, Matthews, PSJ, Whalley, LK, Brooks, B, Goddard, A, Baeza-Romero, MT, Heard, DE. 2013. Measurements of uptake coefficients for heterogeneous loss of HO 2 onto submicron inorganic salt aerosols. *Physical Chemistry Chemical Physics* **15**(31): 12829–12845.

Gerosa, G, Finco, A, Mereu, S, Vitale, M, Manes, F, Denti, AB. 2009. Comparison of seasonal variations of ozone exposure and fluxes in a Mediterranean Holm oak forest between the exceptionally dry 2003 and the following year. *Environ Pollut* **157**(5): 1737–1744.

Gordillo-Vazquez, FJ, Pérez-Invernón, FJ, Huntrieser, H, Smith, AK. 2019. Comparison of six lightning parameterizations in CAM5 and the impact on global atmospheric chemistry. *Earth Space Sci* **6**: 2317–2346. DOI: http://dx.doi.org/10.1029/2019EA000873.

Gottschaldt, K, Voigt, C, Jöckel, P, Righi, M, Deckert, R, Dietmüller, S. 2013. Global sensitivity of aviation NO_x effects to the HNO_3-forming channel of the HO_2+ NO reaction. *Atmos Chem Phys* **13**(6): 3003–3025.

Granier, C, et al. n.d. *Changes in anthropogenic emissions over the past four decades in different world regions*, in press.

Granier, C, Bessagnet, B, Bond, T, D'Angiola, A, van der Gon, HD, Frost, GJ, Heil, A, Kaiser, JW, Kinne, S, Klimont, Z, Kloster, J, Lamarque, JF, Liousse, C, Masui, T, Meleux, F, Mieville, A, Ohara, T, Raut, JC, Riahi, K, Schultz, M. 2011. Evolution of anthropogenic and biomass burning emissions of air pollutants at global and regional scales during the 1980–2010 period. *Clim Change* **109**: 163–190. DOI: http://dx.doi.org/10.1007/s10584-011-0154-1.

Grewe, V. 2007. Impact of climate variability on tropospheric ozone. *Sci Total Environ* **374**(1): 167–181.

Griffiths, PT, Murray, LT, Zeng, G, Archibald, AT, Emmons, LK, Galbally, I, Hassler, B, Horowitz, LW, Keeble, J, Liu, J, Moeini, O, Naik, V, O'Connor, FM, Shin, YM, Tarasick, D, Tilmes, S, Turnock, ST, Wild, O, Young, PJ, Zanis, P. 2020. Tropospheric ozone in CMIP6 simulations. *Atmos Chem Phys Discuss*. DOI: http://dx.doi.org/10.5194/acp-2019-1216.

Großmann, K, Frieß, U, Peters, E, Wittrock, F, Lampel, J, Yilmaz, S, Tschritter, J, Sommariva, R, Von Glasow, R, Quack, B, Krüger, K. 2013. Iodine monoxide in the Western Pacific marine boundary layer. *Atmos Chem Phys* **13**(6): 3363–3378.

Guenther, A, Hewitt, CN, Erickson, D, Fall, R, Geron, C, Graedel, T, Harley, P, Klinger, L, Lerdau, M, Mckay, WA, Pierce, T, Scholes, B, Steinbrecher, R, Tallamraju, R, Taylor, J, Zimmerman, PA. 1995. Global-Model of Natural Volatile Organic-Compound Emissions. *J Geophys Res Atmos* **100**(D5): 8873–8892.

Guenther, AB, Karl, T, Harley, P, Wiedinmyer, C, Palmer, PI, Geron, C. 2006. Estimates of global terrestrial isoprene emissions using MEGAN (Model of Emissions of Gases and Aerosols from Nature). *Atmos Chem Phys* **6**: 3181–3210.

Hardacre, C, Wild, O, Emberson, L. 2015. An evaluation of ozone dry deposition in global scale chemistry climate models. *Atmos Chem Phys* **15**(11): 6419–6436.

Harris, SJ, Kerr, JA. 1989. A kinetic and mechanistic study of the formation of alkyl nitrates in the photo-oxidation of n-heptane studied under atmospheric conditions. *Int J Chem Kinet* **21**: 207–218.

Hartley, WN. 1881. On the absorption of solar rays by atmospheric ozone. *J Chem Soc Trans* **39**: 111–128.

Hassler, B, McDonald, BC, Frost, GJ, Borbon, A, Carslaw, DC, Civerolo, K, Granier, C, Monks, PS, Monks, S, Parrish, DD, Pollack, IB, Rosenlof, KH, Ryerson, TB, von Schneidemesser, E, Trainer, M. 2016. Analysis of long-term observations of NOx and CO in megacities and application to constraining emissions inventories. *Geophys Res Lett* **43**: 9920–9930. DOI: http://dx.doi.org/10.1002/2016gl069894.

Hauglustaine, DA, Madronich, S, Ridley, BA, Walega, JG, Cantrell, CA, Shetter, RE, Hüber, G. 1996. Observed and model-calculated photostationary state at Mauna Loa Observatory during MLOPEX 2. *J Geophys Res* **101**(D9): 14681–14696.

Hawkins, E, Sutton, R. 2009. The potential to narrow uncertainty in regional climate predictions. *Bull Amer Meteor* **90**(8): 1095–1108.

Helmig, D, Ganzeveld, L, Butler, T, Oltmans, SJ. 2007. The role of ozone atmosphere-snow gas exchange on polar, boundary-layer tropospheric ozone—A review and sensitivity analysis. *Atmos Chem Phys* **7**: 15–30.

Helmig, D, Lang, EK, Bariteau, L, Boylan, P, Fairall, CW, Ganzeveld, L, Hare, JE, Hueber, J, Pallandt, M. 2012. Atmosphere-ocean ozone fluxes during the TexAQS 2006, STRATUS 2006, GOMECC 2007, GasEx 2008, and AMMA 2008 cruises. *J Geophys Res* **117**: D04305. DOI: http://dx.doi.org/10.1029/2011JD015955.

Hess, PG, Zbinden, R. 2013. Stratospheric impact on tropospheric ozone variability and trends: 1990-2009. *Atmos Chem Phys* **13**(2): 649–674.

Heue, K-P, Coldewey-Egbers, M, Delcloo, A, Lerot, C, Loyola, D, Valks, P, van Roozendael, M. 2016. Trends of tropical tropospheric ozone from 20 years of European satellite measure–ments and perspectives for the Sentinel-5 Precursor. *Atmos Meas Tech* **9**: 5037–5051. DOI: http://dx.doi.org/10.5194/amt-9-5037-2016.

Hoesly, RM, Smith, SJ, Feng, L, Klimont, Z, Janssens-Maenhout, G, Pitkanen, T, Seibert, JJ, Vu, L, Andres, RJ, Bolt, RM, Bond, TC, Dawidowski, L, Kholod, N, Kurokawa, J.-I, Li, M, Liu, L, Lu, Z, Moura, MCP, O'Rourke, PR, Zhang, Q. 2018. Historical (1750–2014) anthropogenic emissions of reactive gases and aerosols from the Community Emissions Data System (CEDS). *Geosci Model Dev* **11**: 369–408. DOI: http://dx.doi.org/10.5194/gmd-11-369-2018.

Holmes, CD, Bertram, TH, Confer, KL, Graham, KA, Ronan, AC, Wirks, CK, Shah, V. 2019. The role of clouds in the tropospheric NOx cycle: A new modeling approach for cloud chemistry and its global implications. *Geophys Res Lett* **46**: 4980–4990. https://doi.org/10.1029/2019GL081990.

Homeyer, CR, Bowman, KP, Pan, LL, Atlas, EL, Gao, RS, Campos, TL. 2011. Dynamical and chemical characteristics of tropospheric intrusions observed during START08. *J Geophys Res Atmos* **116**(D6).

Homeyer, CR, Bowman, KP. 2013. Rossby wave breaking and transport between the tropics and extratropics above the subtropical jet. *J Atmos Sci* **70**(2): 607–626.

Hemispheric Transport of Air Pollution. 2010. Hemispheric transport of air pollution. Part A: Ozone and particulate matter, in Dentener, F, Keating, T, Akimoto, H eds., United Nations. Geneva, Switzerland: 278. ISSN 1014-4625, ISBN 978-92-1-117043-6. Available at http://www.htap.org/publications/2010_report/2010_Final_Report/HTAP%202010%20Part%20A%20110407.pdf. Accessed 13 August 2019.

Hu, L, Jacob, DJ, Liu, X, Zhang, Y, Zhang, L, Kim, PS, Sulprizio, MP, Yantosca, RM. 2017. Global budget of tropospheric ozone: Evaluating recent model advances with satellite (OMI), aircraft (IAGOS), and ozonesonde observations. *Atmos Environ* **167**: 323–334. DOI: http://dx.doi.org/10.1016/j.atmosenv.2017.08.036.

Hu, L, Millet, DB, Baasandorj, M, Griffis, TJ, Turner, P, Helmig, D, Curtis, AJ, Hueber, J. 2015. Isoprene emissions and impacts over an ecological transition region in the US Upper Midwest inferred from tall tower measurements. *J Geophys Res* **120**: 3553–3571. DOI: http://dx.doi.org/10.1002/2014JD022732.

Hudman, RC, Russell, AR, Valin, LC, Cohen, RC. 2010. Interannual variability in soil nitric oxide emissions over the United States as viewed from space. *Atmos Chem Phys* **10**: 9943–9952. DOI: http://dx.doi.org/10.5194/acp-10-9943-2010.

Hughes, C, Johnson, M, von Glasow, R, Chance, R, Atkinson, H, Souster, T, Lee, GA, Clarke, A, Meredith, M, Venables, HJ, Turner, SM, Malin, G, Liss, PS. 2012. Climate-induced change in biogenic bromine emissions from the Antarctic marine biosphere. *Global Biogeochem Cycles* **26**: GB3019. DOI: http://dx.doi.org/10.1029/2012GB004295.

Iglesias-Suarez, F, Badia, A, Fernandez, RP, Cuevas, CA, Kinnison, DE, Tilmes, S, Lamarque, JF, Long, MC, Hossaini, R, Saiz-Lopez, A. 2020. Natural halogens buffer tropospheric ozone in a changing climate. *Nat Clim Change* **10**(2): 147–154.

Ingmann, P, Veihelmann, B, Langen, J, Lamarre, D, Stark, H, Courrèges-Lacoste, GB. 2012. Requirements for the GMES Atmosphere Service and ESA's implementation concept: Sentinels-4/-5 and-5p. *Remote Sens Environ* **120**: 58–69.

Intergovernmental Panel on Climate Change. 2013. Climate change 2013: The physical science basis. Contribution of working group I to the fifth assessment report of the intergovern-mental panel on climate change, in Stocker, TF, Qin, D, Plattner, G-K, Tignor, M, Allen, SK, Boschung, J, Nauels, A, Xia, Y, Bex, V, Midgley, PM eds., Cambridge, UK: Cambridge University Press: 1535.

Jacob, DJ. 2000. Heterogeneous chemistry and tropospheric ozone. *Atmos Environ* **34**(12–14): 2131–2159.

Jacob, DJ, Logan, JA, Murti, PP. 1999. Effect of rising Asian emissions on surface ozone in the United States. *Geophys Res Lett* **26**: 2175–2178.

Jaeglé, L, Wood, R, Wargan, K. 2017. Multiyear composite view of ozone enhancements and stratosphere-to-troposphere transport in dry intrusions of northern hemisphere extratropical cyclones. *J Geophys Res Atmos* **122**(24): 13–436.

Jaffe, DA, Cooper, OR, Fiore, AM, Henderson, BH, Tonnesen, GS, Russell, AG, Henze, DK, Langford, AO, Lin, M, Moore, T. 2018. Scientific assessment of background ozone over the U.S.: Implications for air

quality management. *Elem Sci Anth* **6**(1): 56. DOI: http://dx.doi.org/10.1525/elementa.309.

Jaffe, DA, Wigder, NL. 2012. Ozone production from wildfires: A critical review. *Atmos Environ* **51**: 1–10. DOI: http://dx.doi.org/10.1016/j.atmosenv.2011.11.063.

Jenkin, ME, Saunders, SM, Pilling, MJ. 1997. The tropospheric degradation of volatile organic compounds: a protocol for mechanism development. *Atmos Environ* **31**: 81–104.

Jenkin, ME, Khan, MAH, Shallcross, DE, Bergström, R, Simpson, D, Murphy, KLC, Rickard, AR. 2019. The CRI v2.2 reduced degradation scheme for isoprene. *Atmos Environ* **212**: 172–182.

Jenkin, ME, Watson, LA, Utembe, SR, Shallcross, DE. 2008. A Common Representative Intermediates (CRI) mechanism for VOC degradation. Part 1: Gas phase mechanism development. *Atmos Environ* **42**(31): 7185–7195.

Jöckel, P, Tost, H, Pozzer, A, Brühl, C, Buchholz, J, Ganzeveld, L, Hoor, P, Kerkweg, A, Lawrence, MG, Sander, R, Steil, B, Stiller, G, Tanarhte, M, Taraborrelli, D, van Aardenne, J, Lelieveld, J. 2006. The atmospheric chemistry general circulation model ECHAM5/MESSy1: Consistent simulation of ozone from the surface to the mesosphere. *Atmos Chem Phys* **6**: 5067–5104. DOI: http://dx.doi.org/10.5194/acp-6-5067-2006.

Jöckel, P, Tost, H, Pozzer, A, Kunze, M, Kirner, O, Brenninkmeijer, CAM, Brinkop, S, Cai, D S, Dyroff, C, Eckstein, J, Frank, F, Garny, H, Gottschaldt, K-D, Graf, P, Grewe, V, Kerkweg, A, Kern, B, Matthes, S, Mertens, M, Meul, S, Neumaier, M, Nützel, M, Oberländer-Hayn, S, Ruhnke, R, Runde, T, Sander, R, Scharffe, D, Zahn, A. 2016. Earth System Chemistry integrated Modelling (ESCiMo) with the Modular Earth Submodel System (MESSy) version 2.51. *Geosci Model Dev* **9**: 1153–1200. DOI: http://dx.doi.org/10.5194/gmd-9-1153-2016.

Johnson, D, Marston, G. 2008. The gas-phase ozonolysis of unsaturated volatile organic compounds in the troposphere. *Chemical Society Reviews* **37**(4): 699–716.

Jones, B, O'Neill, BC. 2016. Spatially explicit global population scenarios consistent with the Shared Socioeconomic Pathways. *Environ Res Lett* **11**(8): 084003.

Jones, CE, Hornsby, KE, Dunk, RM, Leigh, RJ, Carpenter, LJ. 2009. Coastal measurements of short-lived reactive iodocarbons and bromocarbons at Roscoff, Brittany during the RHaMBLe campaign. *Atmos Chem Phys* **9**: 8757–8769. DOI: http://dx.doi.org/10.5194/acp-9-8757-2009.

Jones, ITN, Wayne, RP. 1970. The photolysis of ozone by ultraviolet radiation: IV. Effect of photolysis wavelength on primary step. *Proc R Soc* **A319**: 273.

Jonson, JE, Simpson, D, Fagerli, H, Solberg, S. 2006. Can we explain the trends in European ozone levels? *Atmos Chem Phys* **6**: 51–66.

Junge, CE. 1962. Global ozone budget and exchange between stratosphere and troposphere. *Tellus* **14**: 363–377.

Junge, CE. 1972. The cycle of atmospheric gases—Natural and man made. *Q J R Meteorol Soc* **98**: 711–729.

Kasibhatla, P, Sherwen, T, Evans, MJ, Carpenter, LJ, Reed, C, Alexander, B, Chen, Q, Sulprizio, MP, Lee, JD, Read, KA, Bloss, W, Crilley, LR, Keene, WC, Pszenny, AAP, Hodzic, A. 2018. Global impact of nitrate photolysis in sea-salt aerosol on NOx, OH, and O_3 in the marine boundary layer. *Atmos Chem Phys* **18**: 11185–11203. DOI: http://dx.doi.org/10.5194/acp-18-11185-2018.

Keyser, D, Shapiro, MA. 1986. A review of the structure and dynamics of upper-level frontal zones. *Monthly Wea Rev* **114**: 452–499.

Khan, MAH, Cooke, MC, Utembe, SR, Archibald, AT, Derwent, RG, Jenkin, ME, Morris, WC, South, N, Hansen, JC, Francisco, JS, Percival, CJ. 2015. Global analysis of peroxy radicals and peroxy radical-water complexation using the STOCHEM-CRI global chemistry and transport model. *Atmos Environ* **106**: 278–287.

Kleffmann, J. 2007. Daytime sources of nitrous acid (HONO) in the atmospheric boundary layer. *Chem Phys Chem* **8**(8): 1137–1144.

Kleffmann, J, Gavriloaiei, T, Hofzumahaus, A, Holland, F, Koppmann, R, Rupp, L, Schlosser, E, Siese, M, Wahner, A. 2005. Daytime formation of nitrous acid: A major source of OH radicals in a forest. *Geophys Res Lett* **32**(5).

Kim, J, Jeong, U, Ahn, MH, Kim, JH, Park, RJ, Lee, H, Song, CH, Choi, YS, Lee, KH, Yoo, JM, Jeong, MJ. 2020. New era of air quality monitoring from space: Geostationary Environment Monitoring Spectrometer (GEMS). *Bull Amer Meteor Soc* **101**: E1–E22. DOI: http://dx.doi.org/10.1175/BAMS-D-18-0013.1.

Knowland, KE, Ott, LE, Duncan, BN, Wargan, K. 2017. Stratospheric intrusion-influenced ozone air quality exceedances investigated in the NASA MERRA-2 reanalysis. *Geophys Res Lett* **44**(20): 10–691.

Kreher, K, Keys, JG, Johnston, PV, Platt, U, Liu, X. 1996. Ground-based measurements of OClO and HCl in austral spring 1993 at Arrival Heights, Antarctica. *Geophys Res Lett* **23**(12): 1545–1548.

Krotkov, NA, McLinden, CA, Li, C, Lamsal, LN, Celarier, EA, Marchenko, SV, Swartz, WH, Bucsela, EJ, Joiner, J, Duncan, BN, Boersma, KF, Veefkind, JP, Levelt, PF, Fioletov, VE, Dickerson, RR, He, H, Lu, Z, Streets, DG. 2016. Aura OMI observations of regional SO_2 and NO_2 pollution changes from 2005 to 2015. *Atmos Chem Phys* **16**(7): 4605–4629.

Kumar, R, Barth, MC, Madronich, S, Naja, M, Carmichael, GR, Pfister, GG, Knote, C, Brasseur, GP, Ojha, N, Sarangi, T. 2014. Effects of dust aerosols on tropospheric chemistry during a typical pre-monsoon season dust storm in northern India. *Atmos Chem Phys* **14**: 6813–6834.

Kumar, R, Barth, MC, Pfister, GG, Delle Monache, L, Lamarque, JF, Archer-Nicholls, S, Tilmes, S,

Ghude, SD, Wiedinmyer, C, Naja, M, Walters, S. 2018. How will air quality change in South Asia by 2050? *J Geophys Res* 123. DOI: http://dx.doi.org/10.1002/2017JD027357.

Kurokawa, J, Ohara, T, Morikawa, T, Hanayama, S, Janssens-Maenhout, G, Fukui, T, Kawashima, K, Akimoto, H. 2013. Emissions of air pollutants and greenhouse gases over Asian regions during 2000–2008: Regional Emission inventory in ASia (REAS) version 2. *Atmos Chem Phys* **13**(21): 11019–11058.

Kurpius, MR, Goldstein, AH. 2003. Gasphase chemistry dominates O3 loss to a forest, implying a source of aerosols and hydroxyl radicals to the atmosphere. *Geophys Res Lett* **30**(7): 1371. DOI: http://dx.doi.org/10.1029/2002GL016785.

Kurtenbach, R, Becker, KH, Gomes, JAG, Kleffmann, J, Lörzer, JC, Spittler, M, Wiesen, P, Ackermann, R, Geyer, A, Platt, U. 2001. Investigations of emissions and heterogeneous formation of HONO in a road traffic tunnel. *Atmos Environ* **35**(20): 3385–3394.

Lamarque, JF, Bond, TC, Eyring, V, Granier, C, Heil, A, Klimont, Z, Lee, D, Liousse, C, Mieville, A, Owen, B, Schultz, MG, Shindell, D, Smith, SJ, Stehfest, E, Van Aardenne, J, Cooper, OR, Kainuma, M, Mahowald, N, McConnell, JR, Naik, V, Riahi, K, van Vuuren, DP. 2010. Historical (1850–2000) gridded anthropogenic and biomass burning emissions of reactive gases and aerosols: Methodology and application. *Atmos Chem Phys* **10**(15): 7017–7039.

Lamarque, JF, Langford, AO, Proffitt, MH. 1996. Cross-tropopause mixing of ozone through gravity wave breaking: Observation and modeling. *J Geophys Res* **101**: 22969–22976.

Langford, AO, Aikin, KC, Eubank, CS, Williams, EJ. 2009. Stratospheric contribution to high surface ozone in Colorado during springtime. *Geophys Res Lett* **36**(12).

Langford, AO, Pierce, RB, Schultz, PJ. 2015a. Stratospheric intrusions, the Santa Ana winds, and wildland fires in Southern California. *Geophys Res Lett* **42**: 6091–6097. DOI: http://dx.doi.org/10.1002/2015GL064964.

Langford, AO, Senff, CJ, Alvarez Ii, RJ, Brioude, J, Cooper, OR, Holloway, JS, Lin, MY, Marchbanks, RD, Pierce, RB, Sandberg, SP, Weickmann, AM. 2015b. An overview of the 2013 Las Vegas Ozone Study (LVOS): Impact of stratospheric intrusions and long-range transport on surface air quality. *Atmos Environ* **109**: 305–322.

Langford, AO, Alvarez, RJ, Brioude, J, Fine, R, Gustin, MS, Lin, MY, Marchbanks, RD, Pierce, RB, Sandberg, SP, Senff, CJ, Weickmann, AM. 2017. Entrainment of stratospheric air and Asian pollution by the convective boundary layer in the southwestern US. *J Geophys Res Atmos* **122**(2): 1312–1337.

Lee, JD, Helfter, C, Purvis, RM, Beevers, SD, Carslaw, DC, Lewis, AC, Møller, SJ, Tremper, A, Vaughan, A, Nemitz, EG. 2015. Measurement of NOx fluxes from a tall tower in central London, UK and comparison with emissions inventories. *Environ Sci Technol* **49**(2): 1025–1034.

Lefohn, AS, Wernli, H, Shadwick, D, Limbach, S, Oltmans, SJ, Shapiro, M. 2011. The importance of stratospheric-tropospheric transport in affecting surface ozone concentrations in the western and northern tier of the United States. *Atmos Environ* **45**: 4845–4857.

Lefohn, AS, Wernli, H, Shadwick, D, Oltmans, SJ, Shapiro, M. 2012. Quantifying the importance of stratospheric-tropospheric transport on surface ozone concentrations at high- and low-elevation monitoring sites in the United States. *Atmos Environ* **62**: 646–656.

Lefohn, AS, Emery, C, Shadwick, D, Wernli, H, Jung, J, Oltmans, SJ. 2014. Estimates of background surface ozone concentrations in the United States based on model-derived source apportionment. *Atmos Environ* **84**: 275–288.

Lelieveld, J, Crutzen, PJ. 1990. Influences of cloud photochemical processes on tropospheric ozone. *Nature* **343**(6255): 227–233.

Lelieveld, J, Gromov, S, Pozzer, A, Taraborrelli, D. 2016. Global tropospheric hydroxyl distribution, budget and reactivity. *Atmos Chem Phys* **16**: 12477–12493.

Leser, H, Hönninger, G, Platt, U. 2003. MAX-DOAS measurements of BrO and NO_2 in the marine boundary layer. *Geophys Res Lett* **30**: 1537. DOI: http://dx.doi.org/10.1029/2002GL015811.

Leventidou, E, Weber, M, Eichmann, K-U, Burrows, JP, Heue, K-P, Thompson, AM, Johnson, BJ. 2018. Harmonisation and trends of 20-year tropical tropospheric ozone data. *Atmos Chem Phys* **18**: 9189–9205. DOI: http://dx.doi.org/10.5194/acp-18-9189-2018.

Levy, H II. 1971. Normal atmosphere: Large radical and formaldehyde concentrations predicted. *Science* **173**: 141–143.

Levy, H II. 1972. Photochemistry of the lower troposphere. *Planet Space Sci* **20**: 919–935.

Levy, H II. 1973. Photochemistry of minor constituents in the troposphere. *Planet Space Sci* **21**(4): 575–591.

Li, G, Lei, W, Zavala, M, Volkamer, R, Dusanter, S, Stevens, P, Molina, LT. 2010. Impacts of HONO sources on the photochemistry in Mexico City during the MCMA-2006/MILAGO Campaign. *Atmos Chem Phys* **10**: 6551–6567.

Li, K, Jacob, DJ, Liao, H, Shen, L, Zhang, Q, Bates, KH. 2019. Anthropogenic drivers of 2013–2017 trends in summer surface ozone in China. *PNAS* **116**(2): 422. DOI: http://dx.doi.org/10.1073/pnas.1812168116.

Li, Q, Badia, A, Wang, T, Sarwar, G, Fu, X, Zhang, L, Zhang, Q, Fung, J, Cuevas, CA, Wang, S, Zhou, B, Saiz-Lopez, A. 2020. Potential effect of halogens on atmospheric oxidation and air quality in china. *J Geophys Res Atmos* **125**. DOI: https://doi.org/10.1029/2019JD032058.

Li, X, Rohrer, F, Hofzumahaus, A, Brauers, T, Häseler, R, Bohn, B, Broch, S, Fuchs, H, Gomm, S,

Holland, F, Jäger, J. 2014. Missing gas-phase source of HONO inferred from Zeppelin measurements in the troposphere. *Science* **344**(6181): 292–296.

Lim, YB, Ziemann, PJ. 2005. Products and mechanism of secondary organic aerosol formation from reactions of n-alkanes with OH radicals in the presence of NOx. *Environ Sci Technol* **39**: 9229–9236.

Lin, MY, Fiore, AM, Cooper, OR, Horowitz, LW, Langford, AO, Levy, H, II, Johnson, BJ, Naik, V, Oltmans, SJ, Senff, CJ. 2012a. Springtime high ozone events over the western United States: Quantifying the role of stratospheric intrusions. *Geophys Res* **117**: 20. D00V22. DOI: http://dx.doi.org/10.1029/2012JD018151.

Lin, MY, Fiore, AM, Horowitz, LW, Cooper, OR, Naik, V, Holloway, J, Johnson, BJ, Middlebrook, AM, Oltmans, SJ, Pollack, IB, Ryerson, TB, Warner, JX, Widinmyer, C, Wilson, J, Wyman, B. 2012b. Transport of Asian ozone pollution into surface air over the western United States in spring. *J Geophys Res* **117**: 20. D00V07. DOI: http://dx.doi.org/10.1029/2011JD016961.

Lin, MY, Horowitz, LW, Oltmans, SJ, Fiore, AM, Fan, S. 2014. Tropospheric ozone trends at Mauna Loa Observatory tied to decadal climate variability. *Nat Geosci* **7**: 136–143. DOI: http://dx.doi.org/10.1038/ngeo2066.

Lin, MY, Fiore, AM, Horowitz, LW, Langford, AO, Oltmans, SJ, Tarasick, D, Rieder, HE. 2015. Climate variability modulates western US ozone air quality in spring via deep stratospheric intrusions. *Nat Commun* **6**(1): 7105. DOI: http://dx.doi.org/10.1038/ncomms8105.

Lin, MY, Zhang, Z, Su, L, Hill-Falkenthal, J, Priyadarshi, A, Zhang, Q, Zhang, G, Kang, S, Chan, C-Y, Thiemens, MH. 2016. Resolving the impact of stratosphere-to-troposphere transport on the sulfur cycle and surface ozone over the Tibetan Plateau using a cosmogenic 35S tracer. *J Geophys Res* **121**: 439–456. DOI: http://dx.doi.org/10.1002/2015JD023801.

Lin, MY, Horowitz, LW, Payton, R, Fiore, AM, Tonnesen, G. 2017. US surface ozone trends and extremes from 1980 to 2014: Quantifying the roles of rising Asian emissions, domestic controls, wildfires, and climate. *Atmos Chem Phys* **17**. DOI: http://dx.doi.org/10.5194/acp-17-2943-2017

Lin, MY, Malyshev, S, Shevliakova, E, Paulot, F, Horowitz, LW, Fares, S, Mikkelsen, TN, Zhang, L. 2019. Sensitivity of ozone dry deposition to ecosystem-atmosphere interactions: A critical appraisal of observations and simulations. *Global Biogeochem Cy* **33**(10): 1264–1288.

Lin, M, Horowitz, LW, Xie, Y, Paulot, F, Malyshev, S, Shevliakova, E, Finco, A, Gerosa, G, Kubistin, D, Pilegaard, K. 2020. Vegetation feedbacks during drought exacerbate ozone air pollution extremes in Europe. *Nature Climate Change* **10**(5): 444–451.

Liu, SC, Trainer, M, Carroll, MA, Hübler, G, Montzka, DD, Norton, RB, Ridley, BA, Walega, JG, Atlas, EL, Heikes, BG, Huebert, BJ, Warren, W. 1992. A study of the photochemistry and ozone budget during the Mauna Loa Observatory photochemistry experiment. *J Geophys Res* **97**(D10): 10463–10471.

Long-Range Transport of Air Pollution Convention. 2015. Draft Chapter III: Mapping critical levels for vegetation, in *Manual on methodologies and criteria for modelling and mapping critical loads and levels and air pollution effects, risks and trends*. Available at http://icpmapping.org/Mapping_Manual. Accessed 13 August 2019.

Lu, X, Zhang, L, Zhao, Y, Jacob, DJ, Hu, Y, Hu, L, Gao, M, Liu, X, Petropavlovskikh, I, McClure-Begley, A, Querel, R. 2018. Surface and tropospheric ozone trends in the Southern Hemisphere since 1990: Possible linkages to poleward expansion of the Hadley circulation. *Sci Bull*. DOI: http://dx.doi.org/10.1016/j.scib.2018.12.021.

Luhar, AK, Galbally, IE, Woodhouse, MT, Thatcher, M. 2017. An improved parameterisation of ozone dry deposition to the ocean and its impact in a global climate-chemistry model. *Atmos Chem Phys* **17**: 3749–3767. DOI: http://dx.doi.org/10.5194/acp-17-3749-2017.

Luhar, AK, Woodhouse, MT, Galbally, IE. 2018. A revised global ozone dry deposition estimate based on a new two-layer parameterisation for air–sea exchange and the multi-year MACC composition reanalysis. *Atmos Chem Phys* **18**: 4329–4348. DOI: http://dx.doi.org/10.5194/acp-18-4329-2018.

Luo, C, Wang, Y, Koshak, WJ. 2017. Development of a self-consistent lightning NOx simulation in large-scale 3-D models. *J Geophys Res Atmos* **122**: 3141–3154. DOI: http://dx.doi.org/10.1002/2016JD026225.

Mahajan, AS, Gómez Martín, JC, Hay, TD, Royer, S-J, Yvon-Lewis, S, Liu, Y, Hu, L, Prados-Roman, C, Ordóñez, C, Plane, JMC, Saiz-Lopez, A. 2012. Latitudinal distribution of reactive iodine in the Eastern Pacific and its link to open ocean sources. *Atmos Chem Phys* **12**: 11609–11617. DOI: http://dx.doi.org/10.5194/acp-12-11609-2012.

Mahajan, AS, Oetjen, H, Lee, JD, Saiz-Lopez, A, McFiggans, GB, Plane, JM. 2009. High bromine oxide concentrations in the semi-polluted boundary layer. *Atmos Environ* **43**(25): 3811–3818.

Mahajan, AS, Plane, JMC, Oetjen, H, Mendes, L, Saunders, RW, Saiz-Lopez, A, Jones, CE, Carpenter, LJ, McFiggans, GB. 2010. Measurement and modelling of tropospheric reactive halogen species over the tropical Atlantic Ocean. *Atmos Chem Phys* **10**: 4611–4624. DOI: http://dx.doi.org/10.5194/acp-10-4611-2010.

Maljanen, M, Yli-Pirilä, P, Hytönen, J, Joutsensaari, J, Martikainen, PJ. 2013. Acidic northern soils as sources of atmospheric nitrous acid (HONO). *Soil Biology and Biochemistry* **67**: 94–97.

Mao, J, Jacob, DJ, Evans, MJ, Olson, JR, Ren, X, Brune, WH, Clair, JS, Crounse, JD, Spencer, KM, Beaver, MR, Wennberg, PO. 2010. Chemistry of hydrogen

oxide radicals (HOx) in the Arctic troposphere in spring. *Atmos Chem Phys* **10**(13): 5823–5838.

Mao, J, Fan, S, Jacob, DJ, Travis, KR. 2013. Radical loss in the atmosphere from Cu-Fe redox coupling in aerosols. *Atmos Chem Phys* **13**: 509–519.

Marais, EA, Jacob, DJ, Kurosu, TP, Chance, K, Murphy, JG, Reeves, C, Mills, G, Casadio, S, Millet, DB, Barkley, MP, Paulot, F, Mao, J. 2012. Isoprene emissions in Africa inferred from OMI observations of formaldehyde columns. *Atmos Chem Phys* **12**: 6219–6235.

Martin, RV, Jacob, DJ, Yantosca, RM, Chin, M, Ginoux, P. 2003. Global and regional decreases in tropospheric oxidants from photochemical effects of aerosols. *J Geophys Res Atmos* **108**(D3): 1–19.

Matsunaga, A, Ziemann, PJ. 2010. Yields of β-hydroxynitrates, dihydroxynitrates, and trihydroxynitrates formed from OH radical-initiated reactions of 2-methyl-1-alkenes. *PNAS* **107**: 6664–6669.

McDonald, BC, De Gouw, JA, Gilman, JB, Jathar, SH, Akherati, A, Cappa, CD, Jimenez, JL, Lee-Taylor, J, Hayes, PL, McKeen, SA, Cui, YY. 2018. Volatile chemical products emerging as largest petrochemical source of urban organic emissions. *Science* **359**(6377): 760–764.

Mentel, TF, Sohn, M, Wahner, A. 1999. Nitrate effect in the heterogeneous hydrolysis of dinitrogen pentoxide on aqueous aerosols. *Physical Chemistry Chemical Physics* **1**(24): 5451–5457.

Mertens, M, Kerkweg, A, Grewe, V, Jöckel, P, Sausen, R. 2020. Attributing ozone and its precursors to land transport emissions in Europe and Germany. *Atmos Chem Phys* **20**(13): 7843–7873.

Mielke, LH, Furgeson, A, Osthoff, HD. 2011. Observation of $ClNO_2$ in a mid-continental urban environment. *Environ Sci Technol* **45**(20): 8889. DOI: http://dx.doi.org/10.1021/es201955u.

Monks, PS, Archibald, AT, Colette, A, Cooper, O, Coyle, M, Derwent, R, Fowler, D, Granier, C, Law, KS, Mills, GE, Stevenson, DS, Tarasova, O, Thouret, V, von Schneidemesser, E, Sommariva, R, Wild, O, Williams, ML. 2015. Tropospheric ozone and its precursors from the urban to the global scale from air quality to short-lived climate forcer. *Atmos Chem Phys* **15**: 8889–8973. DOI: http://dx.doi.org/10.5194/acp-15-8889-2015.

Monks, PS, Carpenter, LJ, Penkett, SA, Ayers, GP, Gillett, RW, Galbally, IE, Meyer, CP. 1998. Fundamental ozone photochemistry in the remote marine boundary layer: The SOAPEX experiment, measurement and theory. *Atmos Environ* **32**: 3647–3664.

Morgenstern, O, Hegglin, MI, Rozanov, E, O'Connor, FM, Abraham, NL, Akiyoshi, H, Archibald, AT, Bekki, S, Butchart, N, Chipperfield, MP, Deushi, M, Dhomse, SS, Garcia, RR, Hardiman, SC, Horowitz, LW, Jöckel, P, Josse, B, Kinnison, D, Lin, M, Mancini, E, Manyin, ME, Marchand, M, Marécal, V, Michou, M, Oman, LD, Pitari, G, Plummer, DA, Revell, LE, Saint-Martin, D, Schofield, R, Stenke, A, Stone, K, Sudo, K, Tanaka, TY, Tilmes, S, Yamashita, Y, Yoshida, K, Zeng, G. 2017. Review of the global models used within phase 1 of the Chemistry–Climate Model Initiative (CCMI). *Geosci Model Dev* **10**: 639–671. DOI: http://dx.doi.org/10.5194/gmd-10-639-2017.

Murphy, DM, Fahey, DW. 1994. An estimate of the flux of stratospheric reactive nitrogen and ozone into the troposphere. *J Geophys Res* **99**: 5325–5332.

Myhre, G, Shindell, D, Bréon, F-M, Collins, W, Fuglestvedt, J, Huang, J, Koch, D, Lamarque, J-F, Lee, D, Mendoza, B, Nakajima, T, Robock, A, Stephens, G, Takemura, T, Zhang, H. 2013. Anthropogenic and natural radiative forcing, in Stocker, TF, Qin, D, Plattner, G-K, Tignor, M, Allen, SK, Boschung, J, Nauels, A, Xia, Y, Bex, V, Midgley, PM eds., *Climate change 2013: The physical science basis. Contribution of working group I to the fifth assessment report of the intergovernmental panel on climate change*. Cambridge, UK: Cambridge University Press: 1586.

National Oceanic and Atmospheric Administration. 2016. Earth systems research laboratory, global monitoring division. Available at http://www.esrl.noaa.gov/gmd/. Accessed 13 August 2019.

Nath, D, Chen, W, Graf, HF, Lan, X, Gong, H. 2017. Contrasting subtropical PV intrusion frequency and their impact on tropospheric Ozone distribution over Pacific Ocean in El-Niño and La-Niña conditions. *Scientific Reports* **7**(1): 1–13.

Ndour, M, Conchon, P, D'Anna, B, Ka, O, George, C. 2009. Photochemistry of mineral dust surface as a potential atmospheric renoxification process. *Geophys Res Lett* **36**(5): 1–4.

Neu, JL, Flury, T, Manney, GL, Santee, ML, Livesey, NJ, Worden, J. 2014. Tropospheric ozone variations governed by changes in stratospheric circulation. *Nature Geosci* **7**: 340–344. DOI: http://dx.doi.org/10.1038/ngeo2138.

Neu, JL, Lawler, MJ, Prather, MJ, Saltzman, ES. 2008. Oceanic alkyl nitrates as a natural source of tropospheric ozone. *Geophys Res Lett* **35**(13): 1–6.

Newsome, B, Evans, M. 2017. Impact of uncertainties in inorganic chemical rate constants on tropospheric composition and ozone radiative forcing. *Atmos Chem Phys* 17: 14333–14352. DOI: http://dx.doi.org/10.5194/acp-17-14333-2017.

Nozière, B, Barnes, I, Becker, KH. 1999. Product study and mechanisms of the reactions of α-pinene and of pinonaldehyde with OH radicals. *J Geophys Res* **104**: 23645–23656.

Olsen, MA, Schoeberl, MR, Douglass, AR. 2004. Stratosphere-troposphere exchange of mass and ozone. *J Geophys Res* **109**: D24114. DOI: http://dx.doi.org/10.1029/2004JD005186.

Olsen, MA, Douglass, AR, Kaplan, TB. 2013. Variability of extratropical ozone stratosphere–troposphere exchange using microwave limb sounder observations. *J Geophys Res Atmos* **118**(2): 1090–1099.

Oltmans, SJ. 1981. Surface ozone measurements in clean air. *J Geophys Res* **86**(C2): 1174–1180. DOI: http://dx.doi.org/10.1029/JC086iC02p01174.

Oltmans, SJ, Johnson, BJ, Helmig, D. 2008. Episodes of high surface ozone amounts at South Pole during summer and their impact on the long-term ozone variation. *Atmos Environ* **42**: 2804–2816. DOI: http://dx.doi.org/10.1016/j.atmosenv.2007.01.020.

Oltmans, SJ, Karion, A, Schnell, RC, Pétron, G, Helmig, D, Montzka, SA, Wolter, S, Neff, D, Miller, BR, Hueber, J, Conley, S. 2016. O_3, CH_4, CO_2, CO, NO_2 and NMHC aircraft measurements in the Uinta Basin oil and gas region under low and high ozone conditions in winter 2012 and 2013. *Elem Sci Anth* **4**: 1–12.

Orlando, JJ, Tyndall, GS. 2012. Laboratory studies of organic peroxy radical chemistry: An overview with emphasis on recent issues of atmospheric significance. *Chem Soc Rev* **41**(19): 6294–6317.

Osthoff, HD, Roberts, JM, Ravishankara, AR, Williams, EJ, Lerner, BM, Sommariva, R, Bates, TS, Coffman, D, Quinn, PK, Dibb, JE, Stark, H. 2008. High levels of nitryl chloride in the polluted subtropical marine boundary layer. *Nature Geoscience* **1**(5): 324–328.

Oswald, R, Ermel, M, Hens, K, Novelli, A, Ouwersloot, HG, Paasonen, P, Petäjä, T, Sipilä, M, Keronen, P, Bäck, J, Königstedt, R. 2015. A comparison of HONO budgets for two measurement heights at a field station within the boreal forest in Finland. *Atmos Chem Phys* **15**: 799–813.

Pan, LL, Bowman, KP, Atlas, EL, Wofsy, SC, Zhang, F, Bresch, JF, Ridley, BA, Pittman, JV, Homeyer, CR, Romashkin, P, Cooper, WA. 2010. The stratosphere–troposphere analyses of regional transport 2008 experiment. *Bulletin of the American Meteorological Society* **91**(3): 327–342.

Pan, LL, Homeyer, CR, Honomichl, S, Ridley, BA, Weisman, M, Barth, MC, Hair, JW, Fenn, MA, Butler, C, Diskin, GS, Crawford, JH. 2014. Thunderstorms enhance tropospheric ozone by wrapping and shedding stratospheric air. *Geophys Res Lett* **41**(22): 7785–7790.

Parrella, JP, Jacob, DJ, Liang, Q, Zhang, Y, Mickley, LJ, Miller, B, Evans, MJ, Yang, X, Pyle, JA, Theys, N, Van Roozendael, M. 2012. Tropospheric bromine chemistry: Implications for present and pre-industrial ozone and mercury. *Atmos Chem Phys* **12**: 6723–6740. DOI: http://dx.doi.org/10.5194/acp-12-6723-2012.

Parrish, DD, Holoway, JS, Jakoubek, R, Trainer, M, Ryerson, TB, Hübler, G, Moody, FL, Cooper, OR. 2000. Mixing of anthropogenic pollution with stratospheric ozone: A case study from the North Atlantic wintertime troposphere. *J Res* **105**: 24363–24374.

Parrish, DD, Lamarque, J-F, Naik, V, Horowitz, L, Shindell, DT, Staehelin, J, Derwent, R, Cooper, OR, Tanimoto, H, Volz-Thomas, A, Gilge, S, Scheel, H-E, Steinbacher, M, Fröhlich, M. 2014. Long-term changes in lower tropospheric baseline ozone concentrations: Comparing chemistry-climate models and observations at northern mid latitudes. *J Geophys Res Atmos* **119**: 5719–5736. DOI: http://dx.doi.org/10.1002/2013JD021435.

Paulot, F, Ginoux, P, Cooke, WF, Donner, LJ, Fan, S, Lin, MY, Mao, J, Naik, V, Horowitz, LW. 2016. Sensitivity of nitrate aerosols to ammonia emissions and to nitrate chemistry: Implications for present and future nitrate optical depth. *Atmos Chem Phys* **16**(3): 1459–1459.

Paulson, SE, Orlando, JJ. 1996. The reactions of ozone with alkenes: An important source of HOx in the boundary layer. *Geophys Res Lett* **23**(25): 3727–3730.

Perner, D, Platt, U. 1979. Detection of nitrous acid in the atmosphere by differential optical absorption. *Geophys Res Lett* **6**(12): 917–920.

Peeters, J, Nguyen, TL, Vereecken, L. 2009. HO_x radical regeneration in the oxidation of isoprene. *Physical Chemistry Chemical Physics* **11**(28): 5935–5939.

Penkett, SA, Monks, PS, Carpenter, LJ, Clemitshaw, KC, Ayers, GP, Gillett, RW, Galbally, IE, Meyer, CP. 1997. Relationships between ozone photolysis rates and peroxy radical concentrations in clean marine air over the Southern Ocean. *J Geophys Res* **102**: 12805–12817.

Penman, J, Kruger, D, Galbally, IE, Hiraishi, T, Nyenzi, B, Emmanuel, S, Buendia, L, Hoppaus, R, Martinsen, T, Meijer, J, Miwa, K, Tanabe, K eds. 2000. Good practice guidance and uncertainty management in national greenhouse gas inventories [Electronic publication]. Kanagawa, Japan: Intergovernmental Panel on Climate Change. Available at http://www.ipcc-nggip.iges.or.jp/public/gp/english/. Accessed 13 August 2019.

Pitt, JR, Allen, G, Bauguitte, SJ-B, Gallagher, MW, Lee, JD, Drysdale, W, Nelson, B, Manning, AJ, Palmer, PI. 2019. Assessing London CO_2, CH_4 and CO emissions using aircraft measurements and dispersion modelling. *Atmos Chem Phys* **19**: 8931–8945. DOI: http://dx.doi.org/10.5194/acp-19-8931-2019, 2019.

Platt, U, Perner, D. 1980. Direct measurements of atmospheric CH_2O, HNO_2, O_3, NO_2, and SO_2 by differential optical absorption in the near UV. *J Geophys Res Oceans* **85**(C12): 7453–7458.

Pound, RJ, Sherwen, T, Helmig, D, Carpenter, LJ, Evans, MJ. 2020. Influences of oceanic ozone deposition on tropospheric photochemistry. *Atmos Chem Phys* **20**: 4227–4239. DOI: http://dx.doi.org/10.5194/acp-20-4227-2020.

Prados-Roman, C, Cuevas, CA, Fernandez, RP, Kinnison, DE, Lamarque, J-F, Saiz-Lopez, A. 2015. A negative feedback between anthropogenic ozone pollution and enhanced ocean emissions of iodine. *Atmos Chem Phys* **15**: 2215–2224. DOI: http://dx.doi.org/10.5194/acp-15-2215-2015.

Prados-Roman, C, Cuevas, CA, Hay, T, Fernandez, RP, Mahajan, AS, Royer, S-J, Galí, M, Simó, R, Dachs, J, Großmann, K, Kinnison, DE, Lamarque, J-F, Saiz-Lopez, A. 2014. Iodine oxide in the global marine boundary layer. *Atmos Chem Phys* **15**:

583–593. DOI: http://dx.doi.org/10.5194/acp-15-583-2015.

Praske, E, Otkjær, RV, Crounse, JD, Hethcox, JC, Stoltz, BM, Kjaergaard, HG, Wennberg, PO. 2018. Atmospheric autoxidation is increasingly important in urban and suburban North America. *PNAS* **115**(1): 64–69.

Prather, MJ. 2009. Tropospheric O_3 from photolysis of O_2. *Geophys Res Lett* **36**(3): L03811.

Prather, MJ, Zhu, X, Flynn, CM, Strode, SA, Rodriguez, JM, Steenrod, SD, Liu, J, Lamarque, J-F, Fiore, AM, Horowitz, LW, Mao, J, Murray, LT, Shindell, DT, Wofsy, SC. 2017. Global atmospheric chemistry—Which air matters. *Atmos Chem Phys* **17**: 9081–9102. DOI: http://dx.doi.org/10.5194/acp-17-9081-2017.

Prather, MJ, Zhu, X, Tang, Q, Hsu, J, Neu, JL. 2011. An atmospheric chemist in search of the tropopause. *J Geophys Res Atmos* **116**: D04306. DOI: https://doi.org/10.1029/2010JD014939.

Price, C, Penner, J, Prather, M. 1997. NOx from lightning: 1. Global distribution based on lightning physics. *J Geophys Res* **102**: 5929–5941. DOI: http://dx.doi.org/10.1029/96JD03504.

Price, C, Rind, D. 1992. A simple lightning parameterization for calculating global lightning distributions. *J Geophys Res* **97**: 9919–9933. DOI: http://dx.doi.org/10.1029/92JD00719.

Price, JD, Vaughan, G. 1993. The potential for stratosphere-troposphere exchange in cut-off-low systems. *Q J R Meteorol Soc* **119**: 343–365.

Pye, HOT, Liao, H, Wu, S, Mickley, LJ, Jacob, DJ, Henze, DK, Seinfeld, JH. 2009. Effect of changes in climate and emissions on future sulfate-nitrate-ammonium aerosol levels in the United States. *J Geophys Res Atmos* **114**(D01205). DOI: http://dx.doi.org/10.1029/2008JD010701.

Rannik, Ü, Altimir, N, Mammarella, I, Bäck, J, Rinne, J, Ruuskanen, TM, Hari, P, Vesala, T, Kulmala, M. 2012. Ozone deposition into a boreal forest over a decade of observations: Evaluating deposition partitioning and driving variables. *Atmos Chem Phys* **12**: 12165–12182. DOI: http://dx.doi.org/10.5194/acp-12-12165-2012.

Read, KA, Mahajan, AS, Carpenter, LJ, Evans, MJ, Faria, BVE, Heard, DE, Hopkins, JR, Lee, JD, Moller, SJ, Lewis, AC, Mendes, L, McQuaid, JB, Oetjen, H, Saiz-Lopez, A, Pilling, MJ, Plane, JMC. 2008. Extensive halogen-mediated ozone destruction over the tropical Atlantic Ocean. *Nature* **453**: 1232–1235. DOI: http://dx.doi.org/10.1038/nature07035.

Regener, VH. 1938. Neue messungen der vertikalen verteilung des ozons in der atmosphere. *Zeitschrift für Physik* **109**: 642–670.

Regener, VH. 1957. The vertical flux of atmospheric ozone. *J Geophys Res* **62**: 221–228.

Ren, X, Brune, WH, Mao, J, Mitchell, MJ, Lesher, RL, Simpas, JB, Metcalf, AR, Schwab, JJ, Cai, C, Li, Y, Demerjian, KL. 2006. Behavior of OH and HO_2 in the winter atmosphere in New York City. *Atmos Environ* **40**: 252–263.

REVIHAAP. 2013. Review of evidence on health aspects of air pollution—REVIHAAP Project technical report. Bonn, Germany: World Health Organization (WHO) Regional Office for Europe. Available at http://www.euro.who.int/data/assets/pdf_file/0004/193108/REVIHAAP-Final-technical-report-final-version.pdf. Accessed 13 August 2019.

Rickard, AR, Johnson, D, McGill, CD, Marston, G. 1999. OH yields in the gas-phase reactions of ozone with alkenes. *J Phys Chem A* **103**(38): 7656–7664.

Ridley, BA, Madronich, S, Chatfield, R, Walega, J, Shetter, R, Carroll, M, Montzka, D. 1992. Measurements and model simulations of the photostationary state during the Mauna Loa Observatory photochemistry experiment: Implications for radical concentrations and ozone production and loss rates. *J Geophys Res* **97**(D10): 10375–10388.

Ridley, BA, Walega, JG, Dye, JE, Grahek, FE. 1994. Distributions of NO, NOx, NOy and O3 to 12 km altitude during the summer monsoon season over New Mexico. *J Geophys Res* **99**: 25519–25534. DOI: http://dx.doi.org/10.1029/94JD02210.

Riedel, TP, Bertram, TH, Crisp, TA, Williams, EJ, Lerner, BM, Vlasenko, A, Li, SM, Gilman, J, De Gouw, J, Bon, DM, Wagner, NL. 2012. Nitryl chloride and molecular chlorine in the coastal marine boundary layer. *Environ Sci Technol* **46**(19): 10463–10470.

Riedel, TP, Wolfe, GM, Danas, KT, Gilman, JB, Kuster, WC, Bon, DM, Vlasenko, A, Li, S-M, Williams, EJ, Lerner, BM, Veres, PR, Roberts, JM, Holloway, JS, Lefer, B, Brown, SS, Thornton, JA. 2014. An MCM modeling study of nitryl chloride ($ClNO_2$) impacts on oxidation, ozone production and nitrogen oxide partitioning in polluted continental outflow. *Atmos Chem Phys* **14**: 3789–3800. DOI: http://dx.doi.org/10.5194/acp-14-3789-2014.

Roberts, TJ, Braban, CF, Martin, RS, Oppenheimer, C, Adams, JW, Cox, RA, Jones, RL, Griffiths, PT. 2009. Modelling reactive halogen formation and ozone depletion in volcanic plumes. *Chemical Geology* **263**(1–4): 151–163.

Roelofs, G-J, Lelieveld, J. 1997. Model study of the influence of cross-tropopause O3 transports on tropospheric O3 levels. *Tellus B* **49**: 38–55.

Romer, PS, Wooldridge, PJ, Crounse, JD, Kim, MJ, Wennberg, PO, Dibb, JE, Scheuer, E, Blake, DR, Meinardi, S, Brosius, AL, Thames, AB. 2018. Constraints on Aerosol Nitrate Photolysis as a Potential Source of HONO and NOx. *Environ Sci Technol* **52**(23): 13738–13746.

Roth, PM, Roberts, PJW, Liu, M, Reynolds, SD, Seinfeld, JH. 1974. Mathematical modeling of photochemical air pollution—II. A model and inventory of pollutant emissions. *Atmos Environ* **8**: 97–130.

Rowlinson, MJ, Rap, A, Hamilton, DS, Pope, RJ, Hantson, S, Arnold, SR, Kaplan, JO, Arneth, A, Chipperfield, MP, Forster, PM, Nieradzik, L. 2020. Tropospheric ozone radiative forcing uncertainty

due to pre-industrial fire and biogenic emissions. *Atmos Chem Phys* **20**: 10937–10951. DOI: http://dx.doi.org/10.5194/acp-20-10937-202.

Saiz-Lopez, A, Fernandez, RP, Ordóñez, C, Kinnison, DE, Gómez Martín, JC, Lamarque, J-F, Tilmes, S. 2014. Iodine chemistry in the troposphere and its effect on ozone. *Atmos Chem Phys* **14**: 13119–13143. DOI: http://dx.doi.org/10.5194/acp-14-13119-2014.

Saiz-Lopez, A, Lamarque, J-F, Kinnison, DE, Tilmes, S, Ordóñez, C, Orlando, JJ, Conley, AJ, Plane, JMC, Mahajan, AS, Sousa Santos, G, Atlas, EL, Blake, DR, Sander, SP, Schauffler, S, Thompson, AM, Brasseur, G. 2012. Estimating the climate significance of halogen-driven ozone loss in the tropical marine troposphere. *Atmos Chem Phys* **12**: 3939–3949. DOI: http://dx.doi.org/10.5194/acp-12-3939-2012.

Saiz-Lopez, A, Plane, JMC. 2004. Novel iodine chemistry in the marine boundary layer. *Geophys Res Lett* **31**: L04112. DOI: http://dx.doi.org/10.1029/2003GL019215.

Saiz-Lopez, A, Plane, JMC, Shillito, JA. 2004. Bromine oxide in the mid-latitude marine boundary layer. *Geophys Res Lett* **31**: L03111. DOI: http://dx.doi.org/10.1029/2003GL018956.

Saiz-Lopez, A, von Glasow, R. 2012. Reactive halogen chemistry in the troposphere. *Chem Soc Rev* **41**(19): 6448–6472.

Sarwar, G, Roselle, SJ, Mathur, R, Appel, W, Dennis, RL, Vogel, B. 2008. A comparison of CMAQ HONO predictions with observations from the Northeast Oxidant and Particle Study. *Atmos Environ* **42**(23): 5760–5770.

Sarwar, G, Simon, H, Bhave, P, Yarwood, G. 2012. Examining the impact of heterogeneous nitryl chloride production on air quality across the United States. *Atmos Chem Phys* **12**: 6455–6473. DOI: http://dx.doi.org/10.5194/acp-12-6455-2012.

Sarwar, G, Simon, H, Xing, J, Mathur, R. 2014. Importance of tropospheric ClNO2 chemistry across the Northern Hemisphere. *Geophys Res Lett* **41**(11): 4050–4058.

Scheel, HE. 2003. Ozone climatology studies for the Zugspitze and neighbouring sites in the German Alps, in Tropospheric Ozone Research 2, EUROTRAC-2 Subproject Final Report, A. Lindskog, Co-ordinator, EUROTRAC International Scientific Secretariat. München, Germany: 134–139.

Schnell, RC, Oltmans, SJ, Neely, RR, Endres, MS, Molenar, JV, White, AB. 2009. Rapid photochemical production of ozone at high concentrations in a rural site during winter. *Nat Geosci* **2**(2): 120–122.

Schönbein, CF. 1840. On the odour accompanying electricity and on the probability of its dependency on the presence of a new substance. *Philos Mag* **17**: 293–294.

Schroeder, JR, Pan, LL, Ryerson, T, Diskin, G, Hair, J, Meinardi, S, Simpson, I, Barletta, B, Blake, N, Blake, DR. 2014. Evidence of mixing between polluted convective outflow and stratospheric air in the upper troposphere during DC3. *J Geophys Res Atmos* **119**(19): 11–477.

Schultz, MG, Schröder, S, Lyapina, O, Cooper, OR, Galbally, I, Petropavlovskikh, I, Von Schneidemesser, E, Tanimoto, H, Elshorbany, Y, Naja, M, Seguel, RJ. 2017. Tropospheric Ozone Assessment Report: Database and metrics data of global surface ozone observations. *Elem Sci Anth* **5**: 1–26.

Schumann, U, Huntrieser, H. 2007. The global lightning-induced nitrogen oxides source. *Atmos Chem Phys* **7**: 3823–3907.

Scott, RK, Cammas, JP. 2002. Wave breaking and mixing at the subtropical tropopause. *J Atmos Sci* **59**(15): 2347–2361.

Shapiro, MA. 1976. The role of turbulent heat flux in the generation of potential vorticity of upper-level jet stream systems. *Mon Wea Rev* **104**: 892–906.

Shapiro, MA. 1978. Further evidence of the mesoscale and turbulent structure of upper level jet stream-frontal zone systems. *Mon Wea Rev* **106**: 1100–1111.

Shapiro, MA. 1980. Turbulent mixing within tropopause folds as a mechanism for the exchange of chemical constituents between the stratosphere and troposphere. *J Atmos Sci* **37**: 994–1004.

Sherwen, T, Chance, RJ, Tinel, L, Ellis, D, Evans, MJ, Carpenter, LJ. 2019. A machine-learning-based global sea-surface iodide distribution. *Earth Syst Sci Data* **11**: 1239–1262. DOI: http://dx.doi.org/10.5194/essd-11-1239-2019.

Sherwen, T, Evans, MJ, Carpenter, LJ, Andrews, SJ, Lidster, RT, Dix, B, Koenig, TK, Sinreich, R, Ortega, I, Volkamer, R, Saiz-Lopez, A. 2016. Iodine's impact on tropospheric oxidants: A global model study in GEOS-Chem. *Atmos Chem Phys* **16**(2): 1161–1186.

Sherwen, T, Evans, MJ, Carpenter, LJ, Schmidt, JA, Mickley, LJ. 2017a. Halogen chemistry reduces tropospheric O_3 radiative forcing. *Atmos Chem Phys* **17**(2): 1557–1569.

Sherwen, T, Evans, MJ, Sommariva, R, Hollis, LD, Ball, SM, Monks, PS, Reed, C, Carpenter, LJ, Lee, JD, Forster, G, Bandy, B. 2017b. Effects of halogens on European air-quality. *Faraday Discuss* **200**: 75–100.

Shiraiwa, M, Ammann, M, Koop, T, Pöschl, U. 2011. Gas uptake and chemical aging of semisolid organic aerosol particles. *PNAS* **108**(27): 11003–11008.

Silva, SJ, Heald, CL. 2018. Investigating dry deposition of ozone to vegetation. *J Geophys Res Atmos* **123**: 559–573. https://doi.org/10.1002/2017JD027278

Silva, SJ, Heald, CL, Guenther, AB. 2020. Development of a reduced-complexity plant canopy physics surrogate model for use in chemical transport models: A case study with GEOS-Chem v12.3.0. *Geosci Model Dev* **13**: 2569–2585. DOI: http://dx.doi.org/10.5194/gmd-13-2569-2020.

Silva, SJ, Heald, CL, Ravela, S, Mammarella, I, Munger, JW. 2019. A deep learning parameterization for ozone dry deposition velocities.

Geophys Res Lett **46**. DOI: http://dx.doi.org/10.1029/2018GL081049.

Simpson, WR, Von Glasow, R, Riedel, K, Anderson, P, Ariya, P, Bottenheim, J, Burrows, J, Carpenter, LJ, Frieß, U, Godsite, ME, Heard, D. 2007. Halogens and their role in polar boundary-layer ozone depletion. *Atmos Chem Phys* **7**(16): 4375–4418.

Škerlak, B, Pfhal, S, Sprenger, M, Wernli, H. 2019. A numerical process study on the rapid transport of stratospheric air down to the surface over western North America and the Tibetan Plateau. *Atmos Chem Phys* **19**: 6535–6549. DOI: http://dx.doi.org/10.5194/acp-19-6535-2019.

Škerlak, B, Sprenger, M, Wernli, H. 2014. A global climatology of stratosphere-troposphere exchange using the ERA-Interim data set from 1979 to 2011. *Atmos Chem Phys* **14**: 913–937.

Sklaveniti, S, Locoge, N, Stevens, PS, Wood, E, Kundu, S, Dusanter, S. 2018. Development of an instrument for direct ozone production rate measurements: Measurement reliability and current limitations. *Atmos Meas Tech* **11**: 741–761. DOI: http://dx.doi.org/10.5194/amt-11-741-2018.

Söderlund, R, Svensson, BH. 1976. The global nitrogen cycle, in Svensson, BH, Söderlund R eds., *Nitrogen, phosphorus and sulphur—Global cycles. SCOPE Report 7. Ecological Bulletins*. Swedish Natural Science Research Council, NFR, Stockholm, Sweden: 22, 23–73.

Søvde, OA, Hoyle, CR, Myhre, G, Isaksen, ISA. 2011. The HNO_3 forming branch of the HO2+ NO reaction: Pre-industrial-to-present trends in atmospheric species and radiative forcings. *Atmos Chem Phys* **11**(17): 8929–8943.

Squire, OJ, Archibald, AT, Griffiths, PT, Jenkin, ME, Smith, D, Pyle, JA. 2015. Influence of isoprene chemical mechanism on modelled changes in tropospheric ozone due to climate and land use over the 21st century. *Atmos Chem Phys* **15**: 5123–5143. DOI: http://dx.doi.org/10.5194/acp-15-5123-2015.

Staehelin, J, Tummon, F, Revell, LE, Stenke, A, Peter, T. 2017. Tropospheric ozone at northern mid-latitudes: Modeled and measured long-term changes. *Atmosphere* **8**(9): 163.

Stauffer, RM, Thompson, AM, Witte, JC. 2018. Characterizing global ozonesonde profile variability from surface to the UT/LS with a clustering technique and MERRA-2 reanalysis. *J Geophys Res* **123**. DOI: http://dx.doi.org/10.1002/2017JD028465.

Stavrakou, T, Müller, J-F, Bauwens, M, De Smedt, I, Van Roozendael, M, De Mazière, M, Vigouroux, C, Hendrick, F, George, M, Clerbaux, C, Coheur, P-F, Guenther, A. 2015. How consistent are top-down hydrocarbon emissions based on formaldehyde observations from GOME-2 and OMI? *Atmos Chem Phys* **15**(20): 11861–11884.

Stavrakou, T, Müller, J-F, Boersma, KF, van der A, RJ, Kurokawa, J, Ohara, T, Zhang, Q. 2013. Key chemical NOx sink uncertainties and how they influence top-down emissions of nitrogen oxides. *Atmos Chem Phys* **13**: 9057–9082. DOI: http://dx.doi.org/10.5194/acp-13-9057-2013.

Stevenson, DS, Dentener, FJ, Schultz, MG, Ellingsen, K, van Noije, TPC, Wild, O, Zeng, G, Amann, M, Atherton, CS, Bell, N, Bergmann, DJ, Bey, I, Butler, T, Cofala, J, Collins, WJ, Derwent, RG, Doherty, RM, Drevet, J, Eskes, HJ, Fiore, AM, Gauss, M, Hauglustaine, DA, Horowitz, LW, Isaksen, ISA, Krol, MC, Lamarque, J-F, Lawrence, MG, Montanaro, V, Müller, J-F, Pitari, G, Prather, MJ, Pyle, JA, Rast, S, Rodriguez, JM, Sanderson, MG, Savage, NH, Shindell, DT, Strahan, SE, Sudo, K, Szopa, S. 2006. Multimodel ensemble simulations of present-day and near-future tropospheric ozone. *J Geophys Res* **111**: D08301. DOI: http://dx.doi.org/10.1029/2005JD006338.

Stevenson, DS, Young, PJ, Naik, V, Lamarque, JF, Shindell, DT, Voulgarakis, A, Skeie, RB, Dalsoren, SB, Myhre, G, Berntsen, TK, Folberth, GA. 2013. Tropospheric ozone changes, radiative forcing and attribution to emissions in the Atmospheric Chemistry and Climate Model Intercomparison Project (ACCMIP). *Atmos Chem Phys* **13**: 3063–3085.

Stohl, A, Trickl, T. 1999. A textbook example of long-range transport: Simultaneous observation of ozone maxima of stratospheric and North American origin in the free troposphere over Europe. *J Geophys Res Atmos* **104**(D23): 30445–30462.

Stohl, A, Bonasoni, P, Cristofanelli, P, Collins, W, Feichter, J, Frank, A, Forster, C, Gerasopoulos, E, Gäggeler, H, James, P, Kentarchos, T, Kromp-Kolb, H, Krüger, B, Land, C, Meloen, J, Papayannis, A, Priller, A, Seibert, P, Sprenger, M, Roelofs, GJ, Scheel, HE, Schnabel, C, Siegmund, P, Tobler, L, Trickl, T, Wernli, H, Wirth, V, Zanis, P, Zerefos, C. 2003a. Stratosphere-troposphere exchange: A review, and what we have learned from STACCATO. *J Geophys Res* **108**: 8516. DOI: http://dx.doi.org/10.1029/2002JD002490.

Stohl, A, Forster, C, Eckhardt, S, Spichtinger, N, Huntrieser, H, Heland, J, Schlager, H, Wilhelm, S, Arnold, F, Cooper, O. 2003b. A backward modeling study of intercontinental pollution transport using aircraft measurements. *J Geophys Res Atmos* **108**(D12): 1–18.

Stohl, A, Forster, C, Huntrieser, H, Mannstein, H, McMillan, WW, Petzold, A, Schlager, H, Weinzierl, B. 2007. Aircraft measurements over Europe of an air pollution plume from Southeast Asia—Aerosol and chemical characterization. *Atmos Chem Phys* **7**: 913–937.

Stone, D, Whalley, LK, Heard, DE. 2012. Tropospheric OH and HO_2 radicals: Field measurements and model comparisons. *Chemical Society Reviews* **41**(19): 6348–6404.

Streets, DG, Canty, T, Carmichael, GR, de Foy, B, Dickerson, RR, Duncan, BN, Edwards, DP, Haynes, JA, Henze, DK, Houyoux, MR, Jacob, DJ. 2013.

Emissions estimation from satellite retrievals: A review of current capability. *Atmos Environ* **77**: 1011–1042.

Strode, SA, Rodriguez, JM, Logan, JA, Cooper, OR, Witte, JC, Lamsal, LN, Damon, M, Van Aartsen, B, Steenrod, SD, Strahan, SE. 2015. Trends and variability in surface ozone over the United States. *J Geophys Res Atmos* **120**: 9020–9042. DOI: http://dx.doi.org/10.1002/2014JD022784.

Su, H, Cheng, Y, Oswald, R, Behrendt, T, Trebs, I, Meixner, FX, Andreae, MO, Cheng, P, Zhang, Y, Pöschl, U. 2011. Soil nitrite as a source of atmospheric HONO and OH radicals. *Science* **333**(6049): 1616–1618.

Sutton, RT, McCarthy, GD, Robson, J, Sinha, B, Archibald, AT, Gray, LJ. 2018. Atlantic multidecadal variability and the UK ACSIS program. *Bulletin of the American Meteorological Society* **99**(2): 415–425.

Taketani, F, Kanaya, Y, Akimoto, H. 2008. Kinetics of heterogeneous reactions of HO_2 radical at ambient concentration levels with $(NH_4)_2SO_4$ and NaCl aerosol particles. *J Phys Chem A* **112**(11): 2370–2377.

Taketani, F, Kanaya, Y, Akimoto, H. 2009. Heterogeneous loss of HO_2 by KCl, synthetic sea salt, and natural seawater aerosol particles. *Atmos Environ* **43**(9): 1660–1665.

Taketani, F, Kanaya, Y, Pochanart, P, Liu, Y, Li, J, Okuzawa, K, Kawamura, K, Wang, Z, Akimoto, H. 2012. Measurement of overall uptake coefficients for HO_2 radicals by aerosol particles sampled from ambient air at Mts. Tai and Mang (China). *Atmos Chem Phys* **12**(24): 11907–11907.

Tang, Q, Prather, MJ, Hsu, J. 2011. Stratosphere-troposphere exchange ozone flux related to deep convection. *Geophys Res Lett* **38**(3): L03806.

Tarasick, DW, Carey-Smith, TK, Hocking, WK, Moeini, O, He, H, Liu, J, Osman, M, Thompson, AM, Johnson, B, Oltmans, SJ, Merrill, JT. 2019a. Quantifying stratosphere-troposphere transport of ozone using balloon-borne ozonesondes, radar windprofilers and trajectory models. *Atmos Environ* **198**: 496–509. DOI: http://dx.doi.org/10.1016/j.atmosenv.2018.10.040.

Tarasick, DW, Galbally, IE, Cooper, OR, Schultz, MG, Ancellet, G, Leblanc, T, Wallington, TJ, Ziemke, J, Liu, X, Steinbacher, M, Staehelin, J, Vigouroux, C, Hannigan, JW, García, O, Foret, G, Zanis, P, Weatherhead, E, Petropavlovskikh, I, Worden, H, Osman, M, Liu, J, Chang, K-L, Gaudel, A, Lin, M, Granados-Muñoz, M, Thompson, AM, Oltmans, SJ, Cuesta, J, Dufour, G, Thouret, V, Hassler, B, Trickl, T, Neu, JL. 2019b. Tropospheric Ozone Assessment Report: Tropospheric ozone from 1877 to 2016, observed levels, trends and uncertainties. *Elem Sci Anth* **7**(1): 39. DOI: http://dx.doi.org/10.1525/elementa.376.

Tie, X, Brasseur, G, Emmons, L, Horowitz, L, Kinnison, D. 2001. Effects of aerosols on tropospheric oxidants: A global model study. *J Geophys Res Atmos* **106**(D19): 22931–22964.

Thompson, AM, Balashov, NV, Witte, JC, Coetzee, JGR, Thouret, V, Posny, F. 2014. Tropospheric ozone increases over the southern Africa region: Bellwether for rapid growth in Southern Hemisphere pollution? *Atmos Chem Phys* **14**: 9855–9869.

Thompson, AM, Stone, JB, Witte, JC, Miller, SK, Oltmans, SJ, Ross, KL, Kucsera, TL, Merrill, JT, Forbes, G, Tarasick, DW, Joseph, E, Schmidlin, FJ, McMillan, WW, Warner, J, Hintsa, EJ, Johnson, JE. 2007. Intercontinental Transport Experiment Ozonesonde Network Study (IONS, 2004): 2. Tropospheric ozone budgets and variability over northeastern North America. *J Geophys Res* **112**: D12S13. DOI: http://dx.doi.org/10.1029/2006JD007670.

Thornton, JA, Abbatt, JP. 2005. N_2O_5 reaction on submicron sea salt aerosol: Kinetics, products, and the effect of surface active organics. *J Phys Chem A* **109**(44): 10004–10012.

Thornton, JA, Jaeglé, L, McNeill, VF. 2008. Assessing known pathways for HO_2 loss in aqueous atmospheric aerosols: Regional and global impacts on tropospheric oxidants. *J Geophys Res Atmos* **113**(D5).

Tost, H, Jöckel, P, Kerkweg, A, Sander, R, Lelieveld, J. 2006. Technical note: A new comprehensive SCAVenging submodel for global atmospheric chemistry modelling. *Atmos Chem Phys* **6**: 565–574. DOI: http://dx.doi.org/10.5194/acp-6-565-2006.

Travis, KR, Heald, CL, Allen, HM, Apel, EC, Arnold, SR, Blake, DR, Brune, WH, Chen, X, Commane, R, Crounse, JD, Daube, BC, Diskin, GS, Elkins, JW, Evans, MJ, Hall, SR, Hintsa, EJ, Hornbrook, RS, Kasibhatla, PS, Kim, MJ, Luo, G, McKain, K, Millet, DB, Moore, FL, Peischl, J, Ryerson, TB, Sherwen, T, Thames, AB, Ullmann, K, Wang, X, Wennberg, PO, Wolfe, GM, Yu, F. 2020. Constraining remote oxidation capacity with ATom observations. *Atmos Chem Phys* **20**: 7753–7781. DOI: http://dx.doi.org/10.5194/acp-20-7753-2020.

Trickl, T, Eisele, H, Bärtsch-Ritter, N, Furger, M, Mücke, R, Sprenger, M, and Stohl, A. 2011. High-ozone layers in the middle and upper troposphere above Central Europe: Potential import from the stratosphere along the subtropical jet stream. *Atmos Chem Phys* **11**: 9343–9366.

Trickl, T, Feldmann, H, Kanter, H-J, Scheel, HE, Sprenger, M, Stohl, A, Wernli, H. 2010. Deep stratospheric intrusions over Central Europe: Case studies and climatological aspects. *Atmos Chem Phys* **10**: 499–524.

Trickl, T, Vogelmann, H, Fix, A, Schäfler, A, Wirth, M, Calpini, B, Levrat, G, Romanens, G, Apituley, A, Wilson, KM, Begbie, R, Reichardt, J, Vömel, H, Sprenger, M. 2016. How Stratospheric Are Deep Stratospheric Intrusions into the Troposphere? LUAMI 2008. *Atmos Chem Phys* **16**: 8791–8815. DOI: http://dx.doi.org/10.5194/acp-16-8791-2016.

Trickl, T, Vogelmann, H, Flentje, H, Ries, L. 2015. Stratospheric ozone in boreal fire plumes—The 2013

smoke season over Central Europe. *Atmos Chem Phys* **15**: 9631–9649.

Trickl, T, Vogelmann, H, Ries, L, Sprenger, M. 2020. Very high stratospheric influence observed in the free troposphere over the northern Alps – just a local phenomenon? *Atmos Chem Phys* **20**: 243–266. DOI: http://dx.doi.org/10.5194/acp-20-243-2020.

Tuovinen, J-P, Ashmore, MR, Emberson, LD, Simpson, D. 2004. Testing and improving the EMEP ozone deposition module. *Atmos Environ* **38**(15): 2373–2385. ISSN 1352-2310. DOI: http://dx.doi.org/10.1016/j.atmosenv.2004.01.026.

U.S. Environmental Protection Agency. 2013. Integrated science assessment for ozone and related photochemical oxidants. EPA/600/R-10/076F. Office of Research and Development, Research Triangle Park, NC (February).

Utembe, SR, Cooke, MC, Archibald, AT, Jenkin, ME, Derwent, RG, Shallcross, DE. 2010. Using a reduced Common Representative Intermediates (CRIv2-R5) mechanism to simulate tropospheric ozone in a 3-D Lagrangian chemistry transport model. *Atmos Environ* **44**(13)*:* 1609–1622.

van Vuuren, DP, Edmonds, J, Kainuma, M, Riahi, K, Thomson, A, Hibbard, K, Hurtt, GC, Kram, T, Krey, V, Lamarque, J-F, Masui, T, Meinshausen, M, Nakicenovic, N, Smith, SJ, Rose, SK. 2011. The representative concentration pathways: An overview. *Clim Change* **109**: 5–31. DOI: http://dx.doi.org/10.1007/s10584-011-0148-z.

Verstraeten, WW, Neu, JL, Williams, JE, Bowman, KW, Worden, JR, Boersma, KF. 2015. Rapid increases in tropospheric ozone production and export from China. *Nat Geosci* **8**(9): 690–695.

Vinken, GCM, Boersma, KF, Maasakkers, JD, Adon, M, Martin, RV. 2014. Worldwide biogenic soil NOx emissions inferred from OMI NO_2 observations. *Atmos Chem Phys* **14**: 10363–10381. DOI: http://dx.doi.org/10.5194/acp-14-10363-2014.

Vogel, B, Vogel, H, Kleffmann, J, Kurtenbach, R. 2003. Measured and simulated vertical profiles of nitrous acid—Part II. Model simulations and indications for a photolytic source. *Atmos Environ* **37**(21): 2957–2966.

Van Marle, MJ, Kloster, S, Magi, BI, Marlon, JR, Daniau, AL, Field, RD, Arneth, A, Forrest, M, Hantson, S, Kehrwald, NM, Knorr, W. 2017. Historic global biomass burning emissions based on merging satellite observations with proxies and fire models (1750-2015). *Geoscientific Model Development* **10**: 3329–3357.

von Schneidemesser, E, Monks, PS, Allan, JD, Bruhwiler, L, Forster, P, Fowler, D, Lauer, L, Morgan, WT, Paasonen, P, Righi, M, Sindelarova, K, Sutton, MA. 2015. Chemistry and the linkages between air quality and climate change. *Chem Rev* **115**(10): 3856–3897.

Walker, TW, Jones, DBA, Parrington, M, Henze, DK, Murray, LT, Bottenheim, JW, Anlauf, K, Worden, JR, Bowman, KW, Shim, C, Singh, K, Kopacz, M, Tarasick, DW, Davies, J, von der Gathen, P, Thompson, AM, Carouge, CC. 2012. Impacts of midlatitude precursor emissions and local photochemistry on ozone abundances in the Arctic. *J Geophys Res* **117**(D0130). DOI: http://dx.doi.org/10.1029/2011JD016370.

Wallington, TJ, Seinfeld, JH, Barker, JR. 2019. 100 Years of progress in gas-phase atmospheric chemistry research. *Meteorol Monogr* **59**: 10–11.

Wang, X, Jacob, DJ, Eastham, SD, Sulprizio, MP, Zhu, L, Chen, Q, Alexander, B, Sherwen, T, Evans, MJ, Lee, BH, Haskins, JD. 2019. The role of chlorine in global tropospheric chemistry. *Atmos Chem Phys* **19**: 3981–4003.

Wang, T, Tham, YJ, Xue, L, Li, Q, Zha, Q, Wang, Z, Poon, SCN, Dubé, WP, Blake, DR, Louie, PKK, Luk, CWY, Tsui, W, Brown, SS. 2016. Observations of nitryl chloride and modeling its source and effect on ozone in the planetary boundary layer of southern China. *J Geophys Res Atmos* **121**: 2476–2489. DOI: http://dx.doi.org/10.1002/2015JD024556.

Waugh, DW, Funatsu, BM. 2003. Intrusions into the tropical upper troposphere: Three-dimensional structure and accompanying ozone and OLR distributions. *J Atmos Sci* **60**(4): 637–653.

Wesely, ML. 1989. Parameterization of surface resistances to gaseous dry deposition in regional-scale numerical models. *Atmos Environ* **23**(6): 1293–1304.

Wild, O. 2007. Modelling the global tropospheric ozone budget: exploring the variability in current models. *Atmos.Chem Phys* **7**: 2643–2660. DOI: http://dx.doi.org/10.5194/acp-7-2643-2007.

Williams, JE, Van Velthoven, PFJ, Brenninkmeijer, C. 2013. Quantifying the uncertainty in simulating global tropospheric composition due to the variability in global emission estimates of Biogenic Volatile Organic Compounds. *Atmos Chem Phys* **13**(5): 2857–2891.

Wong, AYH, Geddes, JA, Tai, APK, Silva, SJ. 2019. Importance of dry deposition parameterization choice in global simulations of surface ozone. *Atmos Chem Phys* **19**: 14365–14385. DOI: http://dx.doi.org/10.5194/acp-19-14365-2019.

Wong, KW, Tsai, C, Lefer, B, Grossberg, N, Stutz, J. 2013. Modeling of daytime HONO vertical gradients during SHARP 2009. *Atmos Chem Phys* **13**(7): 3587–3601.

Xia, L, Nowack, PJ, Tilmes, S, Robock, A. 2017. Impacts of stratospheric sulfate geoengineering on tropospheric ozone. *Atmos Chem Phys* **17**: 11913–11928. DOI: http://dx.doi.org/10.5194/acp-17-11913-2017.

Yang, H, Chen, G, Tang, Q, Hess, P. 2016. Quantifying isentropic stratosphere-troposphere exchange of ozone. *J Geophys Res Atmos* **121**(7): 3372–3387.

Yang, X, Pyle, JA, Cox, RA, Theys, N, Van Roozendael, M. 2010. Snow-sourced bromine and its implications for polar tropospheric ozone. *Atmos Chem Phys* **10**: 7763–7773. DOI: http://dx.doi.org/10.5194/acp-10-7763-2010.

Yates, EL, Iraci, LT, Roby, MC, Pierce, RB, Johnson, MS, Reddy, PJ, Tadic, JM, Loewenstein, M, Gore, W. 2013. Airborne observations and modeling of springtime stratosphere-to-troposphere transport over California. *Atmos Chem Phys* **13**(24): 12481–12494.

Ye, C, Zhou, X, Pu, D, Stutz, J, Festa, J, Spolaor, M, Tsai, C, Cantrell, C, Mauldin, RL, Campos, T, Weinheimer, A, Hornbrook, RS, Apel, EC, Guenther, A, Kaser, L, Yuan, B, Karl, T, Haggerty, J, Hall, S, Ullmann, K, Smith, JN, Ortega, J, Knote, C. 2016. Rapid cycling of reactive nitrogen in the marine boundary layer. *Nature* **532**: 489–491. DOI: http://dx.doi.org/10.1038/nature17195.

Yeung, LY, Murray, LT, Martinerie, P, Witrant, E, Hu, H, Banerjee, A, Orsi, A, Chappellaz, J. 2019. Isotopic constraint on the twentieth-century increase in tropospheric ozone. *Nature* **570**(7760): 224.

Yin, X, Kang, S, de Foy, B, Cong, Z, Luo, J, Zhang, L, Ma, Y, Zhang, G, Rupakheti, D, and Zhang, Q. 2017. Surface ozone at Nam Co in the inland Tibetan Plateau: Variation, synthesis comparison and regional representativeness. *Atmos Chem Phys* **17***:* 11293–11311. DOI:https://doi.org/10.5194/acp-17-11293-2017.

Young, PJ, Archibald, AT, Bowman, KW, Lamarque, J-F, Naik, V, Stevenson, DS, Tilmes, S, Voulgarakis, A, Wild, O, Bergmann, D, Cameron-Smith, P, Cionni, I, Collins, WJ, Dalsøren, SB, Doherty, RM, Eyring, V, Faluvegi, G, Horowitz, LW, Josse, B, Lee, YH, MacKenzie, IA, Nagashima, T, Plummer, DA, Righi, M, Rumbold, ST, Skeie, RB, Shindell, DT, Strode, SA, Sudo, K, Szopa, S, Zeng, G. 2013a. Pre-industrial to end 21st century projections of tropospheric ozone from the Atmospheric Chemistry and Climate Model Intercomparison Project (ACCMIP). *Atmos Chem Phys* **13**: 2063–2090. DOI: http://dx.doi.org/10.5194/acp-13-2063-2013.

Young, PJ, Archibald, AT, Bowman, KW, Lamarque, J-F, Zeng, G. 2013b. Corrigendum to "Pre-industrial to end 21st century projections of tropospheric ozone from the Atmospheric Chemistry and Climate Model Intercomparison Project (ACCMIP)" published in *Atmos Chem Phys* 13, 2063–2090, 2013. *Atmos Chem Phys* **13**: 5401–5402. DOI: http://dx.doi.org/10.5194/acp-13-5401-2013.

Young, PJ, Naik, V, Fiore, AM, Gaudel, A, Guo, J, Lin, MY, Neu, J, Parrish, D, Reider, HE, Schnell, JL, Tilmes, S. 2018. Tropospheric Ozone Assessment Report: Assessment of global-scale model performance for global and regional ozone distributions, variability, and trends. *Elem Sci Anth* **6**(1): 1–49.

Zhang, L, Jacob, DJ, Boersma, KF, Jaffe, DA, Olson, JR, Bowman, KW, Worden, JR, Thompson, AM, Avery, MA, Cohen, RC, Dibb, JE. 2008. Transpacific transport of ozone pollution and the effect of recent Asian emission increases on air quality in North America: An integrated analysis using satellite, aircraft, ozonesonde, and surface observations. *Atmos Chem Phys* **8**(20): 6117–6136.

Zhang, L, Wang, T, Zhang, Q, Zheng, J, Xu, Z, Lv, M. 2016a. Potential sources of nitrous acid (HONO) and their impacts on ozone: A WRF-Chem study in a polluted subtropical region. *J Geophys Res Atmos* **121**: 3645– 3662. DOI: http://dx.doi.org/10.1002/2015JD024468.

Zhang, Q, Streets, DG, He, K, Wang, Y, Richter, A, Burrows, JP, Uno, I, Jang, CJ, Chen, D, Yao, Z, Lei, Y. 2007. NOx emission trends for China, 1995–2004: The view from the ground and the view from space. *J Geophys Res Atmos* **112(**D22): 1–18.

Zhang, R, Tie, X, Bond, DW. 2003. Impacts of anthropogenic and natural NOx sources over the US on tropospheric chemistry. *PNAS* **100**(4): 1505–1509.

Zhang, Y, Cooper, OR, Gaudel, A, Thompson, AM, Nédélec, P, Ogino, S-Y, West, JJ. 2016b. Tropospheric ozone change from 1980 to 2010 dominated by equatorward redistribution of emissions. *Nat Geosci.* DOI: http://dx.doi.org/10.1038/NGEO2827.

Ziemke, JR, Chandra, S, Bhartia, PK. 2005. A 25-year data record of atmospheric ozone in the Pacific from Total Ozone Mapping Spectrometer (TOMS) cloud slicing: Implications for ozone trends in the stratosphere and troposphere. *J Geophys Res* **110**: D15105. DOI: http://dx.doi.org/10.1029/2004JD005687.

Ziemke, JR, Oman, LD, Strode, SA, Douglass, AR, Olsen, MA, McPeters, RD, Bhartia, PK, Froidevaux, L, Labow, GJ, Witte, JC, Thompson, AM, Haffner, DP, Kramarova, NA, Frith, SM, Huang, L-K, Jaross, GR, Seftor, CJ, Deland, MT, Taylor, SL. 2019. Trends in global tropospheric ozone inferred from a composite record of TOMS/OMI/MLS/OMPS satellite measurements and the MERRA-2 GMI simulation. *Atmos Chem Phys* **19**: 3257–3269. DOI: http://dx.doi.org/10.5194/acp-19-3257-2019.

Zoogman, P, Liu, X, Suleiman, RM, Pennington, WF, Flittner, DE, Al-Saadi, JA, Hilton, BB, Nicks, DK, Newchurch, MJ, Carr, JL, Janz, SJ. 2017. Tropospheric emissions: Monitoring of pollution (TEMPO). *J Quant Spectrosc Radiat Transf* **186**: 17–39.

How to cite this article: Archibald, AT, Neu, JL, Elshorbany, Y, Cooper, OR, Young, PJ, Akiyoshi, H, Cox, RA, Coyle, M, Derwent, R, Deushi, M, Finco, A, Frost, GJ, Galbally, IE, Gerosa, G, Granier, C, Griffiths, PT, Hossaini, R, Hu, L, Jöckel, P, Josse, B, Lin, MY, Mertens, M, Morgenstern, O, Naja, M, Naik, V, Oltmans, S, Plummer, DA, Revell, LE, Saiz-Lopez, A, Saxena, P, Shin, YM, Shaahid, I, Shallcross, D, Tilmes, S, Trickl, T, Wallington, TJ, Wang, T, Worden, HM, Zeng, G. 2020. Tropospheric ozone assessment report: A critical review of changes in the tropospheric ozone burden and budget from 1850 to 2100. *Elem Sci Anth*. 8: 1. DOI: https://doi.org/10.1525/elementa.2020.034

Domain Editor-in-Chief: Detlev Helmig, Boulder AIR, LLC, Boulder, CO, USA

Associate Editor: Alastair Lewis, National Centre for Atmospheric Science, University of York, York, United Kingdom

Knowledge Domain: Atmospheric Science

Part of an Elementa Special Feature: Tropospheric Ozone Assessment Report (TOAR): Global Metrics for Climate Change, Human Health and Crop/Ecosystem Research

Published: December 30, 2020 **Accepted:** October 12, 2020 **Submitted:** March 24, 2020

ELEMENTA Science of the Anthropocene

Elem Sci Anth is a peer-reviewed open access journal published by University of California Press.

OPEN ACCESS